PRODUCTION AND CHARACTERIZATION OF ACTIVATED CARBON FROM HAZELNUT SHELL AND HAZELNUT HUSK

A THESIS SUBMITTED TO
THE GRADUATE SCHOOL OF NATURAL AND APPLIED SCIENCES
OF
MIDDLE EAST TECHNICAL UNIVERSITY

BY

ÇİĞDEM ÇUHADAR

IN PARTIAL FULFILLMENT OF THE REQUIREMENTS
FOR
THE DEGREE OF MASTER OF SCIENCE
IN
CHEMICAL ENGINEERING

JUNE 2005

Approval of the Graduate School of Natural and Applied Sciences

Prof. Dr. Canan Özgen
Director

I certify that this thesis satisfies all the requirements as a thesis for the degree of Master of Science.

Prof. Dr. Nurcan Baç
Head of Department

This is to certify that we have read this thesis and that in our opinion it is fully adequate, in scope and quality, as a thesis and for the degree of Master of Science.

Prof. Dr. N. Suzan Kıncal
Co-Supervisor

Prof. Dr. Hayrettin Yücel
Supervisor

Examining Committee Members

Prof. Dr. Timur Doğu (METU, CHE) _____

Prof. Dr. Hayrettin Yücel (METU, CHE) _____

Prof. Dr. N. Suzan Kıncal (METU, CHE) _____

Dr. Cevdet Öztin (METU, CHE) _____

Prof. Dr. Zeki Aktaş (AÜ, CHE) _____

I hereby declare that all information in this document has been obtained and presented in accordance with academic rules and ethical conduct. I also declare that, as required by these rules and conduct, I have fully cited and referenced all material and results that are not original to this work.

Çiğdem ÇUHADAR

ABSTRACT

PRODUCTION AND CHARACTERIZATION OF ACTIVATED CARBON FROM HAZELNUT SHELL AND HAZELNUT HUSK

ÇUHADAR, Çiğdem

M.Sc. Department of Chemical Engineering

Supervisor: Prof. Dr. Hayrettin YÜCEL
Co-Supervisor: Prof. Dr. N. Suzan KINCAL

June 2005, 110 pages

In this study, the pore structures and surface areas of activated carbons produced from hazelnut shell and hazelnut husk by chemical activation technique using phosphoric acid (H_3PO_4), at relatively low temperatures (300, 400 and 500^oC), were investigated. Raw materials were impregnated with different H_3PO_4 solutions of 30%, 40%, 50% and 60% by weight. To produce activated carbon, acid impregnated samples were heated; at a heating rate of 20 ^oC/min to the final carbonization temperature and held at that temperature for 2 hours.

The volume and surface areas of mesopores (2-50 nm) and BET surface areas of the samples were determined by N_2 gas adsorption technique at -195.6^oC. The pore volume and the area of the micropores with diameters less than 2 nm were determined by CO_2 adsorption measurements at 0^oC by the application of Dubinin Radushkevich equation.

N_2 (BET) surface areas of the hazelnut shell and hazelnut husk based activated carbons were in the range of 242-596 m^2/g and 705-1565 m^2/g, respectively. CO_2 (D-R) surface areas of the hazelnut shell and hazelnut husk based activated carbons were in the range of 433-576 m^2/g and 376-724 m^2/g, respectively.

The highest BET surface area was obtained as 596 m^2/g among hazelnut shell based samples (HS 60.4; shell impregnated with 60 wt.% H_3PO_4, carbonized at 400 ºC) and as 1565 m^2/g among hazelnut husk based samples (HH 40.4; husk impregnated with 40 wt.% H_3PO_4, carbonized at 400 ºC). Hazelnut shell based activated carbons were mainly microporous while hazelnut husk based ones were mesoporous.

Keywords: Activated Carbon, Hazelnut Shell, Hazelnut Husk, Pore Structure, H_3PO_4 Activation

ÖZ

FINDIK KABUĞU VE FINDIK ÇOTANAĞINDAN AKTİF KARBON ÜRETİMİ VE KARAKTERİZASYONU

Çuhadar, Çiğdem

Yüksek Lisans, Kimya Mühendisliği Bölümü

Tez Yöneticisi: Prof. Dr. Hayrettin YÜCEL

Ortak Tez Yöneticisi: Prof. Dr. N. Suzan KINCAL

Haziran 2005, 110 sayfa

Bu çalışmada, kimyasal aktivasyon tekniği ile aktive edici madde olarak fosforik asit (H_3PO_4) kullanılmak suretiyle oldukça düşük sıcaklıklarda (300, 400 ve 500^oC) fındık kabuğu ve fındık çotanağından üretilen aktif karbonların gözenek yapıları ve yüzey alanları incelenmiştir. Hammaddelere 30%, 40%, 50% ve 60% ağırlıksal derişimdeki H_3PO_4 çözeltileri emdirilmiş; asit emdirilmiş örnekler aktif karbon üretmek için 20^oC/dak. ısıtma hızıyla son karbonizasyon sıcaklıklarına kadar ısıtılıp 2 saat süreyle sabit sıcaklıkta tutulmuştur.

Ürünlerin mezogözenek (2-50 nm) yüzey alanları ve hacimleri ve BET yüzey alanları -195.6^oC de N_2 gaz adsorbsiyon tekniği kullanılarak, çapları 2 nm den küçük olan mikrogözeneklerin gözenek hacmi ve yüzey alanı 0^oC de CO_2 adsorpsiyon ölçümleriyle Dubinin-Radushkevich denkleminin kullanılmasıyla elde edilmiştir.

Fındık kabuğu ve fındık çotanağından üretilen aktif karbonların BET yüzey alanlarının sırasıyla 242-596 m^2/g ve 705-1565 m^2/g aralıklarda olduğu ölçülmüştür. Ürünlerin CO_2 (D-R) yüzey alanları fındık kabuğundan üretilenler için 433-576 m^2/g ve fındık çotanağından üretilenler için 376-724 m^2/g aralıklarında bulunmuştur.

Fındık kabuğundan üretilen aktif karbonlar içinde en yüksek BET yüzey alanını HS 60.4 örneği (ağırlıkça 60% asit derişimi ve 400 ^oC karbonizasyon sıcaklığı) 596 m^2/g olarak, fındık çotanağından üretilenler içinde ise HH 40.4 örneği (ağırlıkça 40% asit derişimi ve 400 ^oC karbonizasyon sıcaklığı) 1565 m^2/g olarak vermiştir. Fındık kabuğundan üretilen aktif karbonların çoğunlukla mikrogözenekli, fındık çotanağından üretilen aktif karbonların ise mezogözenekli oldukları tespit edilmiştir.

Anahtar Kelimeler: Aktif Karbon, Fındık Kabuğu, Fındık Çotanağı, Gözenek Yapısı, H_3PO_4 Aktivasyonu

To My Family,

ACKNOWLEDGEMENTS

I wish to express my deepest gratitude to my thesis supervisors Prof. Dr. Hayrettin Yücel and Prof. Dr. N. Suzan Kıncal for all their understanding, support and sound advice in all aspects of my research work. I am very much obliged for their objective and tolerant attitude, creating very pleasant working conditions.

I should mention, Özge Yazıcıoğlu, Emrah Irmak, Yalçın Yılmaz, Nahide Özkan, Oluş Özbek, Salih Obut, İsmail Doğan, Açelya Gökalp, Deniz Akkaş, my laboratory mates Wisam Abdallah and Ural Yağşi, my dear brother Özgür Çuhadar and many others that I could not mention here, who gave me helpful suggestions for the improvement of the document and moral support.

I would like to thank Ms. Gülten Orakcı, Ms. Mihrican Açıkgöz, Ms. Kerime Güney, Mr. Selahattin Uysal, Dr. Necati Özkan and Dr. Kemal Behlülgil for their help in the chemical and physical analysis of the samples.

Thanks are due to all the staff of the Chemical Engineering Department.

TABLE OF CONTENTS

LIST OF TABLES

Table

LIST OF FIGURES

Figure

LIST OF SYMBOLS

A_m : Cross-sectional area of the adsorbate, nm^2

C : A constant in equation 3.1

CSA_{N2} : Cross sectional area of nitrogen molecule, nm^2

D_p : Pore diameter, μm

E_i : Adsorption potential, kJ/mol

ΔG : Gibbs free energy change of the reaction, kJ/mol

I : Intercept of the BET plot

K : A constant in equation B.1

M : Adsorbate molecular weight, g/mol

N_A : Avagadro's constant, $6.023*10^{23}$ molecules/mol

P_i : Partial pressure of the gas i, atm, Pa, psia, mmHg

P : Pressure, atm, Pa, psia, mmHg

P_0 : Saturation pressure, mmHg

q_1 : Heat of adsorption of the first layer, kJ/mol

q_2 : Heat of adsorption of the second and subsequent layers, kJ/mol

R : The gas constant, $8.314x10^7$erg/mole-K, $8.314x10^{-3}$ KJ/mole-K

r_p : Actual pore radius, mean radius of the liquid meniscus, nm or μm

r_K : Kelvin radius, nm

r_{KAVE} : Average Kelvin radius, nm

r_{PAVE} : Average pore radius, nm

S : Slope of the BET plot

S_{BET} : BET surface area, m^2/g

S_{cum} : Cumulative pore surface area, m^2/g

S_{meso} : Mesopore surface area m^2 /g

t : Thickness of the adsorbate layer, nm

t_m : Thickness of the monolayer, nm

T : Temperature, °C

T_a : Ambient temperature, °C

T_c : Critical temperature of the adsorption, °C

V : Volume adsorbed, cm^3/g

V_0 : Micropore Volume, cm^3/g

V_{cum} : Cumulative volume, cm^3/g

V_m : Monolayer volume, cm^3/g STP

V_{meso} : Mesopore volume, cm^3/g

V_{mol} : Molar volume of the nitrogen, $34.6x10^{24}$ A^3/mol at -195.6°C

ΔV_{gas} : Incremental molar adsorbed gas volume, cm^3/g

ΔV_{Liq} : Incremental molar adsorbed liquid volume, cm^3/g

W_0 : Limiting adsorption space volume, cm^3

W_a : The quantity of adsorbed at a particular relative pressure, cm^3

W_m : The quantity of adsorbed at correspond to BET monolayer, cm^3

Greek Letters

μm : Micrometer (10^{-6} meter)

Å : Angstrom (10^{-10} meter)

ρ : Liquid density, g/cm^3

ρ_{He} : Helium (True Density), g/cm^3

θ : Contact angle of liquid meeting the pore wall

σ : Cross sectional area of a CO_2 molecule, nm^2

γ : Surface tension, erg/cm^2

CHAPTER I

INTRODUCTION

Activated carbon is a predominantly amorphous solid that has an extraordinarily large internal surface area and pore volume. These unique characteristics are responsible for its adsorptive properties, which are exploited in many different liquid- and gas-phase applications. Through choice of precursor, method of activation, and control of processing conditions, the adsorptive properties of products are tailored for applications as diverse as the purification of potable water and the control of gasoline emissions from motor vehicles.

The structure of activated carbon is best described as a twisted network of defective carbon layer planes, cross-linked by aliphatic bridging groups. X-ray diffraction patterns of activated carbon reveal that it is nongraphitic, remaining amorphous. This property of activated carbon contributes to its most unique feature, namely, the highly developed and accessible internal pore structure. Activated carbon is generally considered to exhibit a low affinity for water, which is an important property with respect to the adsorption of gases in the presence of moisture. Commercial activated carbon products are produced from organic materials that are rich in carbon, particularly coal, lignite, wood, nut shells, peat, pitches, and cokes. (Kirk-Othmer, 2003)

The pyrolysis of starting material with the exclusion of air and without addition of chemical agent usually results in an inactive material with a specific surface area of the order of several m^2/g and low adsorption capacity. One can prepare a carbon with a large adsorption capacity by activating the carbonized products with a reactive gas. The majority of activated carbon used throughout the world

is produced by steam activation (physical activation). In this process, the carbonized product is reacted with steam over 900^{o}C. Another procedure used in the production of activated carbon involves the use of chemical activating agents before the carbonization step. The most commonly used activating agents are phosphoric acid, zinc chloride and salts of sodium and magnesium. Chemical agents act as dehydration agents and they may restrict the formation of tar during carbonization. Chemical activation is usually carried out at lower temperatures than the simple pyrolysis and the activation process with steam or carbon dioxide. The production at lower temperatures promotes the development of a porous structure, because under these conditions elementary crystallites of smaller dimensions are formed. (Smisek and Cerny, 1970)

Most of the available surface area of activated carbon is nonpolar in nature. However, during production the interaction of surface with oxygen produces specific active sites giving the surface of slightly polar nature. As a result, carbon adsorbents tend to be hydrophobic and organophilic. (Ruthven, 1984)

Activated carbon may not be pure carbon but also contain some impurities depending on the type of starting material. It must be noted that, the adsorption characteristics of activated carbon for certain uses (such as adsorption of electrolytes and non-electrolytes from solutions) are significantly influenced by even small amounts of ash. Moreover, the adsorption of gases is also influenced by the ash content. Therefore, the raw material should contain as small ash as possible. On the other hand, the raw material must have relatively low cost (Balcı, 1992).

To meet the engineering requirements of specific applications, activated carbons are produced and classified as granular, powdered, or shaped products. Activated carbon is a recyclable material that can be regenerated. Thus the economics, especially the market growth, of activated carbon is affected by industry regeneration capacity. Landfill disposal is becoming more restrictive environmentally and more costly (Kirk-Othmer, 2003).

According to the IUPAC definition, pores can be distinguished in three groups with respect to their dimensions (Reinoso, 1985).

Table 1.1 Pore Sizes of Activated Carbon

Macropores	Pores with diameters larger than 50 nm (500 Å)
Mesopores	Pores with diameters between 2 nm and 50 nm (20- 500 Å)
Micropores	Pores with diameters less than 2 nm (20 Å)

Most activated carbons contain pores of different sizes; micropores, transitional mesopores and macropores. Therefore they are considered as adsorbents with wide variety of applications.

Activated carbons for use in liquid-phase applications differ from those used in gas-phase applications primarily in pore size distribution. Liquid-phase carbons have significantly more pore volume in the macropore range, which permits liquids to diffuse more rapidly into the mesopores and micropores. Liquid-phase activated carbon can be applied either as a powder, granular, or shaped form. Granular and shaped carbons are used generally in continuous systems where the liquid to be treated is passed through a fixed bed. Liquid-phase applications of activated carbon include potable water treatment, industrial and municipal wastewater treatment, sweetener decolourization, groundwater remediation, and miscellaneous uses including chemical processing, mining and the production of food, beverages, cooking oil, and pharmaceuticals.

Gas-phase applications of activated carbon include separation, gas storage, and catalysis. Most of the activated carbon used in gas-phase applications is granular or shaped. Applications include solvent recovery, automotive/gasoline recovery, industrial off-gas control, and catalysis, among others. Separation processes comprise the main gas-phase applications of activated carbon.

Some of the major raw materials used, are agricultural by-products. Although they have very high volatile content and hence give low yields of activated carbon, they are relatively inexpensive and economical starting materials. In Turkey, agricultural by products including hazelnut shell and husk are abundantly available.

Turkey is the largest hazelnut producer and exporter in the world. It covers approximately 70 percent and 82 percent of the world's production and export respectively. About 60 percent of the crop is produced in the Eastern Black Sea Region, 15 percent is produced in the Central Black Sea Region and the remaining 25 percent is produced in the Western Black Sea Region. Turkey's average in-shell production is 350-400 000 t, this value has reached up to 500 000 t in recent years (Köksal, 2000). Accordingly, 140,000 tons of hazelnut shell and 110,000 tons of hazelnut husks are obtained as waste. Hazelnut shell is mainly used for heating purposes in the Black Sea Region but hazelnut husk is mostly left to decay because of moist climate.

Most of the studies have shown that, activated carbons obtained from agricultural by-products can be favorably compared with other activated carbons used in industry with respect to their adsorptive properties (Balcı, 1992).

The objective of this study is to produce activated carbon from agricultural wastes; hazelnut shell and hazelnut husk by chemical activation using phosphoric acid and characterize these products in terms of pore volume and surface area by BET (Braunauer, Emmet, Teller) method, BJH (Barrett, Joyner, Hallenda) Method, DR (Dubinin, Radushkevich) Method and Helium Pycnometer.

The major novelty of this work is the production of activated carbons from phosphoric acid impregnated hazelnut shell and hazelnut husk samples by chemical activation technique in a temperature range of 300^{o}C to 500^{o}C and with different acid concentrations. The applicability of hazelnut husk for the production of activated carbon was investigated for the first time in this study.

CHAPTER II

ACTIVATED CARBON

2.1. Definition and Properties

Activated carbon is a microcrystalline, nongraphitic form of carbon. X-ray analysis of activated carbons shows a structure which is much more disordered than that of graphite, having crystallites only a few layers in thickness and less than 10 nm in width (Smisek and Cerny, 1970). The spaces between the crystallites of activated carbon constitute the microporous structure with a large internal surface area of 250 m^2/g-2500 m^2/g. Its chemical structure allows it to preferentially adsorb organic materials and other nonpolar compounds from the gas or liquid streams. Because of these properties, they have been used for many decades for the purification of gases, the separation of gas mixtures, purification of exhausted air, especially the recovery of solvents, removal of heavy metals, decolourization of solutions and purification of water. Carbonaceous adsorbents found greater use in the solution of environmental problems related to water purification and removal of air pollutants (Smisek and Cerny, 1970; Hassler, 1974).

The removal of impurities from gases and liquids by activated carbon takes place by adsorption. Adsorption is a term, which describes the existence of a higher concentration of a substance at the interface between a fluid and a solid than is present in the fluid. Adsorption process can be considered as either physical adsorption or chemisorption.

In physical adsorption the impurities are held on the surface of the carbon by weak van der Waals forces while in chemisorption, the forces are relatively strong and adsorption occurs at active sites on the surface. Therefore, in chemisorption the efficiency of carbon will depend upon its accessible surface area and also upon the presence of active sites on the surface where chemisorption may occur (Balcı, 1992).

The porous structure and chemical nature of an activated carbon is a function of the raw materials used in its preparation and the activation method used. This is the reason why surface area or pore volume of activated carbons can vary widely from one kind to another. Pore structure of activated carbon (from TEM) is shown in Figure 2.1.

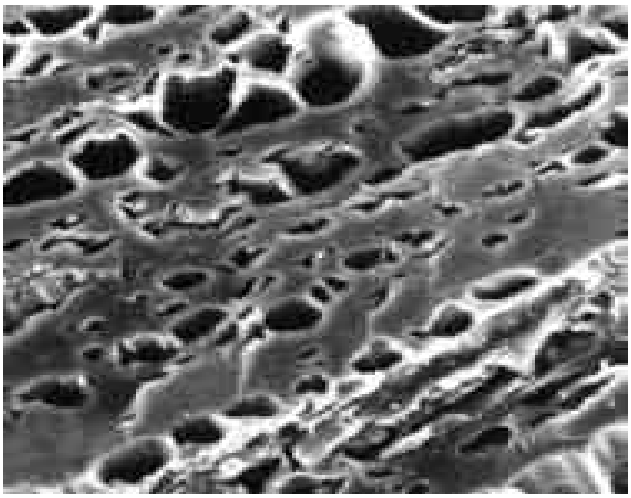

Figure 2.1 Pore Structure of Activated Carbon (TEM) (Yağşi, 2004)

The internal surface area of activated carbons can be determined by the adsorption of nitrogen, but there is no guarantee that the entire surface is available for the adsorption of organic compounds. Since organic molecules are

much larger than a nitrogen molecule and if the pores are the same size as molecular dimensions, it is possible to have a sieving action. Thus, it is essential for an adsorptive carbon to have a large accessible surface area which in turn is directly related to pore size distribution (Balcı, 1992).

2.2. Principle of Activation Process

During carbonization of a carbonaceous material (i.e., pyrolysis in the absence of air and without addition of chemical agents), most of the noncarbon elements (hydrogen, oxygen, traces of sulphur and nitrogen) are first removed in a gaseous form by pyrolytic decomposition.

The atoms of elementary carbon thus released are grouped into organized crystallographic formations known as elementary graphitic crystallites. The mutual arrangements of these crystallites is irregular, so that free interstices remain between them, and, apparently as the result of deposition and decomposition of tarry substances, these become filled or blocked by disorganized carbon. The resulting carbonized product generally has only a small adsorption capacity. Activation of the carbonized material is possible via two routes: chemical activation and physical activation (Wigmans, 1989).

2.2.1. Raw Materials

The quality of the resulting activated carbon is considerably influenced by the raw material. Although the activation procedure employed mainly determines the chemical nature of the surface oxides and the surface area of the resultant product, the structure of the pores and the pore size distributions are largely predetermined by the nature of the starting material. Any cheap substance with a high carbon and low ash content can be used as a raw material. Raw materials for the production of activated carbon include number of carbonaceous

materials, especially wood, peat, brown coal, bituminous coal, lignite, coconut shells, almond shells, pits from peaches and other fruit, petroleum-based residues and pulp mill residues (Balcı, 1992).

Since the manufacturing process involves the removal of volatile matter, the economic relationship between price, availability and quality of raw materials on one side and volatile content on the other side, is an important one. The most important advantages of using bituminous coal and anthracite are their relatively low volatile content and hence high yield of product.

Fixed carbon contents of some raw materials are given in Table 2.1. On the other hand, the younger fossil materials-wood, (mainly birch wood and beech wood) peat and wastes of vegetable origin (such as fruit stones, almond shell, coconut shell, saw dust) can be activated easily and give high quality products. (Smisek and Cerny, 1970; Martin, 1981; Holden, 1982)

Table 2.1 Fixed Carbon Contents of Raw Materials Employed in Activated Carbon Manufacture (Holden, 1982).

Material	Percent Carbon Content
Soft Wood	40
Hard Wood	40
Coconut Shell	40
Lignite	60
Bituminous Coal	75
Anthracite	90

2.2.2. Production Methods

Activated carbon can be prepared by one of the following two methods:

- Carbonization after addition of substances, which restrict the formation of tar. In this way, a carbonized product with the properties of a good activated carbon can be obtained in a single operation. Yet, the activation agent like $ZnCl_2$, H_3PO_4, KOH, K_2S or KCNS that has to be applied in large quantities has to be removed via washing in order to reveal the porous structure and to make the material practically applicable. This route is generally called "chemical activation."

- Partial gasification, generally called "physical activation." The activation agents most often used are steam, carbon dioxide, and air or a combination of these. During activation of the intermediate product, the disorganized carbon (depending on the carbonization procedure, 10-20% burn-off) is first removed to expose the surface of the elementary crystallites to the action of the activation agent. The further development of the porosity on increasing burn-off depends on the mechanism of carbon removal via active site formation and the relative rate of reaction in the direction parallel with the plane of the graphitic layers compared to carbon removal in the direction perpendicular to this plane (Wigmans, 1989).

The basic production processes can be combined in different ways. Sometimes the chemically activated carbon is subjected to additional activation with gaseous environment in order to change the pore structure of the final product.

In contemporary technologies both types of activation, chemical and physical are widely used. Although high quality products can be obtained by both procedures, sometimes, they are not equally good for all purposes. For example, for the recovery of solvent, chemically activated carbons are preferred, whereas for

water treatment, carbon activated with steam appears to be preferable. (Smisek and Cerny, 1970)

2.2.2.1. Chemical Activation

In chemical activation the precursor is impregnated with a given chemical agent and pyrolyzed after that. As a result of the pyrolysis process, a much richer carbon content material with a much more ordered structure is produced, and once the chemical agent is eliminated after the heat treatment, the porosity is highly developed. Several activating agents have been reported for the chemical activation process: phosphoric acid, zinc chloride and alkaline metal compounds. Phosphoric acid and zinc chloride are activating agents usually used for the activation of lignocellulosic materials which have not been previously carbonized; while, alkaline metal compounds, usually KOH, are used for activation of coal precursors or chars.

An important advantage of chemical activation is that the process normally takes place at a lower temperature and for a shorter time than those used in physical activation. In addition, very high surface area activated carbons can be obtained. Moreover, the yields of carbon in chemical activation are usually higher than those in physical activation because the chemical agents used are substances with dehydrogenation properties that inhibit formation of tar and reduce the production of other volatile products. On calcinations, the impregnated chemicals dehydrate the raw materials, which results in changing and aromatization of the carbon skeleton by the creation of a porous structure and surface area. However, the general mechanism for the chemical activation is not so well understood as for the physical activation. Other disadvantages of chemical activation process are the need of an important washing step because of the incorporation of impurities coming from the activating agent, which may affect the chemical properties of the activated carbon, and the corrosiveness of the chemical activation process (Lozano-Castello, 2001; Balcı, 1992).

The material mainly used in the production of activated carbon consists predominantly of cellulose, and therefore in a discussion of the mechanism of chemical activation, the action of the chemical agent on cellulose must first be considered. Cellulose is composed of elongated macromolecules, up to 1800-2000 nm long, orientated in the direction of their longitudinal axes, which form agglomerates known as micelles. The orientated chains of molecules are laterally bounded by bonds of different types of strength. The electrolytic action of the activation agent causes the cellulose to undergo a change known as swelling, during which the arrangement of the molecules in the direction of the longitudinal axis remain unchanged, but the lateral bonds are broken down with the result that the inter-and-intra micelle voids increase until finally the cellulose is dispersed. Simultaneously other reactions, hydrolytic or oxidative, take place, by which the macromolecules are gradually depolymerized. The processes lead to the formation of a homogeneous plastic mass consisting of the partially depolymerized substance uniformly saturated with the activation agent (Browning, 1963, Smisek and Cerny, 1970).

An important factor in chemical activation is the degree of impregnation. This weight ratio of the anhydrous activation agent to the dry materials is defined as the coefficient of impregnation. The effect of the degree of impregnation on the porosity of the resulting product is apparent from the fact that the volume of salt in the carbonized material is equal to the volume of pores, which are freed by its extraction. For small degrees of impregnation, a small increase in impregnation amount causes an increase in the total pore volume of the product showing an increase in the volume of smaller pores. When the degree of impregnation is further raised, the number of larger diameter pores increases and the volume of the smallest pores decreases (Balcı, 1992).

The activated carbons produced through chemical activation, especially when $ZnCl_2$ is used, must be cleaned from the chemical agent before their commercial use. One advantage of using phosphoric acid in chemical activation is that, it can be cleaned from the activated carbon by rinsing with boiling pure water (Yağşi, 2004).

2.2.2.2. Physical Activation

a. Carbonization

The method of production of the carbonized intermediate product has a marked effect on the quality of the final activated carbon product. The main aim of carbonization is to reduce the volatile content of the source material in order to convert it to a suitable form for activation. During the phase of the carbonization, carbon content of the product attains a value of about 80 percent. By carbonization most of the non-carbon elements, hydrogen and oxygen are first removed in gaseous form by pyrolytic decomposition of the starting material and the freed atoms of elementary carbon are grouped into organized crystallographic formation known as elementary graphitic crystallites (Balcı, 1992).

Carbonization of lignocellulosic material starts above 170^{o}C and it is nearly completed around 500^{o}C- 600^{o}C. In the production of charcoal, it is desirable to carry out its pyrolysis sufficiently quickly, in order to reduce the time of contact of the carbon formed with the decomposition products. The rate of pyrolysis is significantly influenced by the moisture content of the starting material. Further important factors are uniform heating of the retort and the temperature of carbonization, which must not be very high (Yağşi, 2004).

In the simple carbonization product, the mutual arrangement of the crystallites is irregular, so that free interstices remain between them. However, as a result of deposition and decomposition of tarry substances, these become filled or at least blocked by disorganized (amorphous) carbon. The resulting carbonized product has small adsorption capacity. Presumably, at least for carbonization at lower temperatures, part of the formed tar remains in the pores between the crystallites and on their surface. Such carbonized materials can then be partially activated by removing the tarry products by heating them in a stream of an inert gas, or by extracting them with a suitable solvent, or by a chemical reaction (for

example, heating in an atmosphere of sulphur vapor at temperatures lower than those at which reactions with carbon take place). (Smisek and Cerny, 1970; Wigmans, 1985)

b. Activation of Carbonized Intermediate Product with Gaseous Agents

A carbon with a large adsorption capacity can also be produced by activating the carbonized material under such conditions that the activating agent reacts with the carbon. The most common activation agents are steam, carbon dioxide and oxygen (air). The activation step is generally conducted at temperatures between 800^{o}C and 1100^{o}C. The active oxygen in the activating agent basically burns away the more reactive portion of the carbon skeleton as carbon monoxide and carbon dioxide, depending on the gaseous agent employed.

The reaction of carbon with carbon dioxide is endothermic and, for a given carbon in the absence of a catalyst, takes place at a rate several orders of magnitude slower than the carbon-oxygen reaction at the same temperature: it proceeds very slowly at temperatures below 1000 K (727 ^{o}C). The endothermic reaction between carbon and water vapor (steam) is favored by elevated temperature and reduced pressure and occurs slowly at temperatures below 1200 K. The reactions of carbon with molecular oxygen are favored thermodynamically at all temperatures up to 4000 K.

Activation takes place in two stages. In the initial stage, when the burn off is not higher than 10 percent, disorganized carbon is burnt out preferential and the closed and clogged pores between the crystallites are freed. By the removal of disorganized carbon, the surface of the elementary crystallites became exposed to the action of the activation agent. The burning out of the crystallites must proceed at different rates on different parts of the surface exposed to reaction; otherwise new pores could not be formed. The removal of nonorganized carbon and the non-uniform burn out of elementary crystallites leads to the formation of new pores, and to the development of the macroporous structures. The effect which becomes increasingly significant is the widening of existing pores, or the

formation of larger size pores by the complete burn out of walls between adjacent micropores.

According to the type of the gaseous activation agent, some difficulties may arise. Activation with steam and carbon dioxide are carried out at temperatures between 800 ºC and 1100 ºC. At lower temperatures, reactions are too slow. However, the temperature must be carefully chosen to make the chemical reaction between carbon and gaseous agent the rate determining factor. In kinetics control region, reactions take place at the interior surface of the carbon. Hence the removing of carbon from the pore walls causes the enlargement of the pores. However at much higher temperatures reactions become diffusion controlled and occurs on the outside of the carbon particle (Balcı, 1992).

The reaction of oxygen with carbon is exothermic. Therefore, for the activation of the carbonized product with oxygen it may be difficult to maintain the correct temperature in the oven. Possible local overheating prevents uniform activation. Furthermore, due to the very aggressive action of oxygen, burn out is not limited to pores but also occur on the external surface of the grain by causing great loss. It must be noted that, carbons activated with oxygen have a large amount of surface oxides. Due to the difficulties and disadvantages explained, oxygen (air) activation is rarely used (Balcı, 1992).

The main factors that influence the rates of the reactions of carbon with carbon dioxide, steam and oxygen are: i) the concentration of the active sites on the carbon surface, ii) the crystallinity and structure of the carbon, iii) the presence of inorganic impurities and iv) the diffusion of reactive gases to the active sites.

Generally, carbonization and activation steps are carried out separately, but recently there is an increasing tendency to conduct the two processes together. (Smisek and Cerny, 1970; Hassler, 1974; Wigmans, 1985; Rodriguez-Reinoso, 1991)

2.3. Physical Structure of Activated Carbon

The structure studies of Franklin (1951) on carbonized materials showed two distinct well defined classes; nongraphitizing carbons and graphitizing carbon. (Figure 2.2)

In general, the nongraphitizing carbons are formed from substances containing little hydrogen or more oxygen. Such substances develop a strong system of cross linking of crystallites on heating at low temperature, forming a porous mass. The graphitizing carbons are prepared from substances containing more hydrogen. The crystallites remain relatively mobile during the early stages of carbonization and cross linking is much weaker. As a result, softer and less porous carbon is obtained (Balcı, 1992).

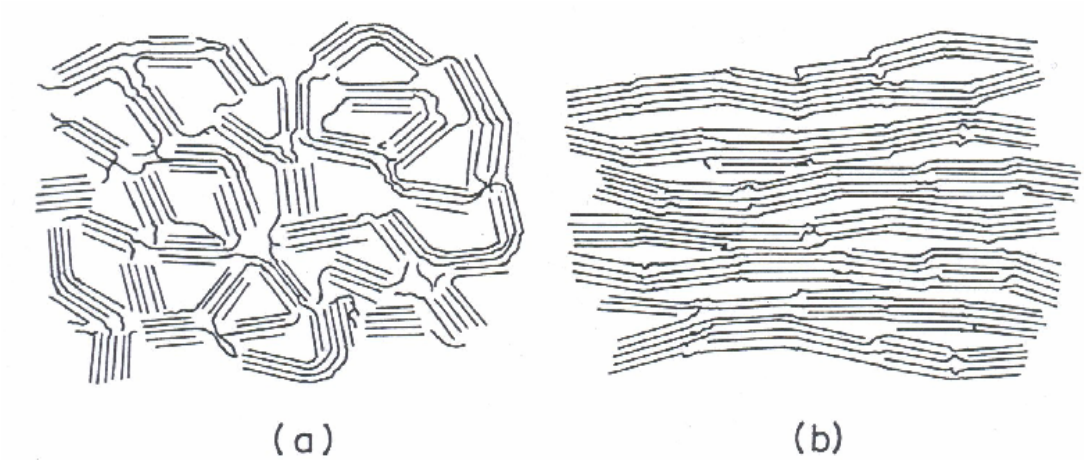

Figure 2.2 Schematic Representation of (a) Nongraphitizing and (b) Graphitizing Structure of Carbon (Smisek and Cerny, 1970)

Activated carbons, together with other types of chars, form a group of carbonaceous materials of which the structure and the properties depending on it are more or less similar to the structure and properties of graphite. Graphite is composed of layer planes formed by carbon atoms ordered in regular hexagons, similar to those in the rings of aromatic organic compounds. The interatomic distance between the carbon atoms in the individual layer planes is 0.142 nm. The layer planes are in parallel array with an interlayer spacing of 0.335 nm, shown in Figure 2.3. However, the structure of activated carbon differs somewhat from that of graphite. During carbonization process, several aromatic nuclei, having a structure similar to that of graphite are formed. Planar separation distance in carbon is approximately 0.36 nm. From X-ray spectrograph, these structures have been interpreted as microcrystallite consisting of fused hexagonal rings of carbon atoms structurally, carbon can therefore be considered to consist of rigid interlinked cluster of microcrytallites. Each microcrystallite comprises a stack of graphite planes (Smisek and Cerny, 1970).

Microcrystallites are interconnected by interaction of functional groups terminating the graphitic planes. The diameter of the planes forming the microcrystallites, as well as the stacking height, has been estimated at 2 -5 nm indicating that each microcrystallite consists of about 5-15 layers of graphite planes (Wolff, 1959).

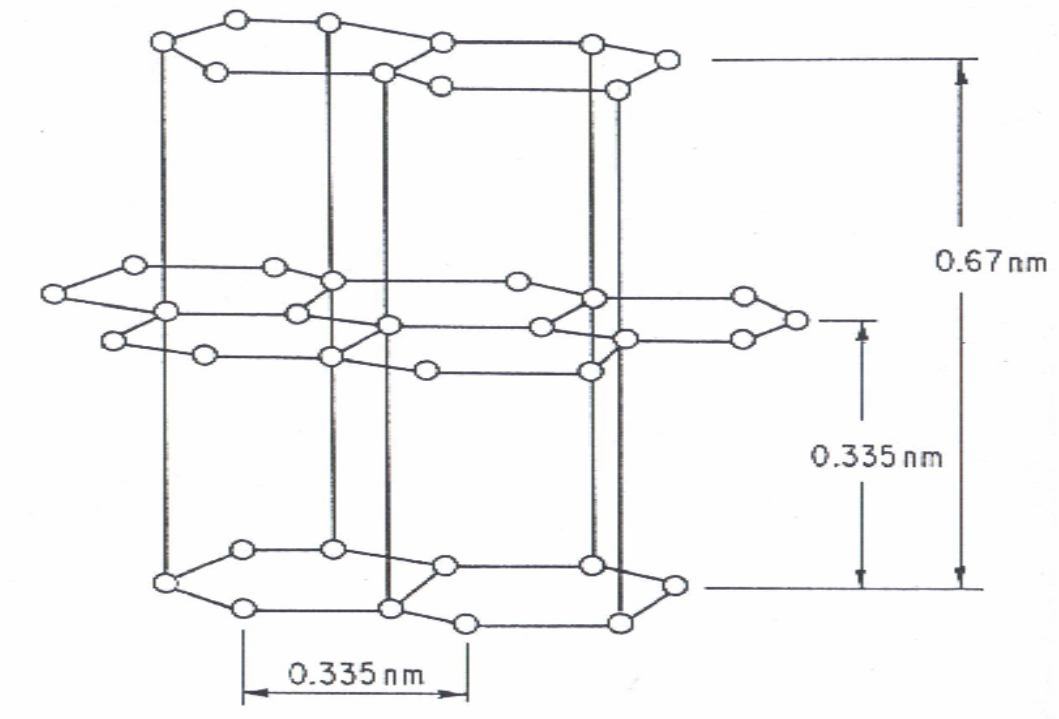

Figure 2.3 Carbon Atom Arrangements in Graphite Crystal**.**

2.4. Porosity

During the process of activation, the spaces between the elementary crystallites become cleared of various carbonaceous compounds and nonorganized carbon. Carbon is also removed partially from the graphitic layers of the elementary crystallites. The resulting voids are termed as pores. Results seem to indicate that, there are pores with a contracted entrance (ink-bottle shaped), pores in the shape of capillaries open at both ends or with one end closed, pores in the shape of more or less regular slits between two planes, v-shaped, tapered pores, and other forms (Smisek and Cerny, 1970).

In most cases, it is difficult to determine the pore shapes reliably. However, the calculation of diameters of pores assuming cylindrical capillary shapes yields values which approach the actual dimensions of the pores. Activated carbon usually has pores belonging to several groups, each group having a certain range of values for the effective dimensions.

Pores of an effective diameter larger than about 50 nm, are classified as macropores. Their volume in the activated carbon is generally between 0.2 cm^3/g and 0.5 cm^3/g and their surface area is 0.5 m^2/g to 2 m^2/g.

Transitional pores are those in which capillary condensation with the formation of a meniscus of the liquefied adsorbate can take place. This phenomenon usually produces a hysteresis loop on the adsorption isotherm. The effective diameters of transitional pores are in the range of 2 nm to 50 nm. Their specific surface area is generally around 5 % of the total surface area of the activated carbon.

Pores with an effective diameter of less than about 2 nm are called micropores. The micropore volume is generally around 0.15 cm^3/g to 0.50 cm^3/g. Usually the specific surface area of micropores amounts to over 90 % of the total specific surface area. Each of these three groups of pores has its specific function in the process of adsorption on activated carbon. According to the type of application, the percentages of the transitional pores and the micropores could be adjusted employing special production procedures. (Gregg and Sing, 1967; Smisek and Cerny, 1970; Rodriguez Reinoso, 1989; Balcı, 1992).

The suitability of active carbon for a particular application depends on the ratio in which pores of different sizes are present. Thus, for the adsorption of vapors and gases from mixtures in which they are present in small concentrations, markedly microporous active carbons are the most suitable. But active carbons used for the recovery of vapors of industrial organic solvents from waste gases and removal of heavy metals from solutions should contain a certain fraction of transitional pores (Smisek and Cerny, 1970).

2.5. Chemical Properties of Activated Carbon

The adsorptive properties of activated carbon are determined not only by its pore structure but also by its chemical composition. The decisive component of the adsorption forces on a highly ordered carbonaceous surface is the dispersion component of the van der Waals forces. Disturbances in the elementary microcrystalline structure as, for example, by the presence of imperfect graphitic layers in the crystallites, obviously change the arrangement of the electron clouds in the carbon skeleton. As a result incompletely saturated valences or unpaired electrons appear, and this influences the adsorptive properties of the active carbon, especially for polar substances.

Activated carbon contains two types of admixtures. One of them is represented by chemically bonded elements, in the first place oxygen and hydrogen. These are derived from the starting material and remain in the structure of activated carbon as a result of imperfect carbonization or become chemically bonded to the surface during activation. The other type of admixture consists of ash, which is not an organic part of the product. The ash content and its composition vary widely with the kind of active carbon. In adsorption of electrolytes and non-electrolytes from solutions, the adsorption characteristics of active carbon are significantly influenced even by small amounts of ash (Smisek and Cerny, 1970).

The elemental composition of activated carbon typically comprises 85-90 % C, 0.5 % H, 0.5 % N, 5 % O, and 1 % S, the balance of 5-6 % representing inorganic (ash) constituents. However, these values can not serve as specification for activated carbon's quality or properties (Faust and Aly, 1983).

Surface areas generated by the more reactive edges of the microcrystallite contain a wide variety of functional groups and are accordingly quite heterogeneous in nature. The nature of the relevant functional groups is determined to a large extent by the method of activation as well as by the type

of raw material from which the activated carbon is produced (Cookson, 1980; Wigmans, 1985).

The oxygen content of starting material has a considerable influence on the arrangement and size of the elementary crystallites formed in carbonaceous adsorbents. In adsorbents prepared from materials of high oxygen content, the distance between the parallel graphitic layers is appreciably smaller. Moreover, the course of carbonization and the required carbonization temperature depend strongly on the oxygen content of raw material. On the other hand, if oxidizing gases possess the oxygen, this oxygen also be chemisorbed and bound as surface oxides on the edge of the layer planes. The presence of chemisorbed oxygen on the surface of activated carbon has important effects on its capacity to adsorb water vapor and other polar adsorbate vapors. The oxygen content of activated carbon ranges between 1 % and 25 % and has been shown to vary considerably with the activation temperatures. The oxygen content generally decreases with an increase in the activation temperature (Balcı, 1992).

Carbons activated at lower temperatures, 200^{o}C-500^{o}C, termed as L-carbons, generally will develop acidic surface oxides. The acidic surface oxides could mainly include phenolic hydroxyl groups. The carbons activated by chemical treatment in aqueous solutions with such oxidizing agents as chloride, permanganate, persulfate, hydrogen peroxide and nitric acid, develop the same characteristics as L-carbon. The carbons activated at higher temperatures, 800^{o}C–1000^{o}C, termed as H-carbons, will develop basic surface oxides. Adsorption of electrolytes is affected by the presence of basic or acidic surface oxides. The presence of surface oxygen complexes will also impart a polar character to the activated carbon surface, which should result in preferential adsorption of comparatively polar organic compounds (Balcı, 1992).

Materials prior to activation contain hydrogen in the form of hydrocarbon chains and rings attached to border atoms of the hexagon planes. Most of this hydrogen is removed during activation at temperatures below 950^{o}C, but some hydrogen is still held after activation and is not released unless much higher temperatures are reached. It is to be noted that, the evolution of this latter portion of

hydrogen at very high temperatures is paralleled by a simultaneous decrease in adsorptive power. Hydrogen is more strongly chemisorbed than oxygen. Infrared studies showed that hydrogen was present in aromatic and aliphatic form. The aromatic hydrogen was suggested to be bonded covalently to the carbon atoms at the periphery of the aromatic basal planes. The aliphatic hydrogen was suggested to be present in the form of aliphatic chains and alicyclic rings attached to the peripheral aromatic rings. In addition to hydrogen and oxygen, calcined sulphur, nitrogen, chlorine and other elements can also be present in active carbon (Balcı, 1992).

CHAPTER III

METHODS USED IN PHYSICAL CHARACTERIZATION OF ACTIVATED CARBON

3.1. General

Conventional classification of pores according to their diameters, originally proposed by Dubinin and now officially adopted by the International Union of Pure and Applied Chemistry, (IUPAC) is mostly used. (This classification is given in Table 1.1 in Chapter I.)

Table 1.1 Pore Sizes of Activated Carbon

Macropores	Pores with diameters larger than 50 nm (500 Å)
Mesopores	Pores with diameters between 2 nm and 50 nm (20- 500 Å)
Micropores	Pores with diameters less than 2 nm (20 Å)

There are numerous techniques and methods for the characterization of pore structure of activated carbon. Since the size of the pores vary in a wide range, (e.g. macro, meso, micro) there is not single technique to provide information in

all ranges of pores. Therefore, in most cases a combination of different methods are used. For the quantitative characterization of the pore structures; estimation of pore surface area, pore volume, and pore size distribution together with the true and apparent density determinations are needed. For this purpose; the adsorption of gases and vapors by standard gravimetric or volumetric techniques helium pycnometry and mercury porosimetry are still classical and convenient approaches to the general characterization of porosity in activated carbon. Complementary techniques, such as, small angle scattering (X-rays or Neutrons), transmission electron microscopy, etc. are also used for the characterization of pores. (Şenel, 1994)

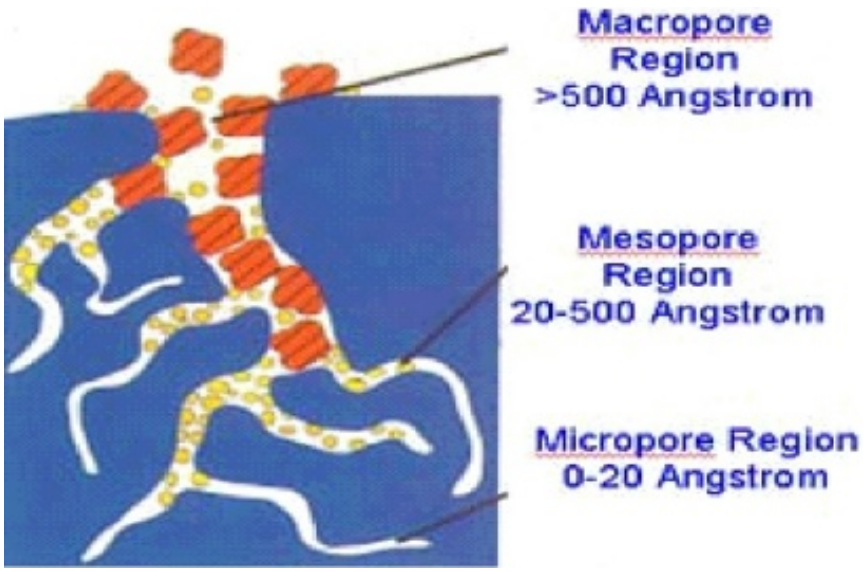

Figure 3.1 Micropore, Mesopore and Macropore Regions of Activated Carbon

Figure 3.1 shows micro, meso and macropore regions of activated carbon. In the following sections of this chapter, the main theory and methods involved in these characterization tests are given.

3.2. Gas Adsorption Phenomena and Standard Isotherms

When a gas (adsorbate) is confined in a closed space in the presence of an outgassed solid (adsorbent), an adsorption process begins. The gas molecules are transferred and accumulated on and in the solid material as a result of the forces between the solid surface and the adsorbate. Physical adsorption includes attractive dispersion forces, repulsive forces, at very short distances well as the contribution from the polarization and electrostatic forces between the permanent electric moment and the electric field of the solid. The amount adsorbed on a solid surface will depend upon the temperature, pressure and the interaction potential between the vapor and the surface. Therefore, at some equilibrium pressure and temperature, a plot of weight of gas adsorbed per unit weight of adsorbent versus relative pressure (P/P_0) is referred as the sorption isotherm of a particular vapor-solid interface.

Brunauer et al. (1940), based upon an extensive literature survey, found that most of the adsorption isotherms fit into one of the five types shown in Figure 3.2. Type I isotherm indicates a microporous adsorbent. Type II isotherms are most frequently encountered when adsorption occurs on nonporous powders or on powders with pore diameters larger than micropores. The inflection point of the isotherm usually occurs near the completion of the first adsorbed monolayer and with increasing relative pressure, second and higher layers are completed until at saturation the number of adsorbed layers becomes infinite.

Type III isotherms are observed when the adsorbate interaction with an adsorbed layer is greater than the interaction with the adsorbent surface. Type IV isotherms occur on porous adsorbents possessing pores mainly in the mesopore range. The slope increases at higher pressures as it is true for the Type II, the knee generally occurs near the completion of the first monolayer. Type V isotherms result from small adsorbate-adsorbent interaction potentials similar to the Type III isotherms. However, they are also associated with the

pores in the same range as those of the Type IV isotherms. A new rare type of isotherm, Type VI recently has been found which exhibits a series of steps (Şenel, 1994).

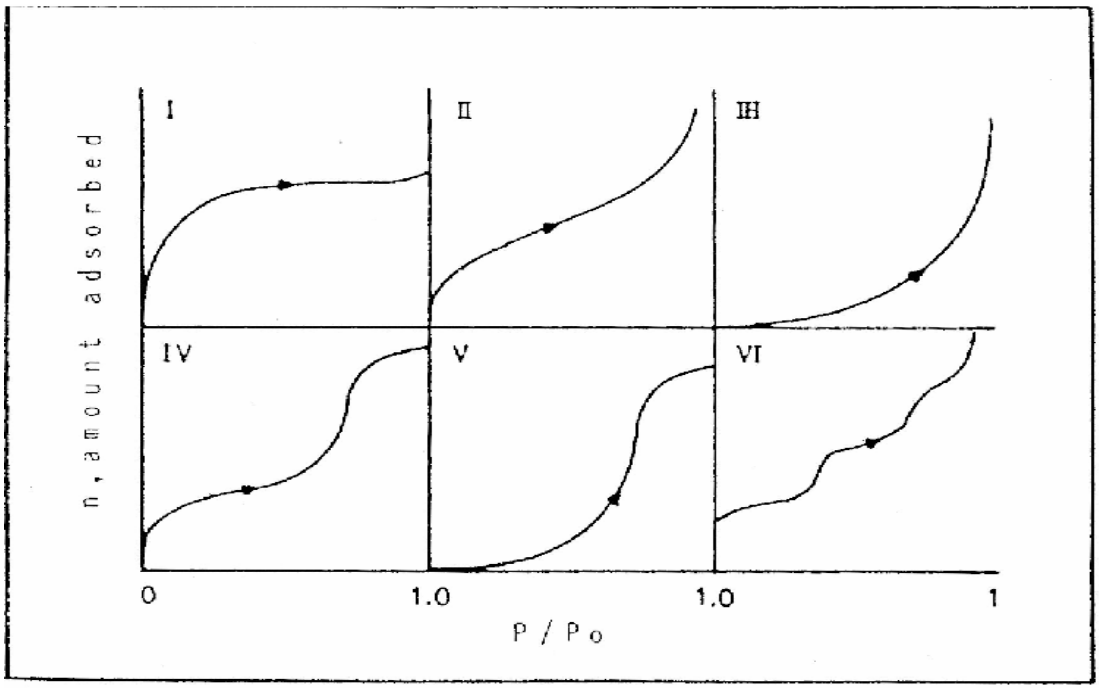

Figure 3.2 Schematic Representations of Different Types of Adsorption Isotherm

3.2.1. The Brunauer, Emmett and Teller (BET) Theory

Although derived over sixty years ago, the BET theory continues to be almost universally used because of its simplicity, and its ability to accommodate each of the five isotherm types. The BET model extends the monolayer Langmuir model to multilayer adsorption. It assumes that the surface is homogeneous and that

the different layers of molecules do not interact. Each adsorbed molecule in the monolayer is assumed to be adsorption site for second layer of molecules, and so on as the relative pressure increases, until bulk condensation occurs.

In the region of relative pressures near the completion of monolayer, the BET theory and experimental isotherms do agree very well leading to a powerful and extremely useful method for the estimation of surface areas of various materials including activated carbon, coal and coal chars. In the final form it is given as;

$$\frac{P}{V\left[P_O - P\right]} = \frac{1}{V_m C} + \frac{C - 1}{V_m C}\frac{P}{P_O} \qquad (3.1)$$

where; 'V" and 'V_m" are the volume adsorbed, at the relative equilibrium pressure P/Po, and the monolayer capacity respectively, "C" is a constant, which is related exponentially to the heat of adsorption at the first and subsequent layers by the equation:

$$C = \exp\left[(q_1 - q_2)/RT\right] \qquad (3.2)$$

where; "q_1" is the heat of adsorption of the first layer, "q_2", is the heat of adsorption of the second and subsequent layers. The determination of surface areas from the BET theory is a straightforward application of equation (3.1). A plot of P/V(P-Po) versus P/Po, will yield a straight line usually in the range of 0.05 < P/Po < 0.35. The slope "S" and the intercept of "I" of a BET plot will give

$$S = \frac{\left[C - 1\right]}{V_m C} \quad \text{and} \quad I = \frac{1}{V_m C} \qquad (3.3)$$

Solving the preceding equations for "V_m" and "C" gives;

$$V_m = \frac{1}{S} + I \quad \text{and} \quad C = S + \frac{1}{I} \qquad (3.4)$$

The BET equation usually gives a good representation of the frequently appearing Type II and IV isotherms within the range of relative pressures 0.05-0.3, and this range is generally used in practice for measurement of the surface area. At higher relative pressures, the BET equation is usually inaccurate because of capillary condensation effect, while at P/Po values below about 0.05, the amount of adsorbed gas is too small to be measured with sufficient accuracy. A poorer description is obtained for the type I, III and V isotherms, but in practice, they too are often analyzed by the BET method. In order to calculate the surface area, it is necessary to know the mean cross-sectional area A_m occupied by one molecule of adsorbate gas. The specific surface area is calculated from the equation,

$$S_{BET} = \frac{V_m N_A A_m}{V_{mol}} \tag{3.5}$$

in which; "V_m" is volume of monolayer, "N_A" is the Avagadro's constant and V_{mol} is the molar volume of the gas. The cross-sectional area of any adsorbed gas molecule can be estimated from the density of the condensed phase of the gas.

For surface area determinations, nitrogen as being the ideal adsorbate, exhibits the unusual property that on almost all surfaces its "C" value is sufficiently small to prevent localized adsorption and yet adequately large to prevent the adsorbed layer from behaving as a two dimensional gas. Thus, the unique properties of nitrogen have led to its acceptance as a universal, standard adsorbate with an assigned cross sectional area of 0.162 nm^2 at its boiling point of -195.6°C (Şenel, 1994). Using BET it is possible to measure pores down to 10 Å.

3.2.2. Pore Characterization by Adsorption / Desorption

Another way to get information on the porous texture of the adsorbent is to look at the shape of the desorption isotherm. It is commonly found for porous solids

that the adsorption and desorption branches are not coincident over the whole pressure range. At relative pressures above 0.3, De Boer (1958) has identified five types of hysteresis loops, which are correlated with various pore shapes; Figure 3.3 shows idealization of the four types of hysteresis (Gregg and Sing, 1982).

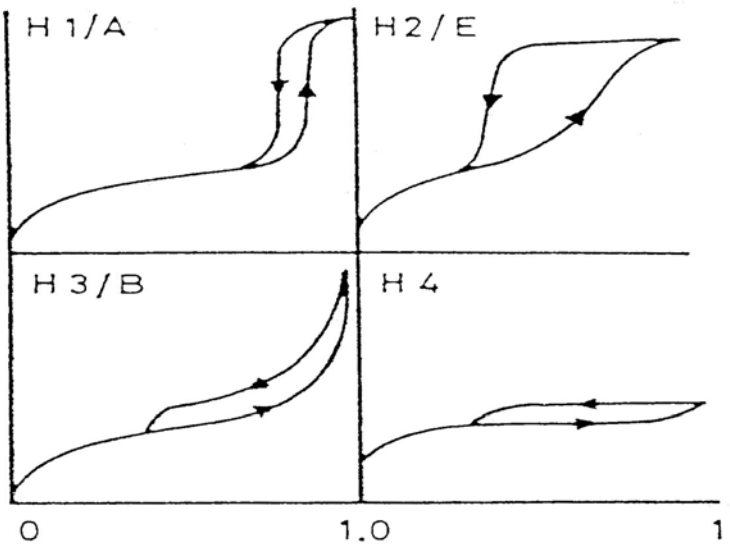

Figure 3.3 Types of Adsorption-Desorption Hysteresis Loops

Type I hysteresis is often associated with capillary condensation in open-ended cylindrical-shaped pores. The formation of a cylindrical meniscus occurs at a higher P/Po than the emptying process, which proceeds through the evaporation from a hemispherical meniscus. Type II corresponds to spheroidal cavities or voids as well as to "ink- bottle" pores. The liquid trapped in the body of the pore until P/Po is reduced to allow evaporation from the neck; therefore, the release of condensate is limited by the neck radius. Type III hysteresis exhibits no limiting adsorption at P/Po = 1 and is indicative of slit shaped pores. Type IV hysteresis is associated with Type I isotherms, that is with microporous

adsorbents. The hysteresis part of the isotherms contains information about the mesopores. There is a relationship between shape and position of the isotherm and the pore geometry, due to condensation and evaporation phenomena. These can be described by Kelvin's capillary condensation equation (Gregg and Sing, 1967) as;

$$r_P = \frac{-2\sigma V_{mol} Cos\ \theta}{RT \ln [P / P_o]} \quad (3.6)$$

where, "r_p" is the mean radius of the liquid meniscus, "σ" is the surface tension, "R" is the gas constant ,"T" is the absolute temperature, "(θ)" is the angle of contact between the condensed phase and the surface of the solid. In finding the pore radius by the Kelvin equation it is necessary to take into consideration the thickness "t" of the adsorbate layer. Then, the actual pore radius "r_p" is given by,

$$r_p = r_k + t \quad (3.7)$$

The term "r_k" indicates the radius into which condensation occurs at the required relative pressure. This radius, called the Kelvin radius or the critical radius, is not the actual pore radius since some adsorption has already occurred on the pore wall prior to condensation, leaving a center core or radius, r_k. Alternatively, during desorption, an adsorbed film remains on the pore wall when evaporation of the center core takes place. Halsey (1948) set up a useful analytical expression for the thickness of the layer "t" as a function of the relative pressure,

$$t = t_m \left[\frac{5}{\ln (P / P_o)} \right]^{1/3} \quad (3.8)$$

Here, "t_m" is the thickness of the monolayer. Thus, replacing equation (3.6) and (3.8) into (3.7) for nitrogen as the adsorbate at its normal boiling point of -195.6^{o}C, with "t_m" as 0.354 nm, the equation:

$$r_P = \frac{4.15}{\log\left(P_O / P\right)} + 3.54\left[\frac{5}{2.303\ \log\left(P_O / P\right)}\right] \qquad (3.9)$$

is obtained. Here, a closely packed hexagonal liquid structure is assumed for the nitrogen molecules. The question of whether or not the adsorption or desorption branch is better suited for calculation of the mesopore size has not yet been answered definitely. For a symmetrical pore geometry, calculation of the size distribution of the mesopores from the adsorption or desorption data permits a simple determination of the mesopore surface area. The gas volumes adsorbed or desorbed upon a change of the relative pressure are taken from the isotherms, and Equation (3.9) is used to calculate the corresponding mesopore radius. Assuming certain pore geometry, the contribution to the surface area from the pores of various sizes can be found from the pore radius distribution.

Stepwise computational methods for finding the pore radius distribution and the mesopore surface area and volume are described by several investigators (Orr, 1959; Broekhoff, 1970). One computational method (BJH), proposed by Barrett, Joyner and Halenda (1951), is frequently used in practice. Derivations of the related equations are given in Appendix A. 1.

3.2.3. Characterization of Microporosity

Adsorption on microporous solids is not very well understood in comparison with that on non-porous or mesoporous solids. Pore sizes of similar order of magnitude as the sizes of the adsorbate molecules lead neither to the progressive completion of a monolayer nor to multilayer adsorption but to the filling up of the micropore volume with the adsorbate in a liquid-like condition. A major development in understanding adsorption of gases and vapors on microporous carbons was provided by the potential theory of adsorption of Polanyi (1932).

Potential theory assumes that at the adsorbent surface the molecules of gases are compressed by attractive forces acting between the surface and the molecules and these forces of attraction decrease with increasing distance from the surface. Polanyi described the adsorption space as a series of equipotential surfaces, each with the adsorption potential E_i, and each enclosing a volume W_i. As one moves away from the surface the values of adsorption potential decrease until it falls to zero and the adsorption space increases up to a limiting value Wo (zero potential). At the surface, W=O and $E_i=E_{max}$. The building up of the volume enclosed within the adsorption space may be described by the function of the type E = f(W).

Polanyi assumed that since dispersion and electrostatic forces are independent of temperature, the adsorption potential at constant volume filling is also temperature independent. This means that the curve E = f(W) should be the same for a given gas and a given adsorbent at all temperatures. This relationship between "E" and "*W*" is called the characteristic curve. Polanyi expressed the adsorption potential for volume filling as the amount of work necessary to compress the adsorbate from its equilibrium vapor pressure P_1 to the compressed adsorbate pressure, P_2.

$$E = \int_{P_1}^{P_2} \frac{RT}{P} dP = RT \ln \frac{P_2}{P_1} \qquad (3.10)$$

Thus, "E" is equal to the ΔG "equivalent free energy change". The state of the compressed adsorbate in the adsorption space depends on the temperature. Polanyi distinguished three different cases. (i) when the temperature is well below the critical temperature of the adsorbate, T_c, the adsorbed vapor may be considered as liquid-like. (ii) when the temperature is just below the T_C most of the adsorbate will be as liquid like but also the adsorbate may be as compressed gas. (iii) when the temperature is above the T_c, the adsorbate will be as compressed gas. The first case is, by far, the most common one. Therefore the adsorption potential will take the form in Equation 3.11.

$$E = RT \ln \frac{P_O}{P} \quad (3.11)$$

In this equation it is assumed that the liquefied adsorbate is incompressible and has the normal density of the liquid at the given adsorption temperature, then it is possible to obtain the volume filled adsorption space by Equation 3.12.

$$W = \frac{nM}{\rho} = nV_{mol} \quad (3.12)$$

where, "n" is the amount adsorbed in moles, "M" is the molecular weight of the adsorbate and ″ρ″ is the liquid density. The temperature-invariance of the adsorption potential which is the fundamental postulate of the Polanyi's theory, has been demonstrated (1966), mainly by Dubinin and co-workers and they have added a second postulate. They stated that for an identical degree of filling of the volume of adsorption space, the ratio of adsorption potentials for any two vapors is constant which is called the affinity coefficient, *″β″.* Dubinin's treatment has been modified by Kaganer to yield a method for calculation of specific surface from the isotherm. Using the experimental data and assuming that pore size distribution is Gaussian, Dubinin and Radushkevich, arrived at an expression which is known as "Dubinin Radushkevich", (D-R) equation;

$$\log W = \log W_O - D \log^2 \left(\frac{P_O}{P} \right) \quad (3.13)$$

where D is 2.303 K (RT / β)^2. A plot of log W against log (Po/P) will be a straight line having an intercept equal to micropore volume, "W_o". Dubinin and Astakhov, assuming a Weibull distribution of pore sizes, rather than a Gaussian, obtained the following "Dubinin - Astakhov, (D-A)" equation;

$$\log W = \log W_O - D' \log^n \left(\frac{P_O}{P} \right) \quad (3.14)$$

where $D' = 2.303^{(n-1)} (RT/E)^n$. It follows from the equation (3.14), that "DR" equation is a special case of "D-A" equation (3.13), when n=2 (Şenel, 1994).

3.3. True Density Determinations

True density of a porous solid is defined as the ratio of the mass to the volume occupied by that mass. Therefore, contribution to the volume made by pores or internal voids must be excluded when measuring the true density. To determine the true density of a solid, one needs to have a non interacting fluid which completely fills all the pores. In reality, no fluid completely fills the pore volume of activated carbons. Therefore, the term, true density should be treated in this way.

Helium is the smallest molecule available with an atomic diameter of 1.7Å. Therefore, it has the best chance of penetrating the entire porosity of activated carbon.

Figure 3.4 depicts a block-diagram of the overall experimental approach. The physical characterization of activated carbon samples were characterized according to this scheme.

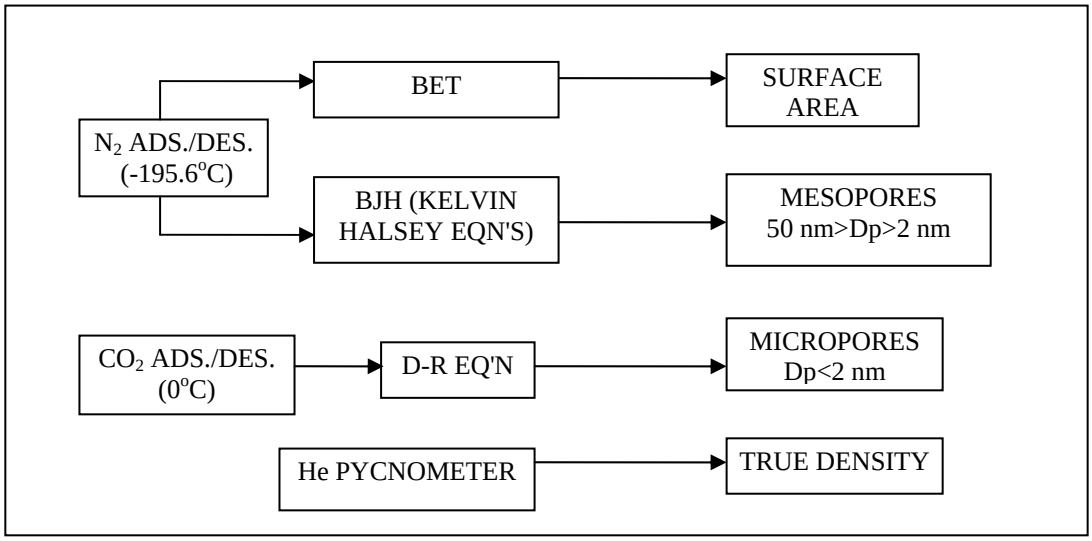

Figure 3.4 Block-Diagram of the Overall Experimental Approach

CHAPTER IV

PREVIOUS WORK ON PREPARATION OF ACTIVATED CARBON

Activated carbon is one of the most commonly used adsorbents in many different liquid- and gas-phase applications in the industry for its adsorptive properties. In this study, production of activated carbon from hazelnut shell and hazelnut husk and the quality of the products have been investigated.

As lignocellulosic materials are heated in an inert atmosphere, they decompose to various pyrolysis products. Depending on their volatility, these products can be grouped into three classes; chars, gases and tars. Char is a carbon-rich nonvolatile solid residue, usually constituting approximately 15-20 percent yield. Gas phase products include all lower molecular weight products (CO, CO_2, CH_4, H_2, etc.) including water. Usually gas phase products constitute 20-25 percent of the total products of pyrolysis. Tars are any of several high molecular weight products that are volatile at carbonization temperatures but condense onto any surface near room temperature. Tar comprises approximately 60-65 percent of the products (Schwenker and Pascu, 1957; Roberts, 1970; Agrawal and Mc Cluskey 1983). Any one of the pyrolysis products could be the most desirable product. Most commercial scale pyrolysis plants are designed to have only one class as the principal product with at least one of the other classes serving as a fuel source. For manufacture of activated carbon, the char is the desirable product.

Pyrolysis of lignocellulosic materials such as shells or stones of fruits etc. is extremely complex. The major components, lignin, cellulose and hemicellulose mainly react independently and the pyrolysis of the lignocellulosic materials is the result of hundreds of cocurrent and consecutive reactions. In order to

investigate mechanism of pyrolysis, it is better to study pyrolysis of each component separately. Cellulose is the major components of plant cells and hemicelluloses have approximately the similar molecular structure with cellulose. So investigation of cellulose pyrolysis mechanism gives an idea about the pyrolysis of lignin and hemicellulose (Balci, 1992).

Pyrolysis of pure cellulose has been widely studied. During heating in an inert atmosphere, molecular bonds will be broken. Since C-O bonds are weaker than the C-C bonds the principal candidates for scission are the 1,4 C-O-C glucosidic and the 1,5 C-O-C acetal linkages in the cellulose macromolecule. The breakage of 1,4 glucosidic bonds results in depolymerization of cellulose and is responsible for the formation of tars. As discussed by Agrawal (1988 a,b) the breakage of 1,5 acetal bonds leads to ring opening and results in formation of gases and chars.

The influence of the experimental conditions such as temperature, heating rate, residence time at high temperature can be interpreted in terms of competition between these two types of cellulose degradation. At temperatures below about 300^{o}C, the ring opening reaction is favored over depolymerization. Higher heating rates cause temperatures favorable to depolymerization to be reached more quickly, and hence give higher tar yield. Trace amount of impurities are thought to catalyze the ring opening reactions. (Agrawal and Mc Cluskey, 1983)

The production of activated carbon is a typical gas-solid reaction. The adsorptive capacities of activated carbon are mainly associated with its internal pore properties such as pore surface area, pore volume and pore size distribution, which develop during the activation of chars (Balcı, 1992).

4.1. Chemical Activation

Aygün et al. (2003) produced activated carbon from almond shell, hazelnut shell, walnut shell and apricot stone through chemical activation using $ZnCl_2$ (30wt. %)

as the activating agent. Highest surface area of activated carbons from the almond shell, hazelnut shell and walnut shell were found with 10 h activation at 750 °C but for apricot stones it was obtained with 18 h activation at 800 °C. Activated carbon from the hazelnut shells had the highest surface area (793 m^2/g) and iodine number (965 mg/g). Iodine molecule gives information on the surface area contributed by pores larger than 10 Å. The order of suitability of raw materials for activated carbon production was established as hazelnut shell > walnut shell ≈ apricot stone > almond shell.

Lozano-Castello et al. (2001) produced activated carbons from Spanish anthracite by using KOH. In this study the activation agent/coal ratio was found to be the most important parameter in a chemical activation process. As activation agent/coal ratio increases micropore volume and surface area increases reaching a maximum ratio of 4:1 giving micropore volume of 1.45 cc/g and a BET surface area of 3290 m^2/g. The higher the temperature and the time of pyrolysis, the higher the micropore volume. In other words, the lower the heating rate during the pyrolysis process, the higher the microporosity development. Also, it was concluded that an acid washing after carbonization could be avoided because the results were not very different from those obtained with water washing. In a next study they used NaOH to produce activated carbon from Spanish anthracite. Nitrogen flow and the activating agent/coal ratio were found to be the most important parameters to achieve the best development of porosity. The highest result was obtained for 960 ml/min nitrogen flow rate and activating agent/coal ratio of 3:1 at 730 °C as BET surface area of 2669 m^2/g, V-DR N_2 as 1.04 cc/g and V-DR CO_2 as 0.64 cc/g. It was concluded that physical mixing of NaOH and coal rendered the best results.

Balcı et al. (1994) carbonized ammonium chloride-impregnated and untreated almond shell and hazelnut shell samples in a flow of nitrogen at relatively low temperatures. It was observed that, chemical activation carried out at 350°C gave products with surface area values above 500 m^2/g. However, the surface area values observed for the products obtained from untreated raw materials were about half of this value. It was also observed that, the surface area of

products obtained from NH_4Cl-impregnated samples reached values of over 700 m^2/g when the carbonization temperature was increased to 700°C.

Girgis et al. (1998) carbonized phosphoric acid impregnated apricot stones at 300, 400 and 500°C. For impregnation, a ratio of acid volume: weight of raw precursor of 1.5/1 was employed and it was observed that, as the temperature increased the BET surface area increased from 700 m^2/g up to 1400 m^2/g. In this study, they used 20%, 30%, 40% and 50% phosphoric acid by weight. The highest BET surface area was obtained from the sample which was impregnated with 30% phosphoric acid and carbonized at 500°C.

Girgis et al. (2002) obtained activated carbon from date pits by using phosphoric acid. The raw material was impregnated with increasing concentrations of H_3PO_4 (30-70 wt. %) followed by pyrolysis at 300, 500 or 700 °C. Carbons obtained at 300 °C were very poorly porous, although with high capacity for the uptake of probe molecules from solution. Carbons obtained at 500 and 700 °C were found to be good to excellent adsorbents. The best porosity development was found at 700 °C with 50 wt. % H_3PO_4 impregnated sample having 945 m^2/g of BET surface area.

Demirbaş et al. (2002) studied the removal of Ni(II) from aqueous solution by adsorption onto hazelnut shell activated carbon. Activated carbons were obtained by impregnation of the raw material with concentrated H_2SO_4 and activation in a hot air oven at 150 °C for 24 h. Activated carbons used in the batch mode adsorption studies had a BET surface area of 441 m^2/g. It was suggested that adsorption data of hazelnut shell based activated carbons fitted best to the Langmuir adsorption isotherm. Adsorption increased with increasing temperature, pH and agitation speed, and decreasing particle size.

Cimino et al. (2000) studied on removal of toxic cations and Cr(VI) from aqueous solution by hazelnut shell as biosorbent substrate. Activated hazelnut shells were prepared by using H_2SO_4 as the activating agent and drying in an air oven at 40 °C for 2 h. Hazelnut shell showed a good efficiency in removing from aqueous solution toxic ions such as three and hexavalent chromium, cadmium

and zinc. Based on the Langmuir isotherm model, at pH_{adj} 4.0 for Cd^{2+}, Cr^{3+} and Zn^{2+} ions the maximum sorption capacities were 5.42, 3.08 and 1.78 g Kg^{-1}, respectively. For hexavalent chromium removal pH interval is 2.5-3.5 and the maximum sorption capacity at pH_{adj} 2.0 is 17.7 g Kg^{-1}.

Toles et al. (1997) prepared activated carbon from almond and pecan shells, which were hard, lignocellulosic precursors for the production of granular activated carbon (GACs) in order to create carbons for the adsorption of both organic compounds and metals. They activated samples either chemically, with H_3PO_4, or physically, with CO_2, under a variety of conditions followed by oxidation at 300 ºC for 4 hours. Chemically produced activated carbons had BET surface areas between 955-1267 m^2/g while surface areas of physically produced activated carbons were in the range of 104-485 m^2/g. Total yield was obtained as 33-41% for chemical activation and 7-22 for physical activation of the raw materials.

Bevla et al. (1984 a,b) produced activated carbon from almond shells through chemical activation. Among several activating agents (H_3PO_4, $ZnCl_2$, K_2CO_3 and Na_2CO_3), $ZnCl_2$ activation gave the best products with high adsorption capacities. Raw material particle size, activation time and impregnation ratio were studied, showing the impregnation ratio to be the most effective variable in increasing the adsorptive power of the products up to 2111 m^2/g. It was observed that, activating reagent recovery and adsorptive capacity increased as the raw material particle size decreased. A maximum adsorption capacity had been observed at 500 ^oC.

Hu et al. (2001) prepared activated carbons from $ZnCl_2$ impregnated coconut shells by pyrolysis under nitrogen flow until temperature reached 800 ^oC, and then switching the gas flow to carbon dioxide. Activating agent/shell ratio (w/w) was between 0.25 and 3. The BET surface area increased with increasing ratio of $ZnCl_2$ to shell from 0.25 to 2 and reached a maximum of 2450 m^2/g. It was indicated that as the activating agent/shell ratio was higher than 2, many micropores were enlarged to mesopores. Also, CO_2 flow resulted in larger mesopore and total pore volumes especially for long-time activated samples.

Ahmedna et al. (2000) produced activated carbon from rice straw, rice hulls, sugarcane bagasse and pecan shells. Rice straw, rice hulls and sugarcane bagasse based activated carbons were obtained by activating with a mixture of nitrogen and carbon dioxide at 900 ^{o}C after the pyrolysis at 750 ^{o}C. Pecan shell based activated carbons were produced by both physical and chemical activation methods. In chemical activation of pecan shells 25% and 50% H_3PO_4 solutions were used as activating agent. Carbonization of pecan shells was performed at 450 ^{o}C under the flow of nitrogen, air or a mixture of both. Chemically activated pecan shells found to have higher surface area values (1200 m^2/g) than physically activated ones. Also, sugarcane bagasse showed a better potential than rice straw or rice hulls as precursor of granular activated carbons with the desirable properties of a sugar decolorizing carbon.

4.2. Physical Activation

Solano et al. (1980) produced activated carbon from direct activation of almond shells with CO_2 or air, or by activation after carbonization under nitrogen atmosphere. It was observed that, direct activation with carbon dioxide in the temperature range of 750^{o}C and 900^{o}C gave activated carbons with similar or larger surface area and micropore volumes than those obtained by carbonization followed by activation. The products obtained by the activation of air in the temperature range from 300 to 400^{o}C, did not show large surface areas. It was also observed that, at low temperatures direct activation with air developed meso and macroporosity to a larger extent than the activation which was preceded by carbonization. However, the reverse case was observed for the high temperature products. The products had surface areas ranging from 150 m^2/g to about 2000 $m^2/$ g for different degrees of burn off and types of production.

Toles et al. (2000) prepared a series of steam or CO_2 activated carbons made from almond shells using six different activation or activation/oxidation methods. They compared the carbons to each other and to two commercial carbons in an effort to ascertain the relative value of the carbons in terms of yield, surface

area, attrition, surface functional groups, organic uptake, metal uptake, as well as estimated cost of production. Of the six methods investigated, the method that produced the best overall performing almond shell carbon and least expensive carbon in terms of production cost was the "Air-Activation" method. This method involved the simultaneous activation and oxidation of almond shells under an air atmosphere.

Arol et al. (2002) tested activated carbons made of hazelnut shells, apricot and peach stones to determine their suitability for gold metallurgy. The raw materials were carbonized under a flow of nitrogen at 650 ^{o}C and then activated with steam at 800 or 900 ^{o}C. Peach stone was found to result in hardest carbon and hazelnut shell the weakest. In terms of BET surface area, peach stones had the largest surface area of 923 m^2/g followed by apricot stones (850 m^2/g) and hazelnut shells (825 m^2/g). It was concluded that active carbons produced from apricot and peach stone can be employed in the recovery of gold from gold cyanide bearing solutions.

Rodriguez-Reinoso et al. (1982) prepared activated carbons from almond shells by means of carbonization in a flow of nitrogen at 750-900 ^{o}C, followed by activation in a flow of carbon dioxide at 650-800 ^{o}C. Activation with carbon dioxide led to the appearance of micropores and to a considerable increase in surface area. The highest BET surface area (adsorption at 77 K) was obtained as 1597 m^2/g for the material carbonized at 850 ^{o}C and activated at 825 ^{o}C for 24 h with 5 ^{o}C/min heating rate.

Yun et al. (2001) investigated the pre-carbonization effect on the porosity development in activated carbons. Two types of activated carbons were manufactured from rice straws, by the one-stage and two-stage processes, respectively. Carbonization was performed at 700, 800 and 900 ^{o}C under nitrogen flow and samples were activated at the same temperatures in CO_2 for 3 h. In pre-carbonization step the raw material was heated until the temperature reached 900 ^{o}C under nitrogen flow and kept at that temperature for 1 h. It was found that the inclusion of pre-carbonization process contributed to the formation of activated carbons with higher values of the BET surface area and

microporosity than those of activated carbons without pre-carbonization. It was found that 800 ^{o}C, 3 h were the optimum activation conditions within the experimental range, resulting in (790 m^2/g).

Wartelle et al. (2000) used macadamia nut shells, hazelnut shells and black walnut shells as the precursors for activated carbon production. Carbonization of raw materials was done at 700-750 ^{o}C under nitrogen flow. Activation was performed at 800 ^{o}C in a mixture of CO_2-N_2 or at 850 ^{o}C with steam. BET surface areas of the products were found as 583, 572 and 829 m^2/g for macadamia nut shells, hazelnut shells and black walnut shells, respectively. A gas chromatographic analysis revealed that macadamia nut shell granular activated carbons seem to be an excellent adsorbent for polar and non-polar compounds from C_3 and C_6-C_{10} tested.

Reinoso et al. (1985) prepared activated carbons from plum and peach stones by carbonization followed by carbon dioxide activation with activation time ranging from 8 hours to 16 hours. The adsorption of N_2, CO_2, i-butane, paranitrophenol and methylene blue had been studied to investigate the microporosity. N_2 adsorption studies gave the micropore volumes ranging from 0.27 cm^3/g to 0.77 cm^3/g for products from plum stones and 0.23 cm^3/g to 0.38 cm^3/g for those obtained from peach stones for various production methods and conditions. Porosimeter results showed that, macro and meso porosities were more developed in carbons prepared from plum stones. Direct activation led to development of these two ranges of porosity, especially macro porosity to larger extents.

Sanchez et al. (2001) prepared three series of activated carbons from *Quercus agrifolia* wood using a two-step process, carbonization followed by physical activation with CO_2. They characterized samples by N_2 and CO_2 adsorption. They used three activation temperatures, 800, 840 and 880^{o}C, covering the 18-85 wt % yield range by variation of residence time. They obtained activated carbons with a well-developed porous structure, predominantly microporous with high BET surface areas. They found no direct relationship between exposed BET surface areas (the surface where activation reaction takes place), evolution and

gasification rate variation. They produced activated carbons with BET surface areas in the range of 400-1200 m^2/g.

Baçaoui et al. (2001) prepared a series of activated carbons from olive-waste cakes by physical activation with steam. They carried out adsorption of N_2 (-195.6°C), CO_2 (0°C) and mercury porosimetry experiments to determine the characteristics of all carbons prepared. They found experimental response varying between: 13–27% for the total yield, 115–490 mg/g for the adsorption of methylene blue, 741–1495 mg/g for the adsorption of iodine, 514–1271 m^2/g for the BET surface area, 0.225–0.377 cm^3/g for the micropore volume, 0.217-0.557 cm^3/g for the volume of pores with a diameter greater than 3.7 nm and 31.3–132 m^2/g for the external surface area. They exploited the results obtained using response surface methodology. They represented these responses and studied in all experimental regions of activation time and activation temperature, the most influential factors in activated carbon preparation. They obtained the optimal activated carbon when using 68 min as activation time and 822°C as activation temperature.

CHAPTER V

EXPERIMENTAL WORK

The main aim of this study was to produce activated carbon from agricultural wastes; hazelnut shell and hazelnut husk and to characterize these products. Chemical activation method was applied by using phosphoric acid as the activating agent. A summary of the experimental procedure is shown in Figure 5.1.

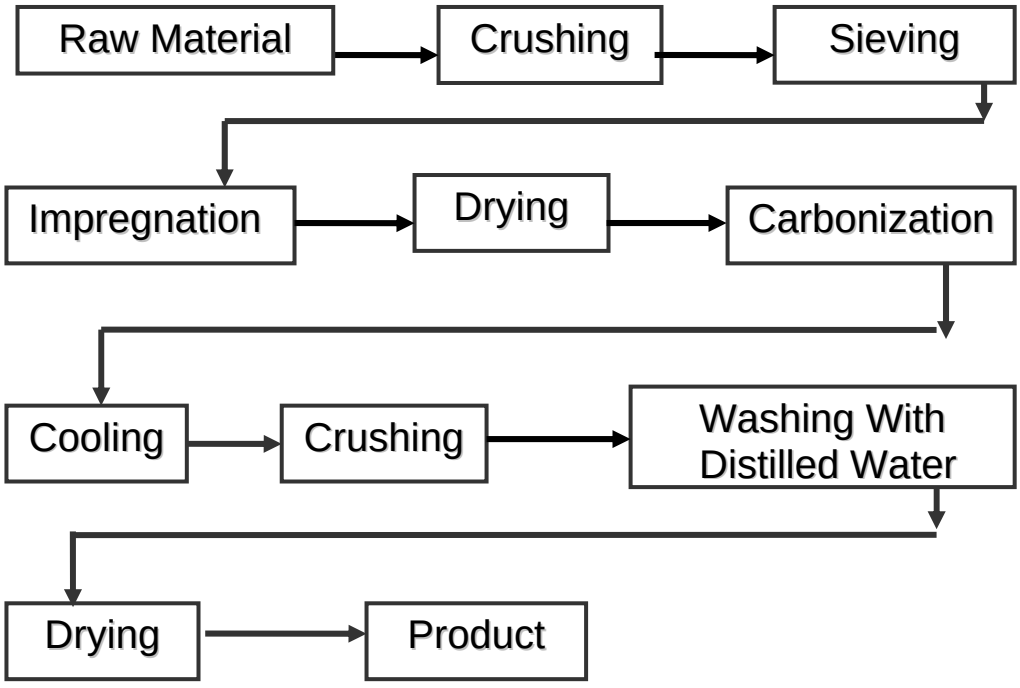

Figure 5.1 Procedure Followed in Experiments

5.1. Properties and Preparation of Raw Materials

5.1.1. Properties of Raw Materials

Hazelnut shells and hazelnut husks used throughout the experiments were obtained from Trabzon and Giresun, respectively.

Elemental analysis of raw materials and activated carbons were carried out using a "Leco CHN Elemental Analyzer". Ash contents of the products were determined by Thermogravimetric Analyzer (TGA) and ash contents of the raw materials were determined by following TS 6879 (Turkish Standards Institution (TSE)). The chemical compositions of raw materials are given in Table 5.1. Ash content of raw hazelnut shell is surprisingly low compared to the husk. Also, in the literature raw materials generally have ash content of 3-5 %. This low ash content might be a specific property for hazelnut shell. Aygün et al. and Balci et al. also reported ash content of hazelnut shell as 0.49% and 1.33%, respectively.

Table 5.1 Chemical Composition of Raw Materials

Raw materials	C% (wt.)	H% (wt.)	N% (wt.)	O %(wt.) (by difference)	Ash% (wt.)
Hazelnut Shell	49.4	6.3	0.3	43.6	0.4
Hazelnut Husk	42.7	5.2	0.9	45.4	5.8

5.1.2. Preparation of Raw Materials

Raw materials were dried at room temperature. Hazelnut shells were crushed by a home blender and hazelnut husks were ground by a laboratory type grinding machine. The resulting particles were sieved and the hazelnut shell particles having sizes 12-18 mesh (1-1.7 mm) and hazelnut husk particles having sizes 20-50 mesh (0.3-0.8 mm) were used in the rest of the experimental work. In the literature particle sizes of raw materials used in activated carbon production is generally in the range of 0.2-2 mm. The choice of using smaller particle size for hazelnut husks is because of heterogeneous physical structure of the material. To have uniform size of hazelnut husk, grinding was required.

Through the experiments the effect of activating agent concentration was investigated. So, raw materials with the desired particle sizes were treated with 60%, 50%, 40% and 30% (wt.) H_3PO_4 solutions separately at 25^oC for 24 hours. As a proportion, in the impregnation of hazelnut shells 1 g. shell was mixed with 2 ml acid solution while 1 g. of hazelnut husk was mixed with 5 ml of acid solution. The reason for choosing these amounts of acid volumes was to obtain homogenous mixtures of raw materials and acid solutions, and allow all particles contact with the acid.

After impregnation, solution was filtered to remove the residual acid. Subsequently, the impregnated samples were air dried at room temperature for 3 days. The ratio of weight of dried samples (impregnated) to the weight of raw material before the impregnation step indicates the weight increase. After this procedure, the dried samples were ready for the carbonization experiments. In Table 5.2, the impregnation ratios and weight increases of the raw materials are given.

Table 5.2 Impregnation Ratios and Weight Increases of the Raw Materials

Raw material	H_3PO_4 conc. (wt. %)	Impregnation ratio (acid : raw material) (w : w)	Weight inc. %
Hazelnut Shell (2 ml acid: 1 g shell)	30	2.32	21
	40	2.50	23
	50	2.66	35
	60	2.82	40
Hazelnut Husk (5 ml acid: 1 g husk)	30	5.80	133
	40	6.25	212
	50	6.65	275
	60	7.05	348

5.2. Carbonization Experiments

5.2.1. Experimental Set-Up

Carbonization experiments were carried out in a horizontal "Lenton Unit C2" furnace. To ensure the inert atmosphere in the furnace by N_2 gas flow, a 20 mm inside (24 mm outside) diameter quartz tube of 90 cm length was placed horizontally into the furnace. The inlet and the outlet of quartz tube were connected with quartz fittings, to avoid the escape of N_2 from the system and to avoid the entrance of air to the system.

To measure the N_2 flow rate passing through the system a N_2 flow meter was connected to inlet of furnace. A bubbler in a cooling bath was used at the outlet of the system to cool the outlet gases and to indicate the N_2 flow by bubbling. After cooling, the outlet gases were purged to the hood by a heat resistant hose. Experimental set up used in the experiments is shown in Figure 5.2.

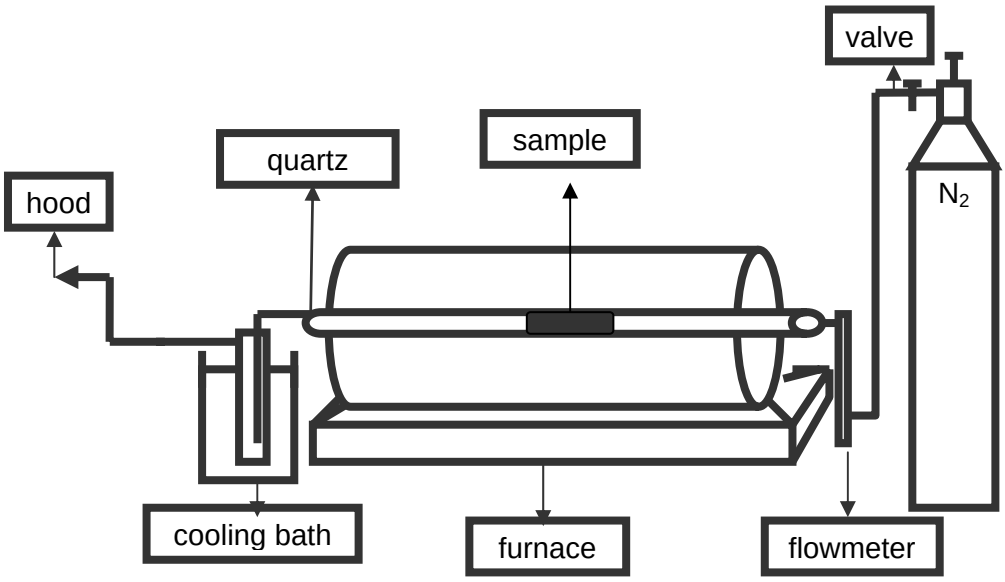

Figure 5.2 Experimental Set-up

5.2.2. Chemical Activation of Samples

In this study, the effect of activating agent concentration and carbonization temperature, on the properties of the products was investigated. For this purpose, raw materials, impregnated with 30%, 40%, 50% and 60% (wt.) H_3PO_4 solutions were carbonized for 2 hours at carbonization temperatures of 300, 400, and 500 ºC.

Activation of phosphoric acid impregnated raw materials was carried out by carbonizing the materials under nitrogen flow (200 cc/min or 64 cm/min) at a heating rate of 20°C/min. In the literature high nitrogen velocities (30 cm/min) were recommended. A faster removal of the gases evolved during carbonization process favors the creation of micropores or, in other words, a lower concentration of these gases produces higher micropore development

(Lozano-Castello, 2001). Samples were placed in the furnace and the N_2 flow started to purge the air in the quartz tube, and continued for 30 minutes. After purging, the furnace was started to heat till the chosen carbonization temperature was achieved, and the temperature was kept constant by the temperature controller of the furnace. Carbonization time was measured from the point when the selected temperature was reached. After 2 hours of carbonization time, the furnace was cooled using a hair dryer. Lastly, when the temperature of furnace decreased down to 100°C, product was taken to a flask and distilled water was added to prevent interaction with the air. Experimental conditions and samples codes are given in Table 5.3 and Table 5.4 for hazelnut shell and hazelnut husk, respectively.

Table 5.3 Experimental Conditions and Sample Codes for Hazelnut Shell

Fixed Parameters		Variable Parameters		
Particle size	12-18 mesh	H_3PO_4 conc. (wt.%)	Carbonization Temp. (ºC)	Sample Code
N_2 flow rate	200 cc/min (velocity: 63 cm/min)	30	300	HS 30.3
			400	HS 30.4
			500	HS 30.5
Heating Rate	20 ºC/min	40	300	HS 40.3
			400	HS 40.4
			500	HS 40.5
Carbonization Time	2 hours	50	300	HS 50.3
			400	HS 50.4
			500	HS 50.5
Mixing Proportion	2:1 (ml acid : g. shell)	60	300	HS 60.3
			400	HS 60.4
			500	HS 60.5

Table 5.4 Experimental Conditions and Sample Codes for Hazelnut Husk

Fixed Parameters		Variable Parameters		
Particle size	20-50 mesh	H_3PO_4 conc. (wt.%)	Carbonization Temp. ºC	Sample Code
N_2 flow rate	200 cc/min (velocity: 63 cm/min)	30	400	HH 30.4
Heating Rate	20 ºC/min	40	400	HH 40.4
Carbonization Time	2 hours	50	400	HH 50.4
Mixing Proportion	5:1 (ml acid : g. husk)	60	300 400 500	HH 60.3 HH 60.4 HH 60.5

5.3 Characterization of the Products

Before the characterization, products were crushed by a mortar in distilled water to obtain smaller particles and rinsed with boiling distilled water until the pH values of the activated carbons reached to 5-6. Decreasing particle size of the products before washing step, results in higher removal of the acid and more effectively opening of pores filled by tarry substances. Suspension pH values of the activated carbons were determined by following TS 5896 (Turkish Standards Institution (TSE)).

Prior to making all characterization tests, the samples were oven dried at 110^{o}C overnight under vacuum. Through the characterization of the products, the effect of activating agent concentration and carbonization temperature to the pore structure, total surface area and true densities of the samples were examined.

5.3.1. Nitrogen Gas Adsorption Measurements

A commercial volumetric gas adsorption apparatus "ASAP 2000", Accelerated Surface Area and Porosimetry System manufactured by Micromeritics Co., USA was used to measure the surface area and to determine the pore size distributions of mesopores using N_2 adsorption data at -195.6°C. Analysis of the micropores was also determined by this unit by CO_2 adsorption at 0°C, the details of which are explained in the following section. Schematic diagram of this apparatus is given in Figure 5.3 (Yağşi, 2004).

To measure the mesopore surface area and the mesopore volume of the samples nitrogen gas adsorption and desorption isotherms were obtained at -195.6°C. For each experimental point, an equilibration time of about 30 minutes was allowed. The cross sectional area of the nitrogen molecule was taken as 0.162 nm^2 (Şenel, 1994). Surface area of the samples was determined by using BET equation. The area and the volumes of the pores as well as their distributions were evaluated from the nitrogen adsorption isotherms using the Barrett, Joyner and Halenda (BJH) method (as indicated in section 3.2.2), (Barrett et al., 1951) considering the IUPAC mesopore range definition which ranges from 50 nm down to 2 nm in terms of the pore diameters of the cylindrical pores.

5.3.2. CO_2 Gas Adsorption Measurements

The micropore volume of the samples was estimated by application of the Dubinin-Radushkevich equation to carbon dioxide adsorption at 0°C. The data were automatically collected and evaluated by using the software/ computer system. A minimum of 30 minutes was allowed for equilibrium to be established at each point of the CO_2 isotherm. Micropore surface area of the samples were calculated from the DR micropore volume, taking the cross sectional area and the density of a CO_2 molecule as 0.17 nm^2 and 1.181 g/cm^3, respectively. The

saturation vapor pressure was taken as 26142.000 mmHg at the analysis temperature of 0^{o}C (Micromeritics ASAP 2000, User Manual, Appendix C, 1993).

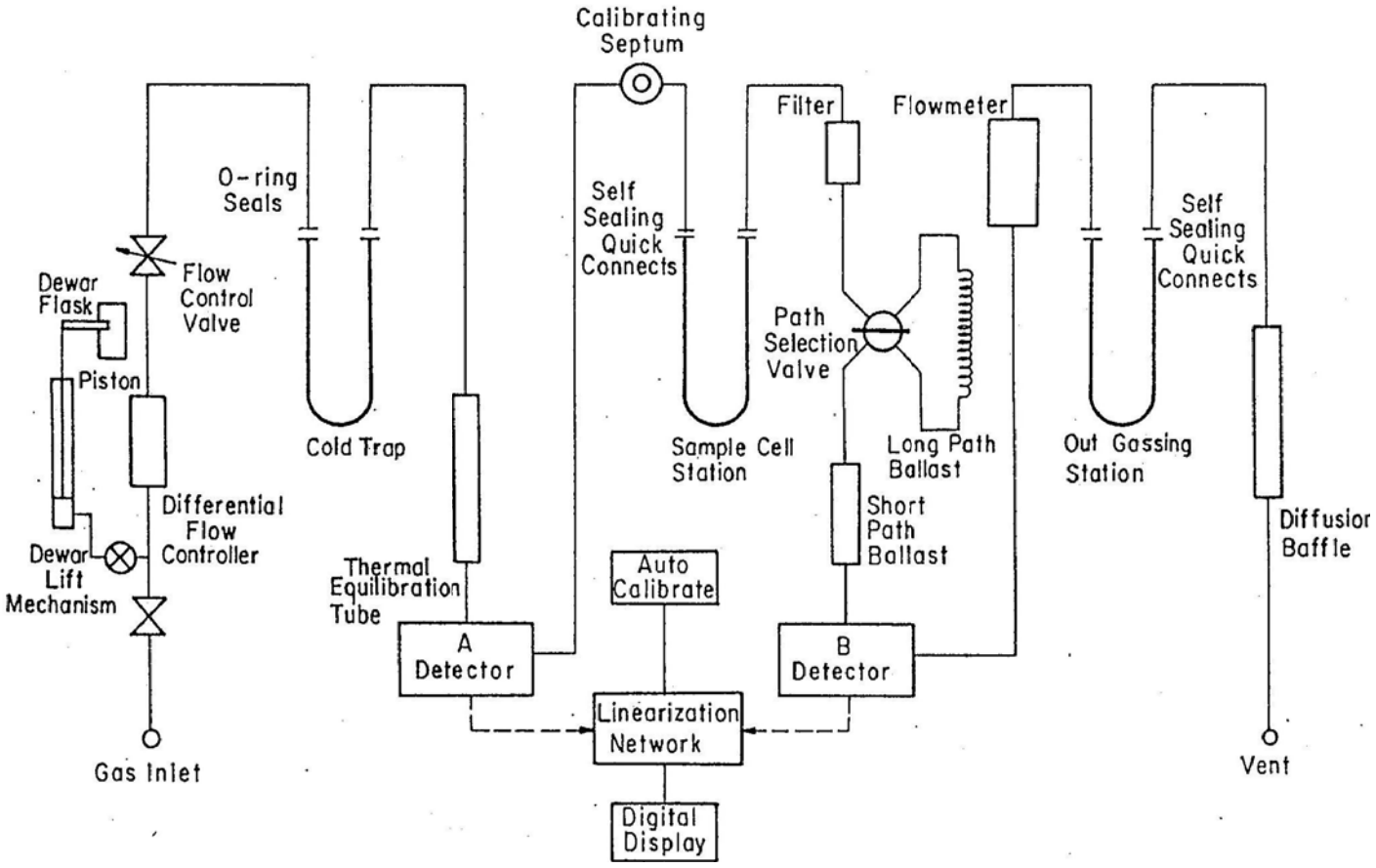

Figure 5.3 Schematic Representation of Surface Analyzer

5.3.3. True Density Determinations

True (Helium) densities of samples were determined by using a commercial Pycnometer. The He Pycnometer instrument is consisted essentially of a sample-holding vessel, a cylinder fitted with a movable piston, the relative position of which is indicated on the front panel dial to five decimal places and a pressure detector. A dial light reveals whether the pressure in the system is the same as that in the detector.

In a typical run, 0.1-0.2 g degassed sample was placed into a propylene cup and then, both were evacuated in the pycnometer chamber for a sufficient time. After filling the system with helium, chamber was opened to atmosphere by means of a 4 position valve. By this way, enough helium is allowed to escape into the system in order to reduce the pressure in the system to the atmospheric reference pressure.

After some time, the valve was turned to gauge position for sealing the helium in the system at atmospheric reference pressure. Once the valve is in gauge position, the variable volume chamber, sample chamber and pressure detector are connected and sealed off as a closed system. When the variable volume is changed so as to decrease the volume of the system, the pressure increase to the point where contact is broken between the bellows of the pressure detector and an electric contact in the detector. This indicates where the reading should be taken. After obtaining three values; for empty cup, for standard volume and for sample as "V_{CELL}", "V_{EXP}" and "V_{SAMP}" values, respectively, true density of the sample was determined using the known weight of sample according to procedure given in Appendix C.

CHAPTER VI

RESULTS AND DISCUSSION

6.1 Preliminary Experiments

At the beginning of the experimental work the plan was to obtain activated carbons from hazelnut husk by physical activation with steam and from hazelnut shell by chemical activation using potassium hydroxide as the activating agent.

In the physical activation of hazelnut husk, carbonization temperature was 400 ºC and activation temperatures were 400, 600 and 800 ºC. BET surface area results showed that samples activated at 400 and 600 ºC had very low surface areas (2-5 m^2/g). The reason for this result could be the choice of lower activating temperatures with respect to the literature values (900 ºC, steam). But, it was also observed that the sample was not resistant to 800 ºC activation temperature, resulting in only 13% yield. A comparison was made with hazelnut shell in order to have an idea on applicability of hazelnut husk in activated carbon production. Physical activation with steam was applied to hazelnut shell using the same parameters with hazelnut husk experiments (400 ºC carbonization, 600 ºC activation temperatures). BET surface area results showed that, under the same conditions with hazelnut husk, hazelnut shell gave higher surface areas (313- 334 m^2/g) with respect to hazelnut husk. These preliminary results led to the conclusion that hazelnut husk was not a proper precursor for activated carbon production by physical activation with steam.

For the production of activated carbon from hazelnut shell, potassium hydroxide (KOH) was tried as the activating agent. Solid KOH was dissolved in 10 ml distilled water and shells were mixed with these solutions in the shell/KOH ratio of 1:1 and 2:1. But, it was observed that gas evolved during carbonization was very dense and the system pressure became unstable. This was attributed to either blockage of the quartz tube or dragging of the sample in the tube. So, the experiments of KOH impregnated samples could not be completed and no product was obtained. Changes in experimental parameters like, gas flow rate, carbonization temperature, input weight of raw material did not solve this problem, the reason probably being the incompatibility of KOH with the structure of hazelnut shell. KOH might have changed the structure of the raw material during impregnation in such a way that the layers of carbon matrix collapsed when carbonization started and the material became nonporous and sticky; resulting in the failure of the experiment.

Since no product could be obtained by using potassium hydroxide as the activating agent, another chemical, phosphoric acid, was tried in the impregnation step for hazelnut shell. 60 wt. % H_3PO_4 solution was mixed with hazelnut shells in the ratio of 2 ml acid: 1 g shell. At carbonization temperature of 400 ºC and under 200 cc/min N_2 flow rate, six experiments were performed. BET surface areas of the products were obtained by using N_2 adsorption data. Surface area results were around 380-420 m^2/g., the average of which was 398.5 m^2/g. For these data the standard deviation was found as 16.3, which was 4% of the average of BET surface areas, showing that the experiments were reproducible. On the other hand, at the same temperature but 130 cc/min gas flow rate, exactly under the same experimental conditions, two activated carbon samples were obtained having BET surface areas of 399 and 512 m^2/g. It was noticed that, this difference in BET surface areas was because of the difference in the amount of raw material placed in the tube. In the production of the activated carbon having 399 m^2/g of BET surface area, 18 gram of raw material was used, while for the production of the sample having 512 m^2/g of BET surface area 6 gram of raw material was used. The less the input weights of the raw material, the higher the surface area of the products. When the sample in the tube was not loose, the tarry substances formed during carbonization might

cover the reaction surface of the material and lower the reaction rate. The rest of the experiments were performed by placing 6-7 grams of impregnated hazelnut shells in the furnace. When phosphoric acid impregnation was applied to hazelnut husks, even higher surface area activated carbons were obtained.

The objective of this study was to investigate the pore structures and surface areas of activated carbons produced from hazelnut shell and hazelnut husk at relatively low temperatures (300, 400 and 500^{o}C) and for different H_3PO_4 concentrations (30%, 40%, 50% and 60% wt.). The pore structure of the activated carbons was characterized by different physical techniques; nitrogen adsorption at -195.6^{o}C and carbon dioxide adsorption at 0^{o}C. By using helium pycnometry true densities of the products were obtained.

In terms of chemical characterization, the analyses were limited to the determination of C, H, N, O elements and ash analysis; to provide information on elemental composition. Under identical experimental conditions, TGA experiments were carried out to supply information in terms of yields of acid impregnated samples.

6.2. Physical Characterization of the Products

The physical characterization of the products was carried out according to the experimental procedures given in Figure 3.4. The samples were characterized by determination of solid (true) density, mesopore area, micropore area, mesopore volume, micropore volume and surface area. BET (N_2) surface area measurement, Helium pycnometry and D-R method (CO_2) were used to determine these values.

6.2.1. Results Based on Nitrogen Gas Adsorption

The nitrogen adsorption measurements of the products include the determination of the (i) BET surface area, (ii) volume of mesopores, and (iii) cumulative surface area of mesopores.

i. Hazelnut Shell Based Activated Carbons

BET surface area values of hazelnut shell based activated carbons are shown in the Figure 6.1. Samples impregnated with 30% H_3PO_4 solution (HS 30.3, HS 30.4, and HS 30.5) had very low values of surface area. Moreover, samples carbonized at 300 ºC gave relatively low results. Sample HS 60.4, which was impregnated with 60% H_3PO_4 and carbonized at 400 ºC, had the highest BET area, 596 m^2/g. In Figure 6.2 the effect of carbonization temperature and phosphoric acid concentration to BET surface areas can be seen more clearly.

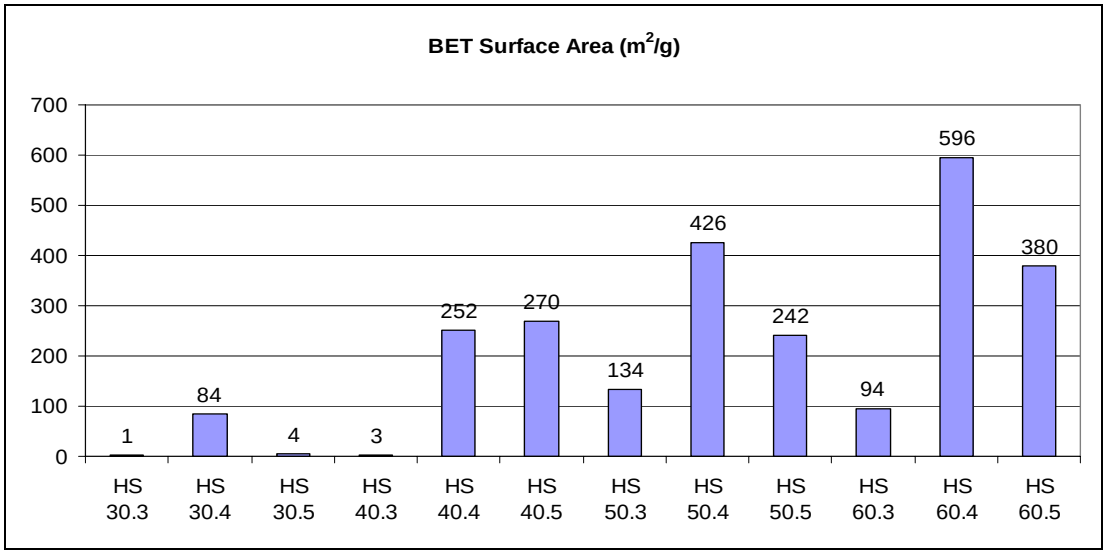

Figure 6.1 BET Surface Areas of Hazelnut Shell Based Samples

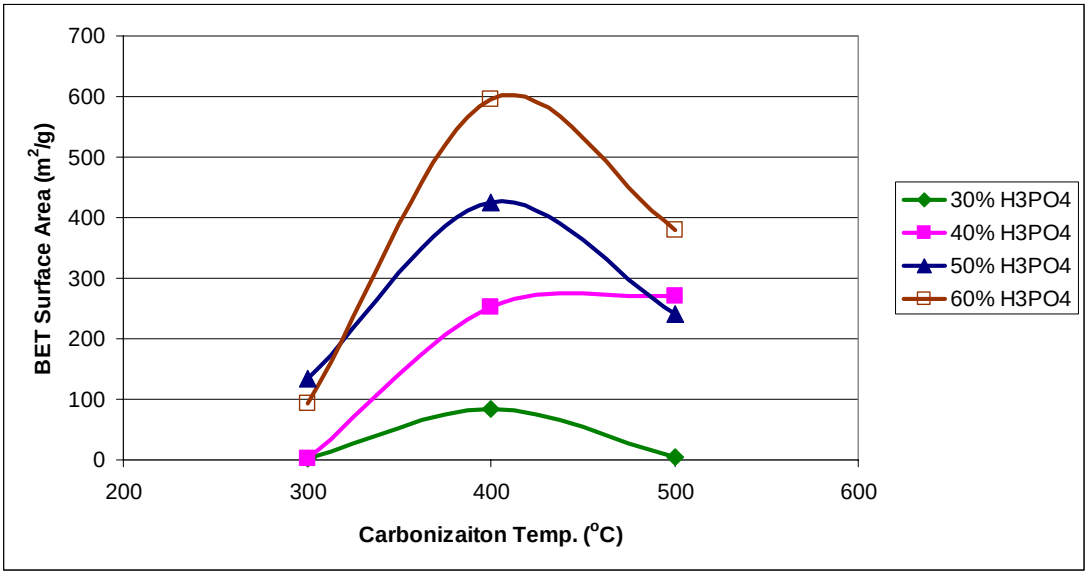

Figure 6.2 BET Surface Areas of Hazelnut Shell Based Samples

As the H_3PO_4 concentration increased, BET surface area values increased. In the literature the impregnation ratio generally shows a maximum point. So, using higher concentrations of phosphoric acid in impregnation can result in higher BET surface areas but probably reaches a maximum, then tends to decrease. In the literature it was shown that in chemical activation there are two different mechanisms: the first one is the micropore formation which starts with the addition of chemicals to the raw materials and the second one is the pore widening which is the result of the chemical effect inside the opened pores. Pore widening normally begins when there are a number of opened pores in the structure; therefore, it becomes significant when the impregnation ratio is reasonably high (Lozano-Castello, 2001). So, to some extent, increasing the impregnation ratio results in mainly formation of micropores and higher surface areas but higher impregnation ratios can result in widening of micropores and formation of meso- and macropores giving lower surface areas.

In Figure 6.2 the appropriate carbonization temperature can be seen to be 400 ºC. 300 ºC was not enough for the formation of pores and obtaining

acceptable areas. Increasing the carbonization temperature to 500 ºC resulted in relatively lower surface areas. In the literature at lower temperatures the ring opening reaction is said to be favored over depolymerization. Ring opening results in formation of char, which is the desirable product in our case. At 500 ºC depolymerization can be favored resulting in the formation of tarry substances hence lower surface areas.

Six activated carbons, which had the highest BET surface areas among twelve hazelnut shell based products, were chosen and other characterization methods were applied. In Figure 6.3 the BJH mesopore areas of the selected products were shown. Activated carbons produced at 500 ºC had lower mesopore areas then the ones carbonized at 400 ºC. Also, as acid concentration increased mesopore areas increased.

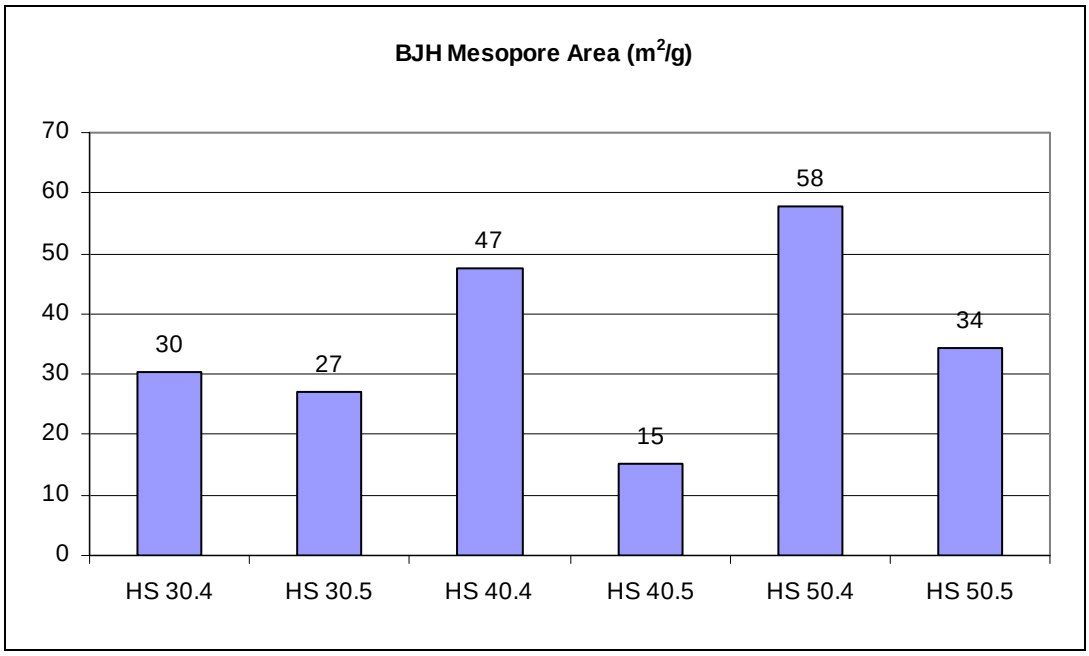

Figure 6.3 BJH Mesopore Areas of Hazelnut Shell Based Samples

Mesopore areas of the samples are in the range of 15 to 58 m^2/g. For all samples mesopore areas are around 9-12 % of the BET surface areas. As it is shown in the Figure 6.4 mesopore volumes of the samples are in the range of 0.009-0.037 cm^3/g. Mesopore volume values are directly related with the mesopore area values.

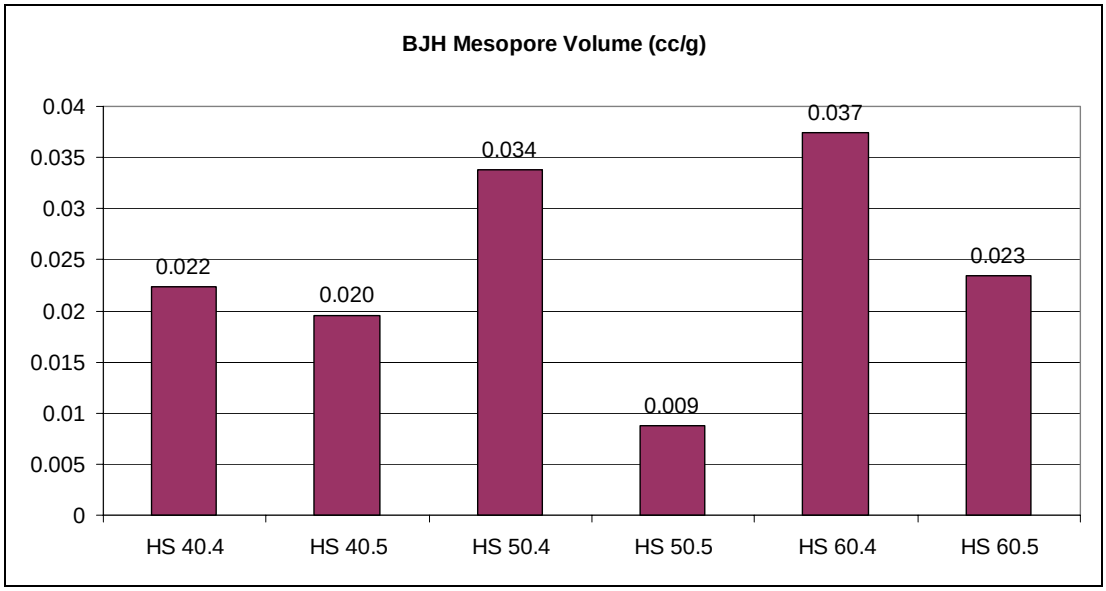

Figure 6.4 Mesopore Volumes of Hazelnut Shell Based Samples

Figures 6.5 shows the N_2 adsorption / desorption isotherms of the samples. Isotherm shapes in the literature which were originally defined by Brunauer et al. (1943) and classified into 6 well-known groups, (as it is shown in Figure 3.2) one may say that all products show similar isotherms to the type I. According to Brunauer, this type of isotherm is observed in the case of microporous solids. As discussed in section 3.2.2, another way of obtaining information on the porous texture of the solids is to compare the shape of the hysteresis loop (Figure 3.3) with the shape of adsorption and desorption branches of the standard shapes which were originally classified by De Boer (1958). But, as it is shown in the

isotherm figures of the samples, there is no distinct hysteresis loops at adsorption / desorption isotherms.

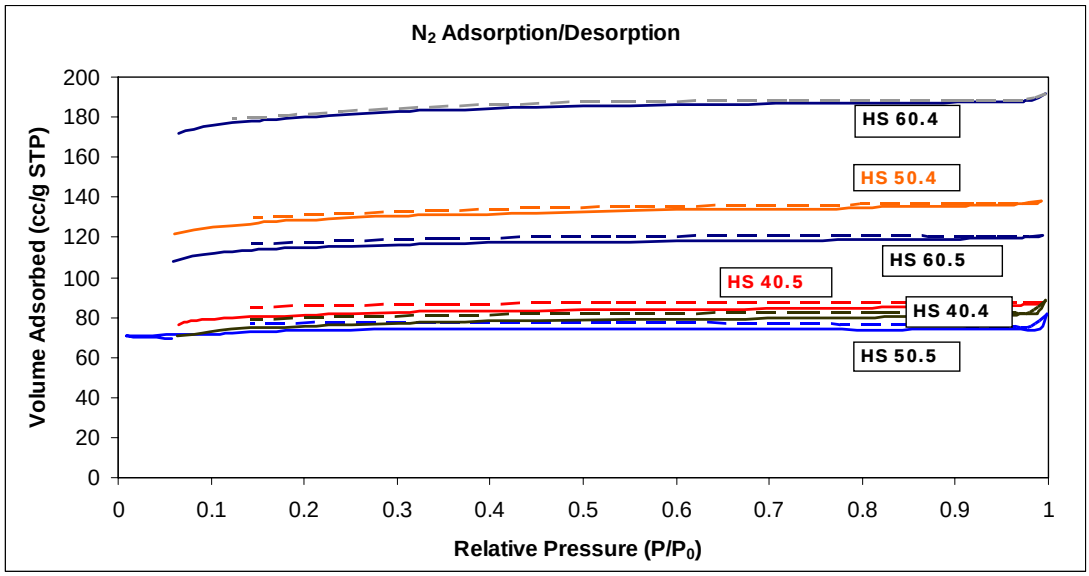

Figure 6.5 N_2 Adsorption/Desorption Isotherms of Hazelnut Shell Based Carbons

ii. Hazelnut Husk Based Activated Carbons

In Figure 6.6 BET surface areas of hazelnut husk based activated carbons are shown. HH 60.3 sample, impregnated with 60% H_3PO_4 solution and carbonized at 300 ºC, had the lowest surface area 705 m^2/g. The highest BET surface area was obtained for the sample impregnated with 40% H_3PO_4 solution and carbonized at 400 ºC as 1565 m^2/g (HH 40.4). In Figure 6.8 the appropriate carbonization temperature was seen as 400 ºC for 60 wt.% H_3PO_4 treatment. Similar to hazelnut shell results, carbonization at 300 ºC and 500 ºC resulted in lower surface areas. But, when compared to the values of hazelnut shell based products, hazelnut husk gave much higher values. (Figure 6.7)

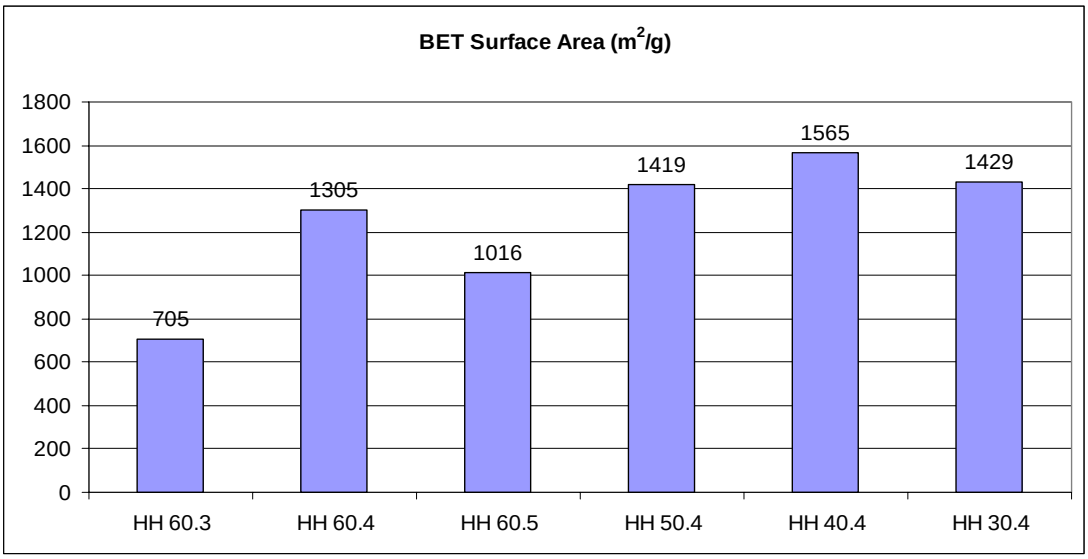

Figure 6.6 BET Surface Areas of Hazelnut Husk Based Products

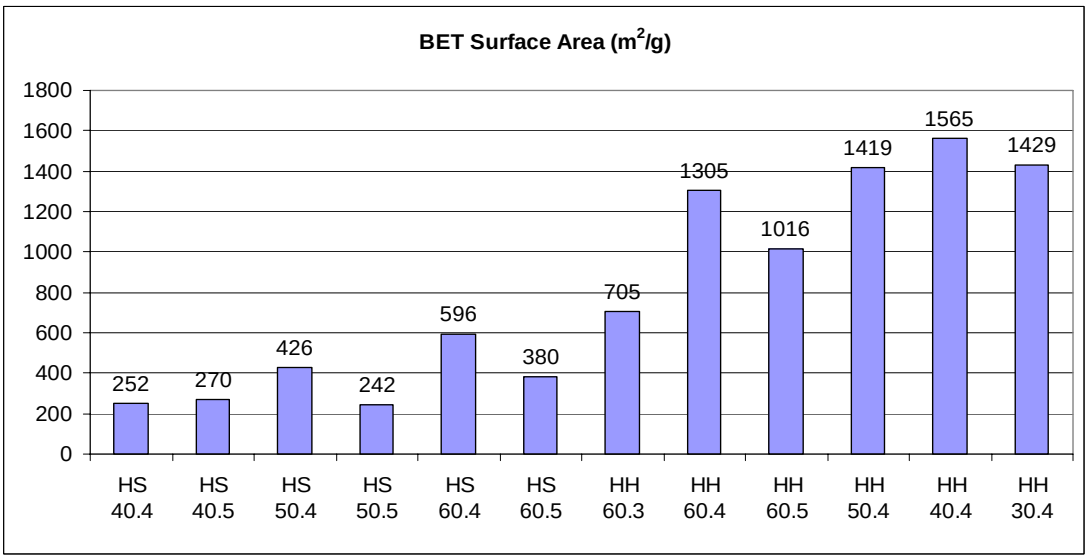

Figure 6.7 Comparison of BET Surface Areas of HS and HH Based Products

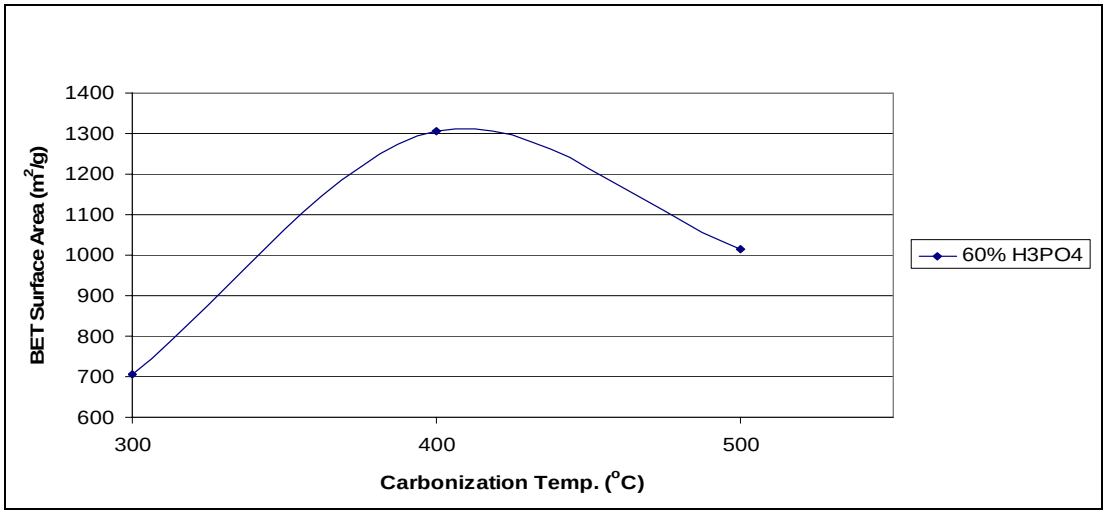

Figure 6.8 BET Surface Areas of Hazelnut Husk Samples Impregnated with 60% H_3PO_4 solution.

In Figure 6.9, the effect of acid concentration to BET surface areas of the samples carbonized at 400 ºC was shown. As discussed earlier for hazelnut shell based carbons, BET surface area showed a maximum for 40% H_3PO_4 impregnated product and decreased as the acid concentration increased.

BJH mesopores areas of the products are shown in Figure 6.10. Mesopore areas of the samples are in the range of 302-1042 m^2/g. For samples HH 60.3 and HH 30.4 the mesopores areas correspond to 43% and 49% of BET surface areas, respectively. For the other samples mesopore areas are around 62-82% of the BET surface areas.

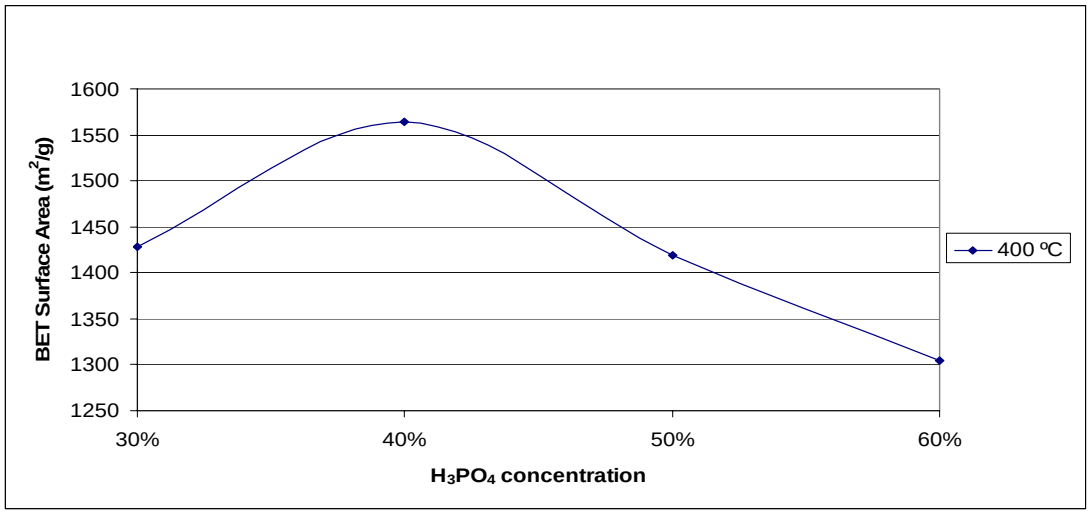

Figure 6.9 BET Surface Areas of Hazelnut Husk Samples at Carbonization Temperature of 400 ºC.

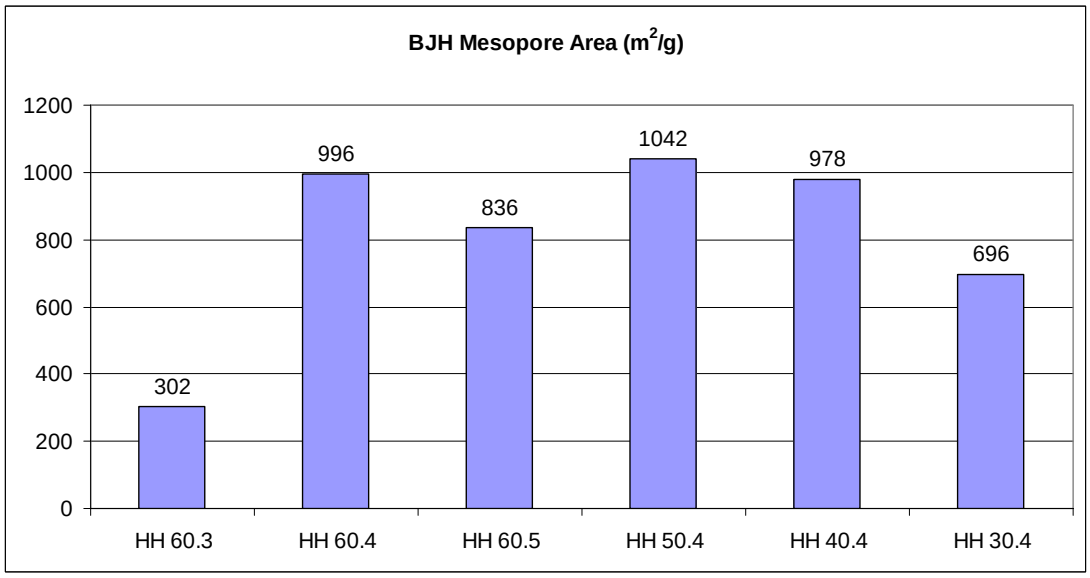

Figure 6.10 BJH Mesopore Areas of Hazelnut Husk Based Samples

As it is shown in Figure 6.11, mesopore volumes of the samples are in the range of 0.22-1.01 cc/g. For the samples impregnated with 60% H_3PO_4 solution, higher carbonization temperatures resulted in higher mesoporosity. Among the samples carbonized at 400 ºC, the product impregnated with 50% H_3PO_4 solution gave the highest mesopore area and volume (1042 m^2/g and 1.01 cc/g). As the acid concentration decreased to 40% and 30 % mesopore area and volume decreased.

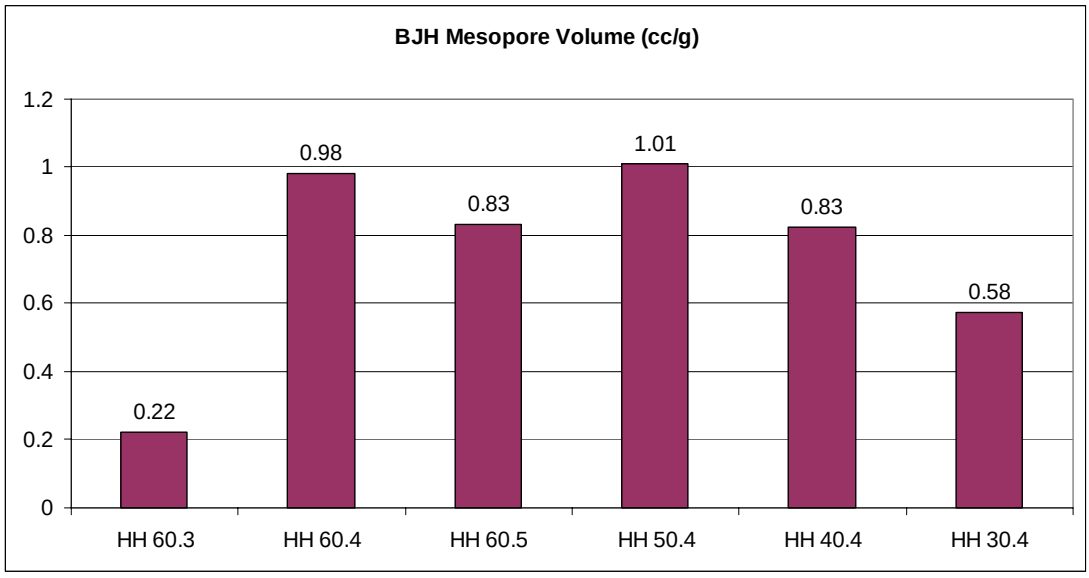

Figure 6.11 BJH Mesopore Volumes of Hazelnut Husk Based Samples

Figures 6.12 and 6.13 show the N_2 adsorption/desorption isotherms of hazelnut husk based activated carbons. Sample HH 60.3 which has the lowest BET area, mesopore area and volume seem to be mainly microporous (Type I isotherm) when the adsorption/desorption isotherm is considered. The isotherms of the other products indicate that they are mainly mesoporous materials (Type II isotherm). Also, type III hysteresis loops of the products, except that of HH 60.3, show that they have slit-shaped pores.

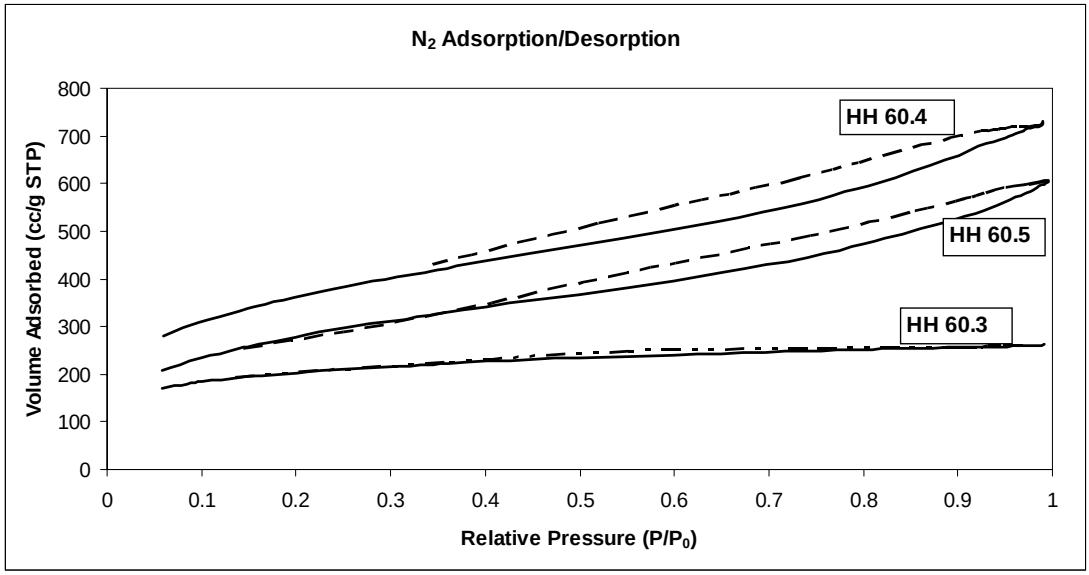

Figure 6.12 N_2 Adsorption/Desorption Isotherms of 60% H_3PO_4 Impregnated Hazelnut Husk Samples.

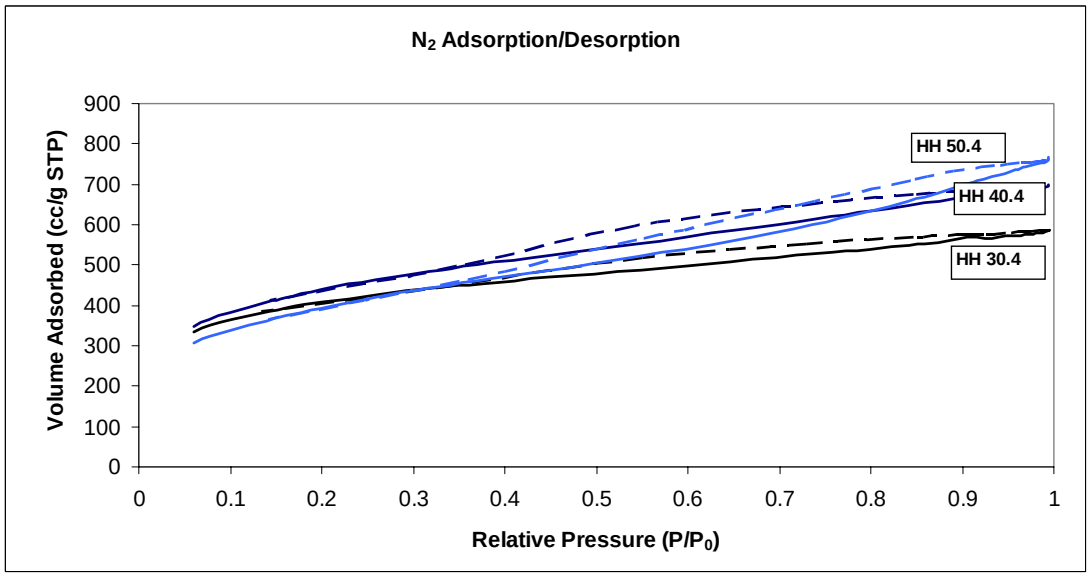

Figure 6.13 N_2 Adsorption/Desorption Isotherms of Hazelnut Husk Samples Impregnated with 30, 40 and 50% H_3PO_4 and Carbonized at 400 ºC.

6.2.2. Carbon Dioxide Gas Adsorption Results

i. Hazelnut Shell Based Activated Carbons

Micropore analysis of the samples was carried out by CO_2 adsorption studies as described in section 5.3.2. This method was applied because CO_2 adsorption at 0^oC is widely used in literature for reporting the micropore volume and the surface area of the activated carbons. For this purpose, the micropore volumes were calculated from intercept of the volume of CO_2 adsorbed, versus $(P/P_o)^2$ in log-log plot, using the Dubinin-Radushkevich (D-R) equation.

Micropore area values of the samples are shown in the Figure 6.14. Similar to BET area, the highest micropore area, 576 m^2/g, was obtained from the HS 60.4 sample. The lowest micropore area 433 m^2/g, was obtained from the HS 40.4 sample. Also, similar to BET area, increase in acid concentration impregnated, resulted in higher micropore areas. As carbonization temperature increased, micropore area decreased for samples impregnated with 50% and 60% acid whereas micropore area increased for 40% acid impregnated samples.

Micropore volumes of the samples are shown in Figure 6.15. Micropore volume values are in the range of 0.15-0.24 cc/g. As it is shown in the figure, micropore volume graph is similar to micropore area graph.

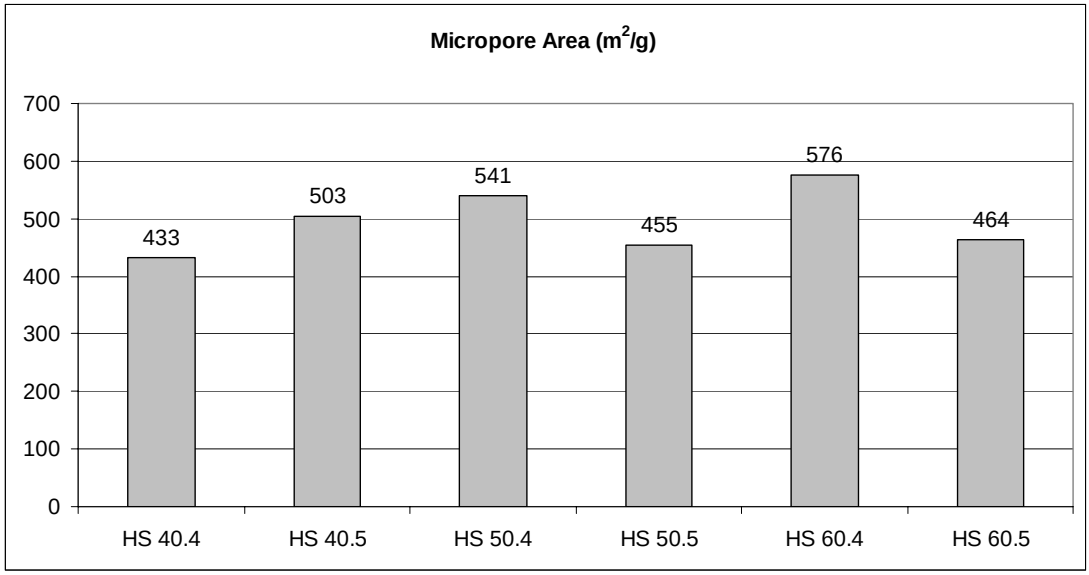

Figure 6.14 Micropore Area Values of Hazelnut Shell Based Products

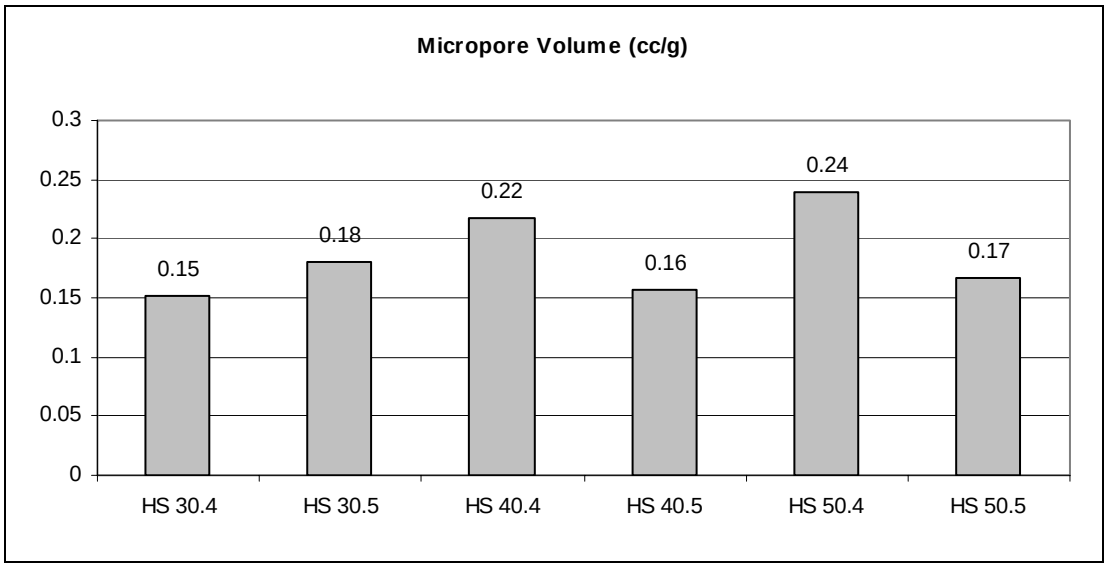

Figure 6.15 Micropore Volume Values of Hazelnut Shell Based Products

BET equation has been used extensively to determine surface areas of activated carbons from nitrogen adsorption isotherms measured at -195.6°C. It is now generally agreed that N_2 adsorption at -195.6°C does not measure the total surface area of activated carbons for two important reasons. First, due to the activated diffusion limitations, N_2 molecules at -195.6°C do not posses enough kinetic energy to readily penetrate into the micropores. Thus, impractically long periods are required for equilibrium to establish. Secondly, the micropores undergo some decrease in their size at low temperatures. Therefore, in some cases, the CO_2 areas greatly exceed those determined from N_2 adsorption at -195.6°C for two reasons. First, minimum dimension of a CO_2 is smaller than that of N_2 molecule. Second, kinetic energy of CO_2 molecules at the adsorption temperatures used far exceeds that of N_2 molecules at -195.6°C. Consequently, rate of diffusion of CO_2 into the activated carbon micropores will be significantly higher than that of N_2 (Senel, 1994).

Other interpretation have also been found in literature that CO_2 adsorption may be influenced by the quadropole moment of CO_2 molecule interacting with the oxygen functionalities present on the carbon surface and that higher surface area may be caused by a CO_2 induced swelling effect (Senel, 1994). CO_2 can measure pores down to 4-5 Å while BET can measure pores down to 10 Å.

As it is shown in the Figure 6.16, for all the samples except for HS 60.4, micropore areas are greater than BET areas. For increasing acid concentrations, BET, micropore and mesopore areas of samples carbonized at 400 ºC were all increased. Mesopore areas of all the samples decreased with increasing carbonization temperature from 400 ºC to 500 ºC. So, it cannot be claimed that the decrease in surface area is because of the enlargement of the micropores to mesopores for samples impregnated with 50% and 60% acid. The 40% acid impregnated sample gave higher results for 500 ºC carbonization temperature. For low acid concentration impregnated samples the difference between BET and micropore areas was more obvious whereas for 60% acid impregnated samples these values were closer.

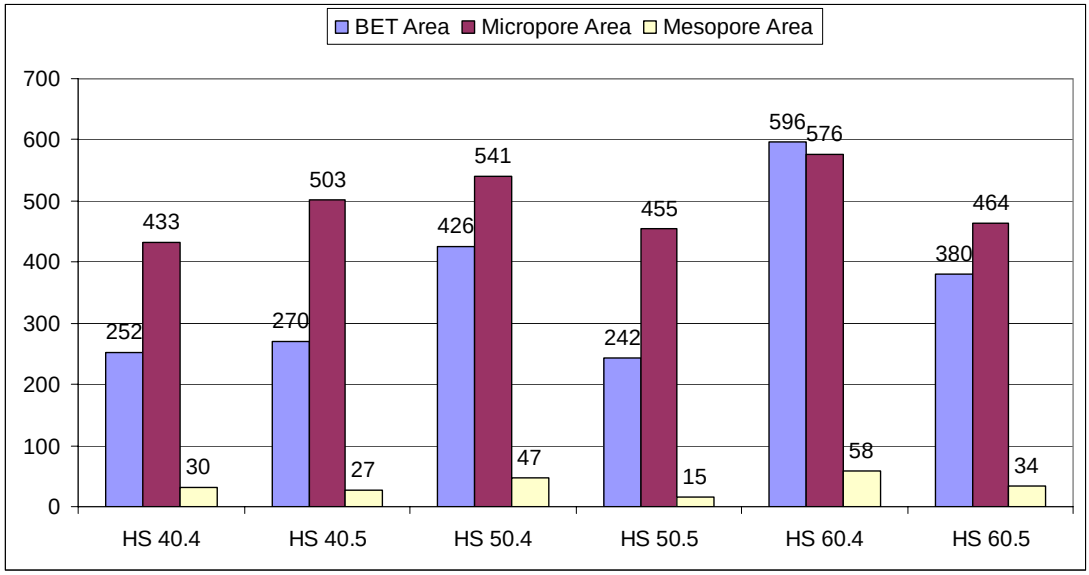

Figure 6.16 Comparisons of BET, D-R and BJH Results of Hazelnut Shell Based Products

ii. Hazelnut Husk Based Activated Carbons

Micropore areas of the hazelnut husk based activated carbons are shown in Figure 6.17. Although the highest BET area was obtained for HH 40.4, in terms of micropore area HH 30.4 was found to have the highest area 724 m^2/g. Samples impregnated with 60% acid, showed similar behavior to BET results; at 400 ºC carbonization temperature gave the highest area (HH 60.4). In terms of acid concentration effect, the samples carbonized at 400 ºC had minimum micropore area for 50% acid impregnated sample and showed more increase as the acid concentration decreased to 40% and 30%.

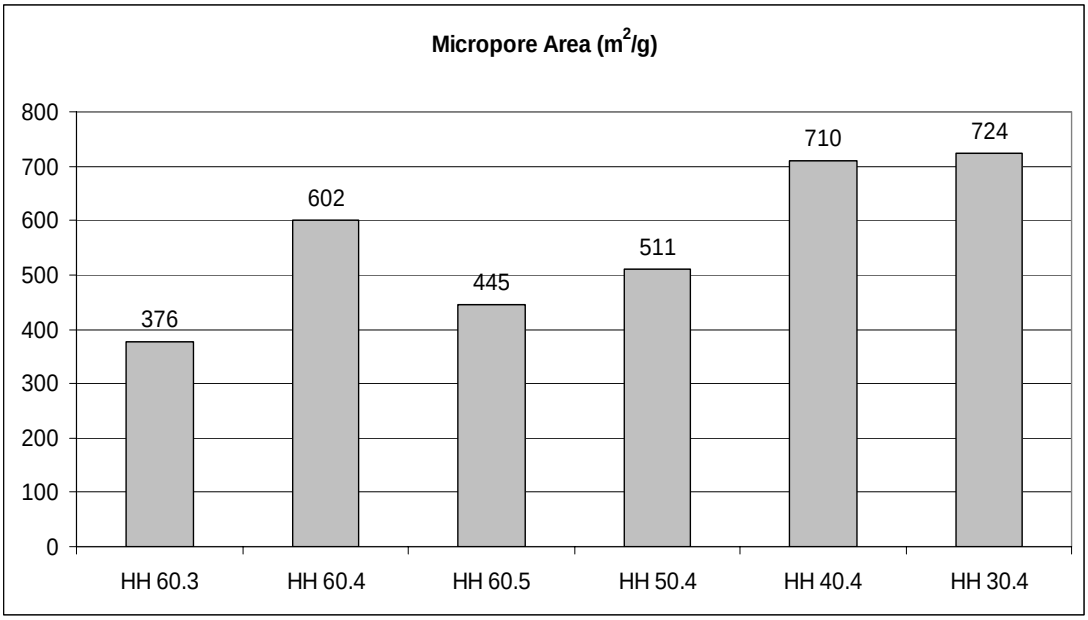

Figure 6.17 Micropore Area Values of Hazelnut Husk Based Products

Micropore volumes of the samples are shown in Figure 6.18. Micropore volumes are in the range of 0.18-0.53 cc/g. Although, HH 40.4 was the second in micropore area values, it had the highest micropore volume 0.53 cc/g. Samples impregnated with 60% acid showed the same behavior like in micropore area graph. In terms of acid concentration effect, the lowest micropore volume was found for 50% acid impregnated sample again as 0.20 cc/g.

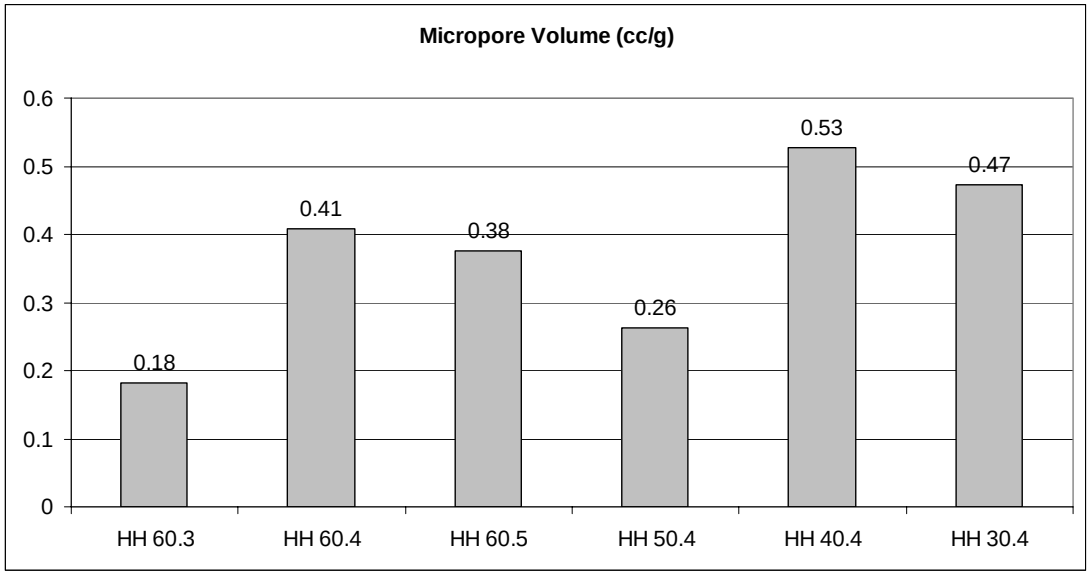

Figure 6.18 Micropore Volume Values of Hazelnut Husk Based Products

In Figure 6.19 BET, mesopore and micropore areas of the samples were compared. Unlike the hazelnut shell based activated carbon results, BET areas were higher than micropore areas. As acid concentration increased from 30% to 50%, the mesopore areas increased while micropore areas decreased but, for sample HH 60.4 an increase in micropore area and a decrease in mesopore area was observed. Except for samples HH 30.4 and HH 60.3, mesopore areas were higher than micropore areas for all samples.

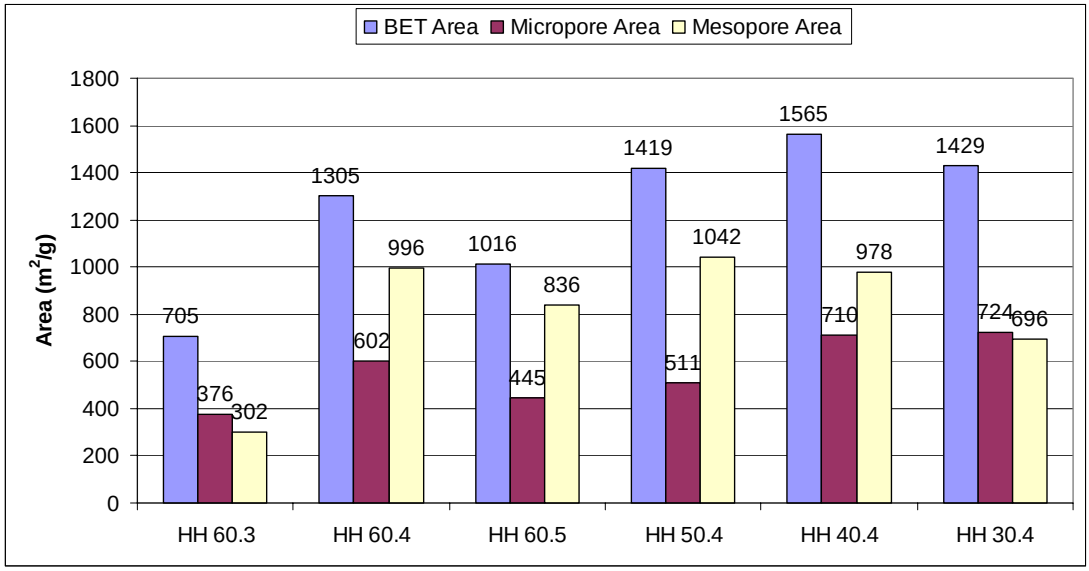

Figure 6.19 Comparisons of BET, D-R and BJH Results for Hazelnut Husk Based Products

Figure 6.20 shows BET, micropore and mesopore areas of all the products to make a comparison between hazelnut shell and hazelnut husk based samples. BET surface areas and mesopore areas of HH based samples were very much higher than those of HS based ones. For samples impregnated with 40 wt. % phosphoric acid and carbonized at 400 ºC, micropore areas were found as 433 m^2/g and 710 m^2/g for HS 40.4 and HH 40.4, respectively. Although activated carbons produced from hazelnut husk were mainly mesoporous, the micropore areas exceeded that of hazelnut shell based samples for most of the products.

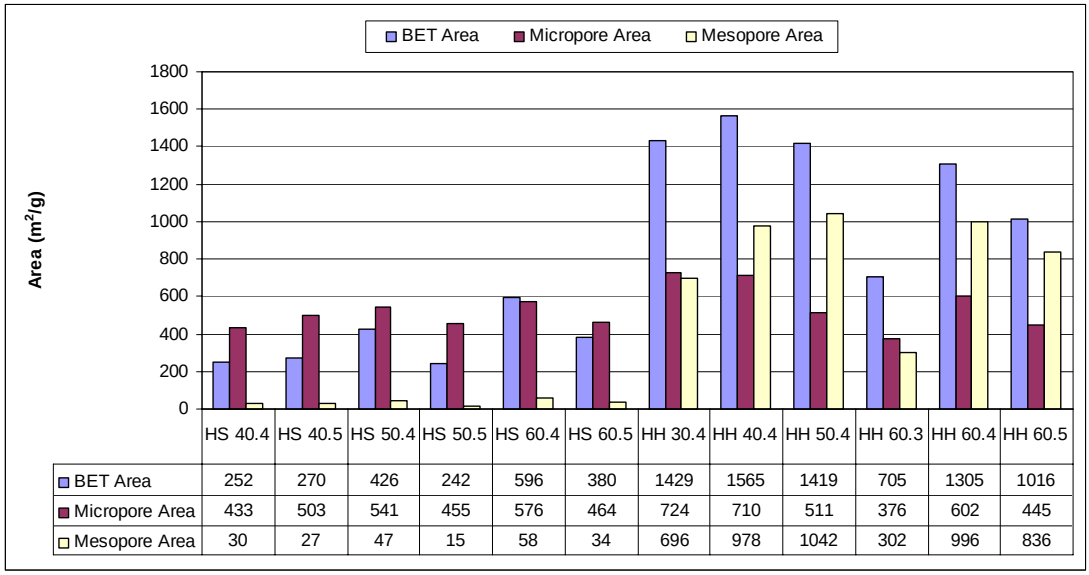

	HS 40.4	HS 40.5	HS 50.4	HS 50.5	HS 60.4	HS 60.5	HH 30.4	HH 40.4	HH 50.4	HH 60.3	HH 60.4	HH 60.5
BET Area	252	270	426	242	596	380	1429	1565	1419	705	1305	1016
Micropore Area	433	503	541	455	576	464	724	710	511	376	602	445
Mesopore Area	30	27	47	15	58	34	696	978	1042	302	996	836

Figure 6.20 Comparison of HH and HS Series in terms of BET, Micro- and Mesopore Areas.

Results in Figure 6.20 can be compared with the literature survey results also. Girgis et al. (1998) produced activated carbon from apricot stone by using 40 wt.% phosphoric acid and 400 ºC carbonization temperature, resulting in 1303 m^2/g surface area. Under similar conditions hazelnut shell sample resulted in 252 m^2/g surface area, but hazelnut husk sample gave a higher result of 1565 m^2/g. Additionally, impregnation with 50 wt. % phosphoric acid and carbonization at 400 ºC gave 1372 m^2/g surface area for apricot stone while HS and HH based samples had 426 and 1419 m^2/g, respectively. Hazelnut shell samples had lower surface areas than apricot stones while hazelnut husks had higher results under similar conditions.

Girgis et al. (2002) produced activated carbons from date pits using phosphoric acid. Impregnation with 50 wt. % acid and carbonization at 500 ºC resulted in BET surface area of 556 m^2/g and micropore area of 464 m^2/g for date pits. Hazelnut shell sample had 242 m^2/g of BET surface area and 455 m^2/g of micropore area under similar conditions. Considering the micropore areas of the

samples it can be stated that hazelnut shells and date pits give close results under similar experimental conditions. But, generally the structure of the starting material very much influences the adsorptive properties and surface chemistry of the products as in the case of apricot stones and hazelnut shell and husk.

6.2.3. True Density Determinations

True densities values of the activated carbons are determined at room temperature by Helium Pycnometry as explained in section 5.3.3 and are shown in Figure 6.21.

As it is shown in figure true density values of hazelnut shell and hazelnut husk based samples are in the range of 1.52-1.75 g/cc and 1.74-2.55 g/cc, respectively. True densities of all the products are increasing with the increasing carbonization temperature. By increasing carbonization temperature, the volatile matter (low density matter) content of the activated carbon might decrease resulting in the increase in true density. Acid concentration has no significant effect on true density of hazelnut shell based products, but true densities of hazelnut husk based activated carbons are increasing with increasing acid concentration.

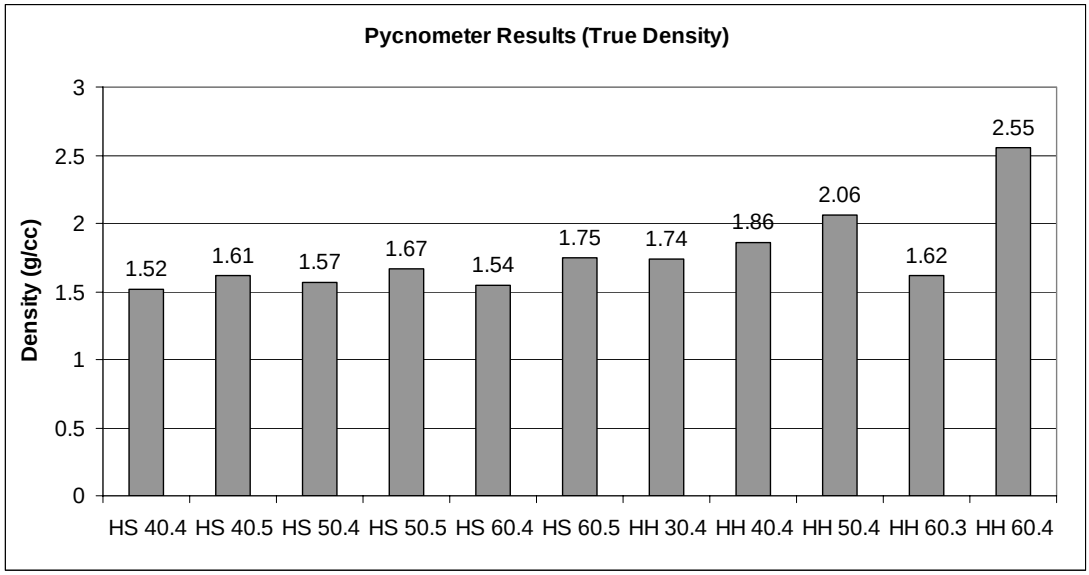

Figure 6.21 True Density Values of the Activated Carbons

6.3. Chemical Analysis of Products

Elemental (C, H, O) analysis of activated carbons and raw materials, which was carried out according to the procedure explained in section 5.1.1, is given in Figure 6.22 and Table D.1 in Appendix D. As it can be seen from this figure, activated carbons produced in this study contain about 70.3-83.1 % carbon, 1.7-2.6 % hydrogen, 12.4-22.6 % oxygen, trace amount of N and 0.8-3.4 % ash.

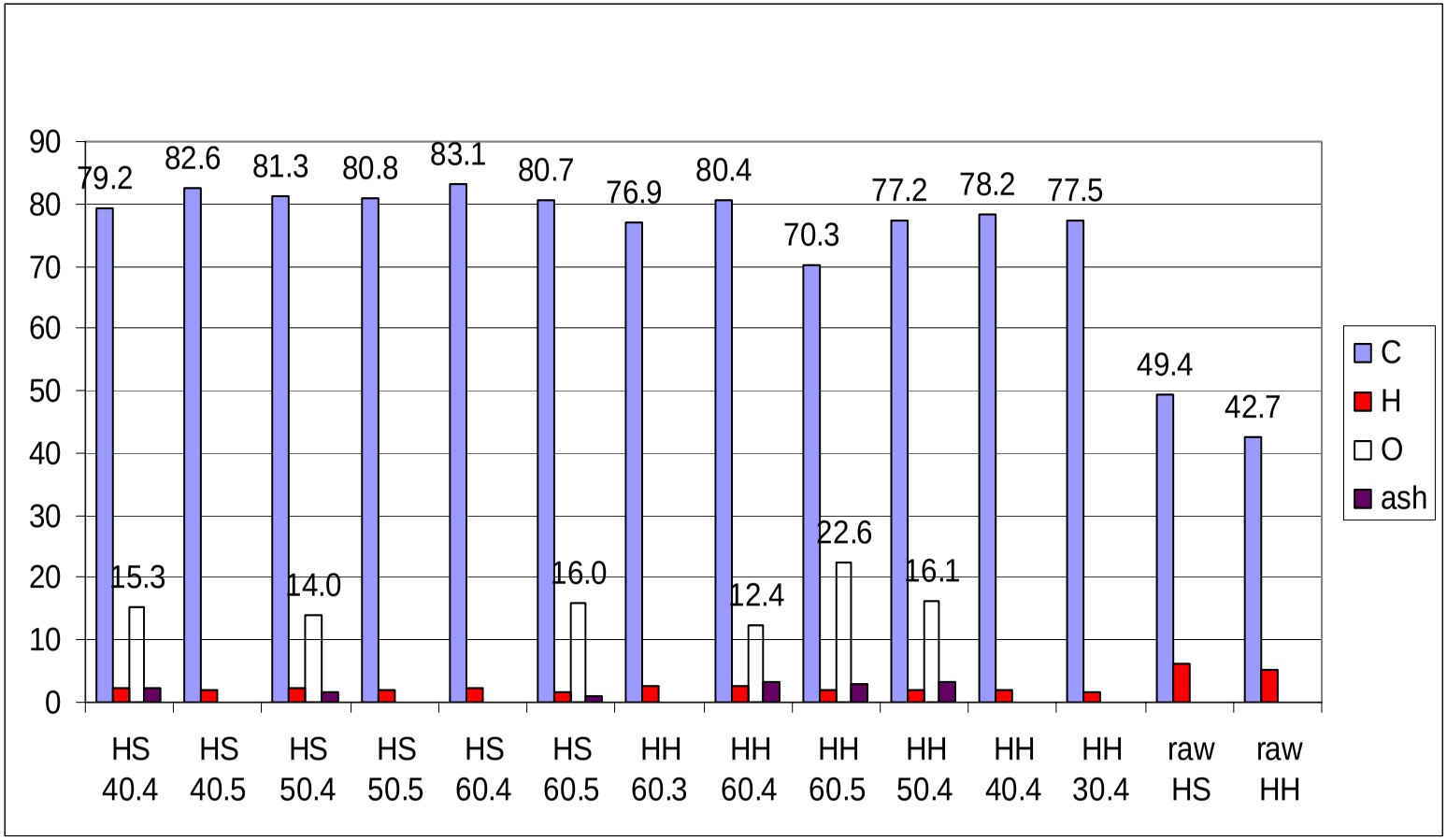

Figure 6.22 Elemental Analysis Results of Activated Carbons and Raw Materials

6.3.1. Carbon Content

Data reported in Figure 6.22. indicates that, for hazelnut shell based activated carbons, 50% and 60% acid impregnated samples have higher carbon content at 400 ºC than 500 ºC. But, carbon content of 40% acid impregnated sample was increased with increasing carbonization temperature. The highest carbon content was found for the hazelnut shell, impregnated with 60% H_3PO_4 and carbonized at 400 ºC as 83.1%.

Carbon content of hazelnut husk, impregnated with 60% acid and carbonized at 500 ºC was found to have the lowest carbon content of all the activated carbons as 70.3%. The highest carbon content was found for sample HH 60.4 as 80.4% for activated carbons produced from hazelnut husk. Raw hazelnut shell and hazelnut husk have 49% and 43% carbon content, respectively. Carbonization of the samples impregnated with H_3PO_4 resulted in higher carbon contents.

For a typical activated carbon, carbon content is reported to be around 85-90 % (Section 2.5, Faust and Aly, 1983). As carbon content of the activated carbon increase it is expected that the BET surface area value increase. BET area value is the most important parameter for activated carbons. High carbon content value is desired to achieve high BET surface area.

6.3.2. Oxygen and Hydrogen Content

The presence of oxygen and hydrogen influence the adsorptive properties of activated carbon. As discussed in Section 2.5 these elements are combined with the atoms of carbon by chemical bonds. The oxygen and hydrogen functional groups provide sites where molecules of water and other polar substances or easily polarizable gases and vapors are adsorbed (Smisek and Cerny, 1970; Hassler, 1974).

However, O and H contents of the samples were slightly higher than typical values. For hazelnut shell based products oxygen content values were in the range of 14-16%. O content of hazelnut husk based activated carbons was in the range of 12.4-22.6 %. As acid concentration increased oxygen content of the products was decreased. As carbonization temperature increased O contents of the products increased. The lowest O value was obtained from HH 60.4 as 12.4%. The hydrogen content of all the products was decreased with increasing carbonization temperature. For hazelnut shell based activated carbons H content decreased with increasing acid concentration. For hazelnut husk based ones the highest H content was for HH 60.4 and the lowest value was found for HH 30.4 as 2.6% and 1.8%, respectively. Since phosphoric acid (H_3PO_4) was used as activating agent and it contained hydrogen and oxygen groups in its structure, these high O and H content values could be obtained. Most probably, the high oxygen content of the products was also because of phosphor content of the acid. In the stated percentages of oxygen, phosphor content might be hidden since oxygen contents were found by adding C, H, N and ash contents and subtracting from 100%. For a typical activated carbon the recommended oxygen content is around 5 % and the hydrogen content is 1 % (Faust and Aly, 1983).

6.3.3. Nitrogen Content

For a typical activated carbon, nitrogen content is less than 1 %. For the products obtained from hazelnut shell by chemical activation have nitrogen contents in small amounts which are less than 1 percent (Figure 6.22). On the other hand, hazelnut husk based products have nitrogen slightly higher than the typical value. During carbonization in nitrogen atmosphere, small amount of nitrogen can be chemisorbed (Smisek and Cerny, 1970;).

6.3.4. Ash content

A good activated carbon must have low ash content. A small increase in ash content causes a decrease in adsorptive properties of activated carbon. The raw hazelnut shell and hazelnut husk have ash content of about 0.4% and 5.8%, respectively (Table 5.1).

The typical ash content of activated carbons is around 5-6 %. However, all the products had lower ash content than the typical activated carbons in the range of 0.8-3.4 %. Moreover, the ash content of the carbonized materials is expected to be high compared with the raw material values.

6.4. TGA of Impregnated Hazelnut Shells and Hazelnut Husks

TGA experiments were carried out to obtain the yield values for selected products. It was not possible to obtain the yield values from the experiments which were done with the experimental set-up since after the carbonization was completed products were immediately taken to a flask and mixed with distilled water to prevent interaction with the air. Yield values of raw hazelnut shell and husk were obtained during preliminary experiments by carbonization at 400 ºC.

TGA experiments were done at same experimental conditions like carbonization time and temperature, particle size, N_2 flow rate, impregnation ratio and heating rate. Yield values of samples for different carbonization temperatures and acid concentrations are given in Table 6.1.

Table 6.1 Yield Values (%) of Selected Products and Raw Materials

Name	Yield%
HS 40.4	51.5
HS 50.4	49.4
HS 60.4	47.0
HS 60.5	43.9
HH 40.4	54.3
HH 50.4	56.5
HH 60.4	56.8
HH 60.5	43.2
Raw HS (400 ºC)	31
Raw HH (400 ºC)	34

As it is seen from the table, yield values of phosphoric acid impregnated samples are higher than that of raw materials for the same temperature. Yield values are decreasing with the increasing carbonization temperature. Hazelnut shell based products gave yield values of 47-51.5% at 400 ºC while yields of samples produced from hazelnut husk were higher, in the range of 54.3-56.8%. As the carbonization temperature was increased to 500 ºC yields were decreased to 43.2-43.9% for both kinds of products. For HS series, increasing acid concentration decreased the yield values while in HH series yield values were increased with increasing acid concentration. Compared with the literature values, products have acceptable yields. Addition of phosphoric acid to the raw materials effects the depolymerization reactions (as indicated in Chapter 4 and Section 2.2.2.1) during the carbonization. Phosphoric acid (H_3PO_4) restricts the formation of tar (Section 2.2.2.1) by its dehydration effect and volatile materials do not evacuate from the structure. Therefore, yield values of acid impregnated samples increase with respect to raw samples. TGA figures of the acid impregnated samples are given in Appendix E.

For a comparison of probable feasibility of hazelnut shell and husk, based on raw materials and phosphoric acid used during the experiments, a material balance was done. Table 6.2 shows the data for HS 40.4 and HH 40.4 samples. 1 gram of hazelnut shell was mixed with 2 ml phosphoric acid solution (40 wt.%), weighting 2.5 g. The weight increase of HS 40 series (impregnated and subsequently dried samples) was 23% (Table 5.2). Weight of input sample was calculated as 1.23 g. Since the yield of HS 40.4 was obtained as 51.5 % (TGA method), the output weight was found as 0.633 g. Similarly, 1 gram of hazelnut husk resulted in 1.69 gram of activated carbon by using 6.25 g H_3PO_4 (40 wt.%) solution.

Table 6.2 Material Balance on Activated Carbon Production
(basis: 1 g raw material)

Raw material	H_3PO_4 (40%) volume (ml)	H_3PO_4 (40%) weight (g)	Carbonization input (g)	Carbonization output (g)
Hazelnut shell	2	2.5	1.23	0.633
Hazelnut Husk	5	6.25	3.12	1.69

Comparison of HS 40.4 and HH 40.4, on the basis of 1 g. raw material, showed that hazelnut husk gave higher amounts of activated carbon from 1 gram of husk. Obtaining product weight less than the raw material weight consumed for that process can be expected. But, when the decomposition of the material during carbonization resulting in leaving of gases and tarry substances from the carbonized sample is considered, obtaining a product weighting higher than the amount of raw material is interesting as in the case of hazelnut husk. Also, considering the availability of the raw materials, since hazelnut shell is used mainly for heating purposes in The Black Sea Region, hazelnut husk might be cheaply obtained in great amounts. On the other hand, weight of phosphoric acid

used for HH 40.4 production was 2.5 times higher than that of used for HS 40.4. This high consumption of phosphoric acid might increase the unit cost of HH 40.4.

Although the material balance was mainly based on the carbonization step, the importance of washing step after carbonization should not be ruled out. It might be more meaningful to determine yield considering the whole production process instead of only carbonization. But during the experiments final activated carbon amounts could not be measured after the removal of acid, since this step caused loss of products to some extent. So, although hazelnut husk based activated carbon production consumed higher amounts of acid, washing step might remove the impregnated acid and lower the unit cost. On the other hand, after washing step the product weight might not change significantly with respect to the carbonization output amount indicating that the unexpected high amount of carbonization output for husk was not a cause of free phosphoric acid. At that point the phosphor content of the products appears to be important.

CHAPTER VII

CONCLUSIONS

From the results of this work, it is concluded that hazelnut shells and hazelnut husks can be used as raw materials for the production of activated carbon by using H_3PO_4 as the activating agent. N_2 and CO_2 adsorption / desorption isotherms show that activated carbons obtained from hazelnut shell have a certain degree of porosity, located mainly in micro size of pores while hazelnut husk based activated carbons are mainly mesoporous.

Novelties of this work are the use of phosphoric acid (H_3PO_4) as the activating agent for hazelnut shell during carbonization and using hazelnut husk for activated carbon production as the starting material. Results showed that, pretreatment of the raw materials with H_3PO_4 solution before carbonization increased the values of surface area of the activated carbons produced at relatively low temperatures. The product obtained from 60% H_3PO_4 impregnated hazelnut shell gave the highest surface area value 596 m^2/g at carbonization temperature of 400^oC. On the other hand, hazelnut husk based products gave much higher surface areas (in the range of 705-1565 m^2/g) for 300, 400 and 500 ºC carbonization temperatures.

Phosphoric acid concentration showed appreciable effects on the properties of activated carbons. By increasing acid concentration from 30% to 60% higher surface area activated carbons were obtained from hazelnut shell. For activated carbons produced from hazelnut husk, 40% phosphoric acid impregnated sample

gave the highest surface area 1565 m^2/g while further increasing the acid concentration decreased the surface areas of the products.

CHAPTER VIII

RECOMMENDATIONS

Activated carbon has many industrial applications depending on its porous structure and adsorption capacity. To increase the BET surface area value of the activated carbons produced from hazelnut shell and hazelnut husk, it is recommended to carry out experiments with different experimental parameters. Some of the most critical parameters are the impregnation ratio, heating rate, carbonization temperature and carbonization time. Increasing phosphoric acid concentration to 70% or 80% for hazelnut shell might give higher BET surface areas but probably tend to decrease after a maximum point. To obtain microporous activated carbon from hazelnut husk the carbonization temperature should be kept low (300 ºC).

The experiments should be performed in a fluidized bed furnace. The preliminary experiments showed that a decrease in the weight of raw material placed in the tube in furnace resulted in higher surface area products. Using fluidized bed will probably result in a more effective carbonization. Also, to have idea about the effective surface areas of the products adsorption of organic materials from solutions may be performed. For further characterization of the products phosphor contents should be investigated to have an idea on surface chemistry. Also, particle size distribution of the products should be determined.

REFERENCES

1. Agrawal, R.K. and Mc Cluskey, R.J., "The Low Pressure Pyrolysis of Newsprint", *J. of AppI. Polv. Sci*., Vol. 27, pp.367-382. (1983)

2. Agrawal, R.K., "Kinetics of Reactions Involved in Pyrolysis of Cellulose I. The Three Reaction Model", *Can. J. of Chem. Eng.,* Vol. 66, pp.403-412. (1988a)

3. Agrawal, R.K., "Kinetics of Reactions Involved in Pyrolysis of Cellulose II. The Modified Kilzer-Broido Model", *Can. J. of Chem. Eng.,* Vol. 66, pp.413-418. (1988b)

4. Ahmedna, M., Marshall, W.E., Rao, R.M., "Surface Properties of Granular Activated Carbons from Agricultural by-products and Their Effects on Raw Sugar Decolorization", *Bioresource Tech.,* 71, pp. 103-112. (2000)

5. Arol, A.I., Yalcin, M., "Gold Cyanide Adsorption Characteristics of Activated Carbon of Non-Coconut Shell Origin", *Hydrometallurgy,* 63, pp. 201-206. (2002)

6. Aygün, A., Yenisoy-Karakaş, S., Duman, I., "Production of Granular Activated Carbon from Fruit Stones and Nutshells and Evaluation of Their Physical, Chemical and Adsorption Properties", *Microporous and Mesoporous Materials*, 66, pp. 189-195. (2003)

7. Baçaoui, A., Yaacoubi, A., Dahbi, A., Bennouna, C., Phan Tan Luu, R., Maldonado- Hodar, F.J., Rivera-Utrilla, J. and Moreno-Castilla, C., "Optimization of Conditions for the Preparation of Activated Carbons from Olive-Waste Cakes", *Carbon* Vol. 39, pp.425-432. (2001)

8. Balcı, S., PhD Dissertation, METU, Ankara (1992)

9. Balcı, S., Doğu, T. And Yücel, H., "Characterization of Activated Carbon Produced from Almond Shell and Hazelnut Shell", *J. Chem. Tech. Biotechnol.* Vol.60, pp.419-426. (1994)

10. Barrett, E. P., Joyner, L. G. and Halenda, P. P., "The Determination of Pore Volume and Area Distribution in Porous Substances. I. Computations from Nitrogen Isotherms", *J. Am. Chem. Soc.*, Vol. 73, pp.373-380. (1951)

11. Bevla, F. R., Rico, D. P. and Gomis, A. F. M., " Activated Carbon from Almond Shells. Chemical Activation. 1. Activating Reagent Selection and Variables Influence", *Ind. Eng. Chem. Prod. Res. Dev.* Vol. 23, pp.266-269. (1984a)

12. Bevla, F. R., Rico, D. P. and Gomis, A. F. M., " Activated Carbon from Almond Shells. Chemical Activation. 2. $ZnCl_2$ Activation Temperature Influence", *Ind. Eng. Chem. Prod. Res. Dev.* Vol. 23, pp.269-271. (1984b)

13. Broekhoff, J. C. P. and Linsen, B. G., Physical and Chemical Aspects of Adsorbents and Catalysts, ed. B. G. Linsen, Academic Press, New York. (1970)

14. Browning, B. L., The Chemistry of Wood, Interscience Pub., New York, London. (1963)

15. Brunauer, S., Demming, L. S., Demming, W. S. and Teller, "On a Theory of the van der Waals Adsorption of Gases" E., *J. Am. Chem. Soc.*, Vol. 62, pp. 1723-1732. (1940)

16. Cimino, G., Passerini, A., Toscano, G., "Removal of Toxic Cations and Cr(VI) from Aqueous Solution by Hazelnut Shell", *Wat. Res.*, Vol. 34, No. 11, pp. 2955-2962. (2000)

17. Cookson, J. T., Carbon Adsorption Handbook. (Edited by Cheremisinoff, P. N. and Ellerbusch, F.) pp.241-279, Ann Arbor Sci., Michigan. (1980)

18. De Boer, J.H., "The Structure and Properties of Porous Materials", ed. D.J. Everett, Butterworths, London, pp. 86 (1958)

19. Demirbaş, E., Kobya, M., Öncel, S, Şencan, S., "Removal of Ni(II) from Aqueous Solution by Adsorption onto Hazelnut Shell Activated Carbon: Equilibrium Studies", *Bioresource Tech.,* 84, pp. 291-293. (2002)

20. Dubinin, M. M., "On Methods for Estimating Micropore Parameters of Carbon Adsorbents", *Carbon*, Vol. 26, pp.97-110. (1988)

21. Faust, S. D. and Aly, O. M., Chemistry of Water Treatment, Butter Wort Pub., Woburn. (1983)

22. Franklin, R. E., "Crystallite Growth in Graphitizing and Nongraphitizing Carbons", *Proc. Roy. Soc.* (London) A 209, 196-218. (1951)

23. Girgis, B. S. and Daifullah, A. A., "Removal of Some Substituted Phenols by Activated Carbon Obtained from Agricultural Waste", *Wat. Res.* Vol. 32, pp.1169-1177, (1998)

24. Girgis, B.S., Abdel-Nasser, A., El-Hendawy, "Porosity Development in Activated Carbons Obtained from Date Pits under Chemical Activation with Phosphoric Acid", *Microporous and Mesoporous Materials,* 52, pp. 105-117. (2002)

25. Gregg, S. J. and Sing, K.S.W., Adsorption, Surface and Porosity, New York Academic Press. (1967)

26. Halsey, G. D., *J. Chem. Phys.*, "Physical adsorption on nonuniform surfaces", Vol. 16, pp.931. (1948)

27. Hassler, J. W., Purification with Activated Carbon, Chem. Pub. Co., New York. (1974)

28. Holden, M. J., "Manufacture and Uses of Activated Carbon", *Eff. and Water Treat. J.* Vol. 22, pp.27-31. (1982)

29. Hu, Z., Srinivasan, M. P. and Yaming Ni, "Novel Activation Process for Preparing Highly Microporous and Mesoporous Activated Carbons", *Carbon* Vol. 39, pp.877-886. (2001)

30. Kirk-Othmer, Encyclopedia of Chemical Technology, John Wiley and Sons Inc. (2003)

31. Köksal, A.İ., "Inventory of hazelnut research, germplasm and references", REU Technical Series - 56, 2000

32. Lozano-Castello, D., Lillo-Rodenas, M.A., Cazorla-Amoros, D., Linares-Solano, A., "Preparation of Activated Carbons from Spanish Anthracite, I. Activation by KOH", *Carbon,* 39, pp. 741-749. (2001)

33. Martin, A. E., Chemistry of Coal Utilization, 2nd Supp. Vol., John Wiley and Sons Inc. (1981)

34. Micromeritics ASAP 2000, User Manual, 1993

35. Orr, C. and Dalla, V. J. M., Fine Particle Measurement, Mc Millian, New York. (1959)

36. Polanyi, M., "Theories of the adsorption of gases. A general survey and some additional remarks", *Trans. Faraday Soc.,* Vol.28, pp.316. (1932)

37. Reinoso, R. F., Martinez, M. J. M., Sabio, M. M., "A Comparison of the Porous Texture of Two CO_2 Activated Botanic Materials", *Carbon,* Vol. 23 pp.19-24. (1985)

38. Roberts, A. F., "A Review of A Kinetic Data for the Pyrolysis of Wood and Related Substances", *Comb. And Flame,* Vol. 14, pp.261-272. (1970)

39. Rodriguez Reinoso, F., Controlled Gasification of Carbon and Pore Structure Development, *Fundamental Issues in Control of Carbon Gasification Reactivity,* pp. 533-571. (1991)

40. Rodriguez-Reinoso, F., "An Overview of Methods for the Characterization of Activated Carbons", *Pure and Appl. Chem.* Vol. 61, No.11, pp.1859-1866. (1989)

41. Rodriguez-Reinoso, F., Lopez-Gonzalez, J. DE D., Berenguer, C., "Activated carbons from Almond Shells-I, Preparation and Characterization by Nitrogen Adsorption", *Carbon,* Vol. 20, No.6, pp.513-518. (1982)

42. Ruthven, D. M., Principle of Adsorption and Adsorption Process, John Wiley and Sons, New York, (1984)

43. Sánchez,A. R., Elguézabal, A. A. and Saenz, L. L. T., "CO_2 Activation of Char from *Quercus Agrifolia* Wood Waste", *Carbon,* Vol. 39, pp.1367-1377. (2001)

44. Schewenker, Jr. R. P. and Pascu, E., "Pyrolytic Degradation Products of Cellulose", *Chem. Eng. Data Ser.2,* No.1, pp.83-88. (1957)

45. Şenel, G. İ., PhD Dissertation, METU, Ankara (1994)

46. Smisek, M. And Cerny, S., Active Carbon Manufacture, Properties and Aplications, Elsevier Pub., Comp., New York. (1970)

47. Solano, L. A., Gonzalez, L. J. de D., Sabio, M. M., "Active Carbons from Almond Shells as Adsorbents in Gas and Liquid Phases", *J. Chem. Tech. Biotech*. Vol. 30, pp.65-72. (1980)

48. Toles, C. A., Marshall, W. E. and Johns, M. M., "Granular Activated Carbons from Nutshells for the Uptake of Metals and Organic Compounds", *Carbon*, Vol.35, No.9, pp.1407-1414. (1997)

49. Toles, C. A., Marshall, W. E., Johns, M. M., Wartelle, L. H. and McAloon A., "Acid-Activated Carbons from Almond Shells: Physical, Chemical and Adsorptive Properties and Estimated Cost of Production", *Bioresource Technology*, Vol. 71, Issue 1, pp.87-92. (2000)

50. TS 6879, Turkish Standards Institution (TSE). Activated Carbon Determination of Total Ash Content

51. TS 5896, Turkish Standards Institution (TSE). Activated Carbon Determination of pH value.

52. Wartelle, L.H., Marshall, W.E., Toles, C.A., Johns, M.M., "Comparison of Nutshell Granular Activated Carbons to Commercial Adsorbents for the Purge-and-Trap Gas Chromatographic Analysis of Volatile Organic Compounds", *Journal of Chromatography A,* 879, pp. 169-175. (2000)

53. Wigmans, T., Carbon and Coal Gasification. (Edited by Figueriedo, J. L. and Moulijn, J. A.,), pp.559-601, Martinus Nijhoff Pub., Lancaster. (1985)

54. Wigmans, T., "Industrial Aspects of Production and Use of Activated Carbons", *Carbon,* Vol. 27, pp. 13-22. (1989)

55. Wolff, W. F., "A Model of Active Carbon", *J. Phys. Chem.* Vol. 63, pp.653-659. (1959)

56. Yağşi, N. U., M.Sc. Dissertation, METU, Ankara (2004)

57. Yun, C.H., Park, Y.H., Park, C.R., "Effects of Pre-carbonization on Porosity Development of Activated Carbons from Rice Straw", *Carbon,* 39, pp. 559-567. (2001)

APPENDIX A

ANALYSIS OF N_2 SORPTION DATA

A.1. Analysis of Mesopores

Adsorption studies reading to measurements of pore sizes and pore size distributions generally make use of the Kelvin equation A.1 which relates the equilibrium vapor pressure of a curved surface such as that of a liquid in a capillary or pore, to the equilibrium pressure of the same liquid on a plane surface (Gregg and Sing, 1982).

$$\ln \frac{P}{Po} = \frac{-2\gamma VmolCos\theta}{r_p RT} \qquad \text{(A.1)}$$

where P is the equilibrium vapor pressure of the liquid contained in a narrow pore of radius r_p and Po is the equilibrium pressure of the same liquid at a plane surface. The terms γ and V_{mol} are surface tension and molar volume of the liquid, respectively. θ is the contact (wetting) angle with which the liquid meets the pore wall.

If the transfer of d_n moles of vapor in equilibrium with the bulk liquid at pressure Po into a pore where the equilibrium pressure P is considered, this process consists of three steps: evaporation from the bulk liquid, expansion of the vapor from Po to P and condensation into the pore. The first and third of these steps

are equilibrium processes and are therefore accompanied by a zero free energy change, whereas the free energy change for the second step is described by

$$dG = \left(RT \ln\left(\frac{P}{Po} \right) \right) dn \qquad \text{(A.2)}$$

When the adsorbate condenses in the pore

$$dG = -(\gamma Cos \quad \theta) dS \qquad \text{(A.3)}$$

where dS is the change in the film-vapor interfacial area and θ is the wetting angle which is taken to be zero since the liquid is assumed to wet completely the adsorbed film. Equations A.2 and A.3, when combined

$$\frac{dn}{dS} = \frac{-\gamma}{RT \ln(P / Po)} \qquad \text{(A.4)}$$

The volume of liquid adsorbate which condenses in a pore of volume V_p is given by

$$dVp = Vmoldn \qquad \text{(A.5)}$$

Substituting equation A.4 into A.5 gives

$$\frac{dVp}{dS} = \frac{-\gamma Vmol}{RT \quad \ln \quad (P \quad / \quad Po \quad)} \qquad \text{(A.6)}$$

The ratio of volume to area within a pore depends upon the geometry. When the shapes of the pores are highly irregular or consisting of a mixture of regular geometries, the volume to area ratio can be too complex to express mathematically. In these cases, or in the absence of specific knowledge of the

pore geometry, the assumption of cylindrical pores is usually made. Since the ratio of volume to area for cylinders is r/2, the equation A.6 gives the Kelvin equation;

$$\ln\left(\frac{P}{Po}\right) = \frac{-2\gamma Vmol}{rRT} \tag{A.7}$$

For nitrogen as the adsorbate at its normal boiling point of -195.6°C, the Kelvin equation can be written as

$$r_k = \frac{2\left(8.85\ \frac{erg}{cm^2}\right)\left(34.6\ \frac{cm^3}{mol}\right)\left(\frac{10^8\ ^o A}{cm}\right)}{\left(8.314\ x10^7\ \frac{erg}{Kmol}\right)(77\ K)(2.303)\log\left(P_o\ /\ P\right)} \tag{A.8}$$

where 8.85 erg/cm^2 is the surface tension and 34.6 cm^3 is the molar volume of liquid nitrogen at -195.6°C. Then equation A.9 can be found as

$$r_k = \frac{4.15}{\log\left(P_o / P\right)} \tag{A.9}$$

The term r_k indicates the radius into which condensation occurs at the required relative pressure. This radius, called the Kelvin radius or the critical radius, is not the actual pore radius since some adsorption has already occurred on the pore wall prior to condensation, leaving a center core or radius r_k. Alternatively, during desorption, an adsorbed film remains on the pore wall when evaporation of the center core takes place. If the depth of the film when condensation or evaporation occurs is t, then the actual pore radius r_p is given by

$$r_p = r_k + t \tag{A.10}$$

This equation can be used to calculate r_p but some means of evaluating t is required if the pore radius is to be determined. Using the assumption that the adsorbed film depth in a pore is the same as that on a plane surface for any value of relative pressure, one can write

$$t = \left(\frac{W_a}{W_m} \right) \tau \qquad \text{(A.11)}$$

Where W_a and W_m are, respectively, the quantity adsorbed at a particular relative pressure and the weight corresponding to the BET monolayer. Essentially equation A.11 asserts that the thickness of the adsorbed film is simply the number of layers times the thickness τ of one layer regardless of whether the film is in a pore or on a plane surface. The t value of τ can be calculated by considering the area S and volume V_{mol} occupied by one mole of liquid nitrogen if it were spread over a surface to the depth of one molecular layer

$$\tau = \frac{V_{mol}}{S} = \frac{\left(34.6 \, x10^{-24}\right) A^3}{\left(16.2 \, \frac{A^2}{mol}\right)\left(6.02 \, x10^{23} \, \frac{1}{mol}\right)} = 3.54 \, A \qquad \text{(A.12)}$$

On nonporous surfaces it has been shown that when the quantity W_a/W_m is plotted versus P/P_o the data all approximately fit a common type II curve above a relative pressure of 0.3. The common curve is described closely by Halsey, (1948) equation which for nitrogen can be written as

$$t = 3.54 \left(\frac{5}{2.303 \log\left(P_o / P\right)} \right)^{1/3} \qquad \text{(A.13)}$$

The thickness of the adsorbed layer which is calculated for a particular relative

pressure from the above equation which becomes thicker and thicker with successive increase in pressure, so that the measured quantity of gas adsorbed in a step is composed of a quantity equivalent to the liquid cores formed in that step plus the quantity adsorbed by the pore walls of pores whose cores have been formed in that and previous steps. Barrett Joyner and Halenda developed the method (BJH) which incorporates these ideas. The algorithm used on the ASAP 2000; the N_2 adsorption apparatus used in the present work, is an implementation of the BJH method. According to this method, ΔV_{gas}, the incremental volume: the change in adsorbed volume between two successive P/P_o values can be determined by subtracting the successive values. The ΔV_{gas} then can be converted to ΔV_{liq} by multiplying by the liquid molar volume for nitrogen at standard temperature and pressure. This is given by

$$\Delta V_{liq} = \frac{\Delta V_{gas}\left(cc/g\right)}{22414\left(cc/mol - STP\right)}\left(34.6\left(cc/mol\right)\right) = \Delta V_{gas}\left(1.54x10^{-3}\right) \quad \text{(A.14)}$$

The actual pore volume was evaluated by

$$\Delta V_{liq} = \pi r^{2}_{KAVE} + \Delta t \sum S \quad \text{(A.15)}$$

In this equation r_{KAVE} is the average Kelvin radius and the term $\Delta t\ \Sigma S$ is the product of the film area and the increase in the film depth, and since,

$$V_p = \pi r^{2}_{PAVE} \quad L \quad \text{(A.16)}$$

where L is the pore length, by combining the equations, A.15 and A.16

$$V_p = \left(\frac{r_{PAVE}}{r_{KAVE}}\right)^2 \left[\Delta V_{liq} - \left(\Delta t \sum S\right)\left(10^{-4}\right)\right] \quad \text{(cc)} \quad \text{(A.17)}$$

The surface area of the pore walls can be calculated from the pore volume by

$$S = \frac{2V_p}{r_{PAVE}}(10^4) \quad (m^2) \qquad (A.18)$$

Then, mesopore volume and surface areas were calculated by using the incremental pore volume and surface area values evaluated from the equations A.17 and A.18:

$$V_{meso} = \left[\sum V_p\Big|_{d_p=0.002\mu m} - \sum V_p\Big|_{d_p=0.05\mu m}\right] \text{(cc/g)} \qquad (A.19)$$

$$S_{meso} = \left[\sum S\Big|_{d_p=0.002\mu m} - \sum S\Big|_{d_p=0.05\mu m}\right] (m^2/g) \qquad (A.20)$$

A.2. Determination of BET Surface Area

BET surface areas of the samples can be obtained from the plot of $P/V(P_o-P)$ versus P/P_o plot, in the relative pressure range 0-0.2, using the following relation (Brunauer et al., 1938).

$$\frac{P}{V[P_O - P]} = \frac{1}{VmC} + \frac{C-1}{V_m C}\frac{P}{P_O} \qquad (A.21)$$

The slope and intercept of this plot which are given as

$$S = \frac{C-1}{V_m C} \quad \text{and} \quad I = \frac{1}{VmC} \qquad (A.22)$$

can be used to evaluate BET surface area by the equation

$$S_{BET} = \frac{\left[\left(CSA_{N_2}\, nm^2\right)\left(6.023x10^{23}\left(1/mol\right)\right)\right]}{\left[\left(22414\left(cm^3/mol-STP\right)\right)\left(10^{18}\left(nm^2/m^2\right)\right)\left((S+I)\left(g/cc-STP\right)\right)\right]} \quad \text{(A.23)}$$

where CSA_{N2} is the cross sectional area of a nitrogen molecule.

A.3. Sample Calculation

Sample Code HH 40.4 (Carbonization Temperature=400°C, Hazelnut Husk impregnated with 40% H_3PO_4 solution)

A.3.1. Calculation of Mesopore Volume and Area

Cumulative Mesopore Volume up to d_p=20 °A (2 nm)=0.845617 cc/g
Cumulative Mesopore Volume up to d_p=500 °A (50 nm)=0.020593 cc/g

Replacing these quantities into equation B.19:

V_{meso}= 0,845617- 0.020593=0,825024 cc/g

Cumulative Pore Surface Area up to d_p=20 °A (2 nm)= 979.2653 m^2/g
Cumulative Pore Surface Area up to d_p=500 °A (50 nm)= 0.896396 m^2/g

Replacing these quantities into equation A.20:

S_{meso}= 979.2653 - 0.896396 = 978.3689 m^2/g

A.3.2. Calculation of BET Surface Area

S=Slope= 0.002768

I=Intercept= 0.000014

CSA_{N_2} =0.162 nm^2 (Walker et al., 1968)

Replacing these quantities into equation A.23:

S_{BET}= 1564.5037 m^2/g

APPENDIX B

ANALYSIS OF CO_2 ADSORPTION DATA

B.1. Analysis of Micropores

The micropore volume of the samples calculated by applying the Dubinin Radushkevich (D-R) equation to the CO_2 adsorption data in the relative pressure range $1x10^{-4}$ – $1x10^{-2}$

$$\log V = \log V_o - 2.303K\left(\frac{RT}{\beta}\right)^2\left[\log\frac{P_o}{P}\right]^2 (cc/gSTP) \qquad \text{(B.1)}$$

A plot of log V versus log $(P/P_o)^2$ gives straight line with an intercept of log V_o from which V_o, the micropore volume (cc/g STP) could be calculated. In this equation, β is a constant which is the ratio of the adsorption potentials. K is also a constant determined by the shape of the pore distribution curve. The micropore volume in the unit of (cc/g STP) which refers to the adsorbate state based on the ideal gas behavior at STP was also converted into the unit of (cc/g) which is based on the specific volume of the adsorbate in the adsorbed state at 0°C by the following equation

$$V_o(cc/g) = \frac{V_o(cc/g - STP)MW_{CO_2}(g/mol)}{(22414\ (cc/mol - STP))(\rho_{CO_2}(g/cc))} \qquad \text{(B.2)}$$

where ρ is the density of the CO_2 molecule. Micropore surface area or so called D-R surface area was then evaluated by

$$S_{DR} = \frac{(\sigma\, nm^{2})V_{o}(cc/g - STP)(6.02\ x10^{23})}{(22414\ \ cc)(10^{18}\ nm^{2}/m^{2})} \qquad \text{(B.3)}$$

where σ is the cross sectional area of a CO_2 molecule.

B.2. Sample Calculation

Sample Code: HH 30.4 (Carbonization Temperature=400°C, Hazelnut Husk impregnated with 30% H_3PO_4 solution)

Micropore volume (cc/g STP) directly obtained from the ASAP 2000M; Micropore Analysis unit which processed the collected CO_2 adsorption data. In these calculations;

Saturation pressure of CO_2 =26142.000 mm Hg at 0°C (Micromeritics ASAP 2000, User Manual, Appendix C, 1993)
Absolute Pressure Range= 7.24243- 901.43604 mm Hg
Corresponding Relative Pressure Range= $2.77x10^{-4}$- $3.44x10^{-2}$

V_{micro}= 158.6431 cc/g STP

Corresponding micropore volume in the units of cc/g was evaluated by taking Density of CO_2 at 0°C=1.181 g/cc (Micromeritics ASAP 2000, User Manual, Appendix C, 1993) and replacing into equation B.2:

V_{micro}= 0.472 cc/g

Micropore surface area (D-R surface area) obtained by taking
Cross Sectional Area of CO_2 molecule =0.17 nm^2 (Micromeritics ASAP 2000, User Manual, Appendix C, 1993)

Replacing into equation B.3

S_{D-R}= 724 m^2/g

APPENDIX C

ANALYSIS OF HELIUM PYCNOMETER DATA

True densities of the samples were determined by helium displacement method. A commercial He Pycnometer apparatus was used to measure true densities of the activated carbons.

Assume that both V_{CELL} and V_{EXP} are at ambient pressure P_a, are at ambient temperature T_a, and that the valve is then closed. V_{CELL} is then charged to an elevated pressure P_1. The mass balance equation across the sample cell, V_{CELL} is

$$P_1\left(V_{CELL} - V_{SAMP}\right) = n_C RT_a \qquad \text{(C.1)}$$

where

n_C= the number of moles of gas in the sample cell,

R= the gas constant, and

T_a= the ambient temperature

The mass equation for the expansion volume is

$$P_a V_{EXP} = n_E RT_a \qquad \text{(C.2)}$$

where,

n_E= the number of moles of gas in the expansion volume.

When the valve is opened, the pressure will fall to an intermediate value, P_2, and the mass balance equation becomes

$$P_2\left(V_{CELL} - V_{SAMP} + V_{EXP}\right) = n_C RT_a + n_E RT_a \qquad \text{(C.3)}$$

Substituting from equations (C.1) and (C.2) into (C.3)

$$V_{CELL} - V_{SAMP} = \frac{P_a - P_2}{P_2 - P_1} V_{EXP} \qquad \text{(C.4)}$$

If we rearrange this equation,

$$V_{SAMP} = V_{CELL} - \frac{V_{EXP}}{\frac{\left(P_1 - P_a\right)}{\left(P_2 - P_a\right)} - 1} \qquad \text{(C.5)}$$

Since P_1, P_2 and P_a are expressed in equations (C.1) through (C.5) as absolute pressures and equation (C.5) is arranged so that P_a is subtracted from both P_1 and P_2 before use, new P_{1g} and P_{2g} may be redefined as gauge pressures

$$P_{1g} = P_1 - P_a \qquad \text{(C.6)}$$

$$P_{2g} = P_2 - P_a \qquad \text{(C.7)}$$

And equation (C.5) rewritten as

$$V_{SAMP} = V_{CELL} - \frac{V_{EXP}}{\frac{P_{1g}}{P_{2g}} - 1} \qquad \text{(C.8)}$$

This equation (C.8) then becomes the working equation for the pycnometer.

APPENDIX D

TABULATED FORM OF CHEMICAL COMPOSITIONS OF ACTIVATED CARBONS

Table D.1 Chemical Compositions of Activated Carbons and Raw Materials

name	C(%)	H(%)	N(%)	O(%)	ash(%)
HS 40.4	79.2	2.4	0.8	15.2	2.4
HS 40.5	82.6	1.9	0.9		
HS 50.4	81.3	2.4	0.8	13.9	1.6
HS 50.5	80.8	1.8	0.8		
HS 60.4	83.1	2.2	0.8		
HS 60.5	80.7	1.7	0.7	16.1	0.8
HH 60.3	76.9	2.6	1.7		
HH 60.4	80.4	2.6	1.5	12.4	3.1
HH 60.5	70.3	1.9	2.3	22.6	2.9
HH 50.4	77.2	1.9	1.4	16.1	3.4
HH 40.4	78.2	2.0	1.5		
HH 30.4	77.5	1.8	1.8		
raw HS	49.4	6.3	0.3	43.6	0.4
raw HH	42.7	5.2	0.9	45.4	5.8

APPENDIX E

TGA RESULTS

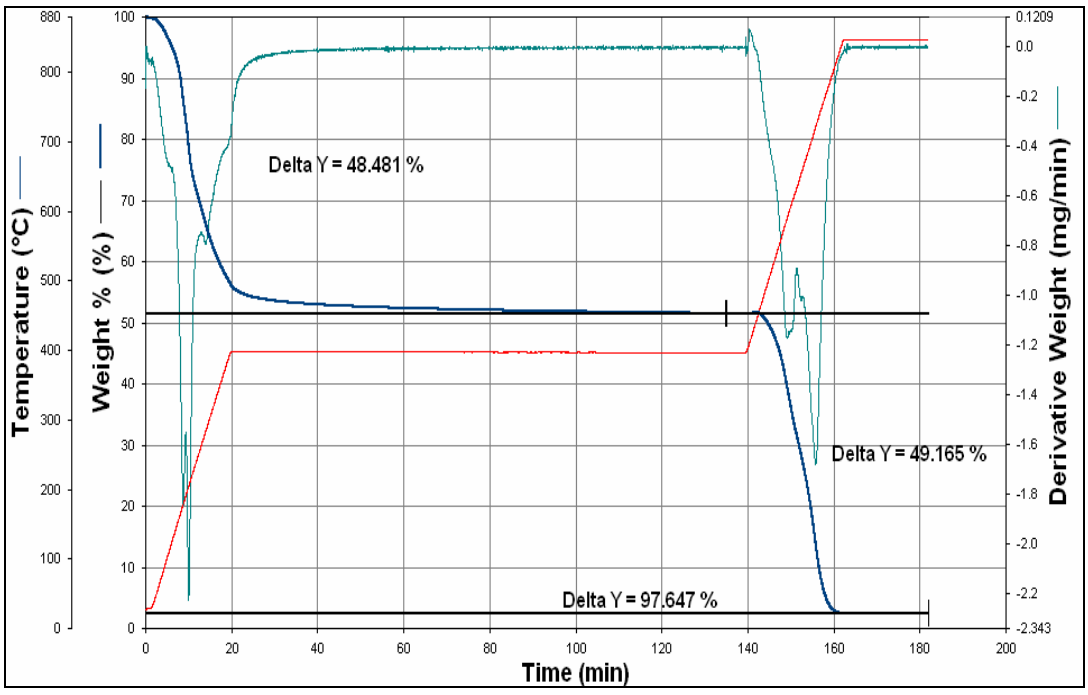

Figure E.1 TGA Result of 40% H_3PO_4 Impregnated Hazelnut Shell at 400 ºC (HS 40.4)

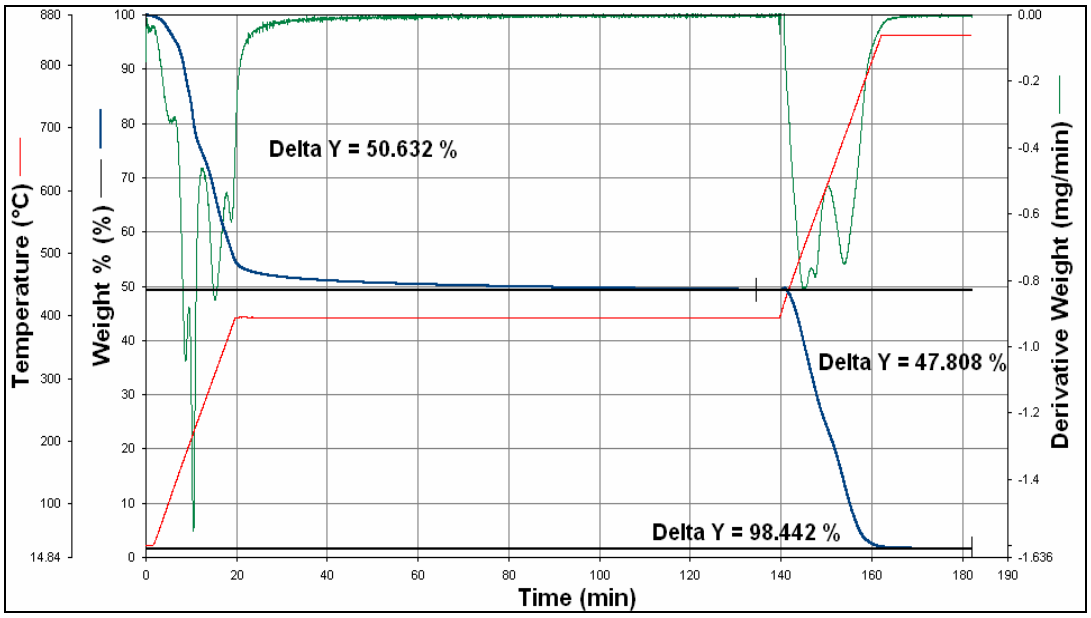

Figure E.2 TGA Result of 50% H_3PO_4 Impregnated Hazelnut Shell at 400 ºC (HS 50.4)

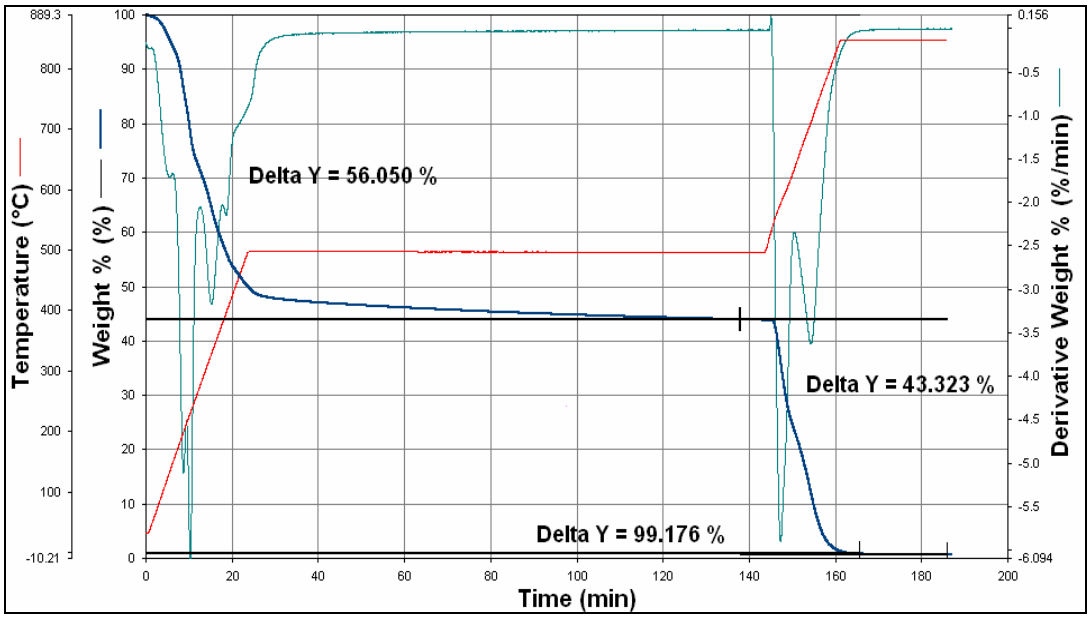

Figure E.3 TGA Result of 60% H_3PO_4 Impregnated Hazelnut Shell at 500 ºC (HS 60.5)

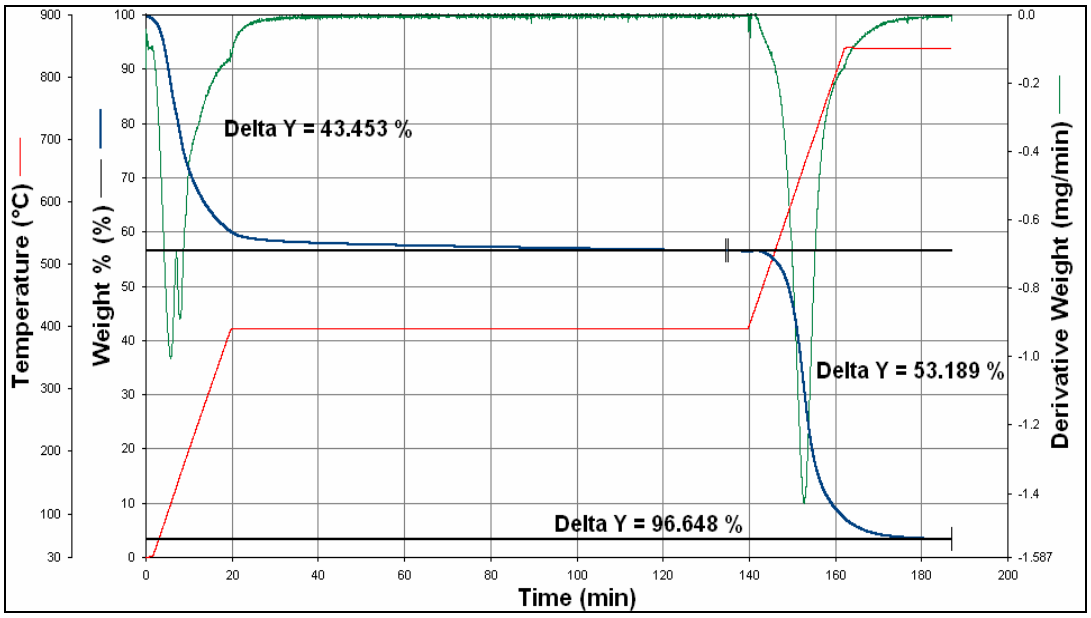

Figure E.4 TGA Result of 50% H_3PO_4 Impregnated Hazelnut Husk at 400 ºC (HH 50.4)

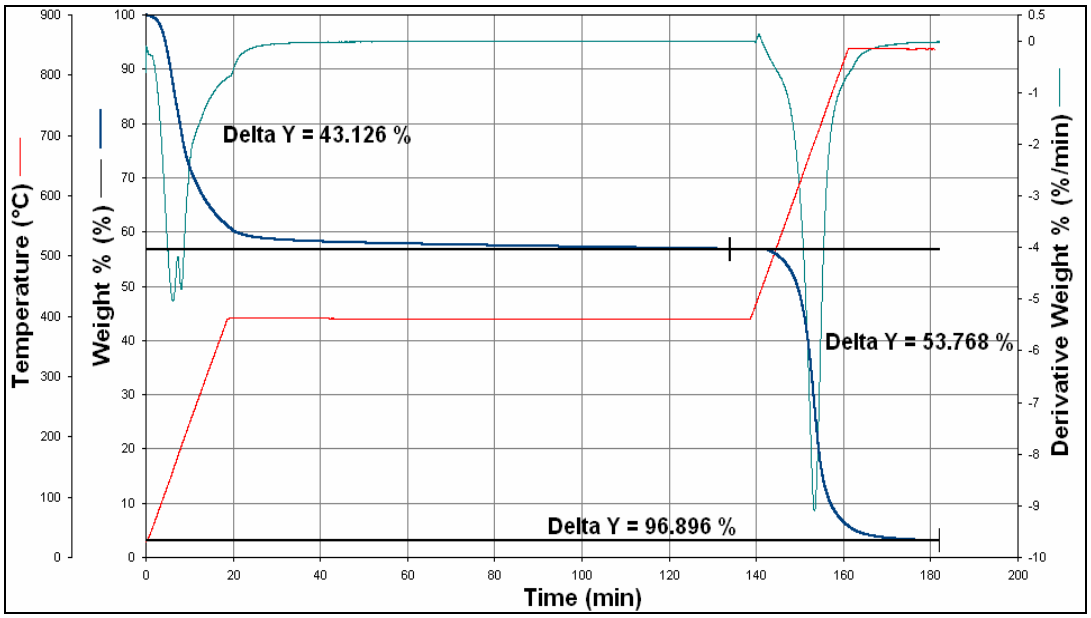

Figure E.5 TGA Result of 60% H_3PO_4 Impregnated Hazelnut Husk at 400 ºC (HH 60.4)

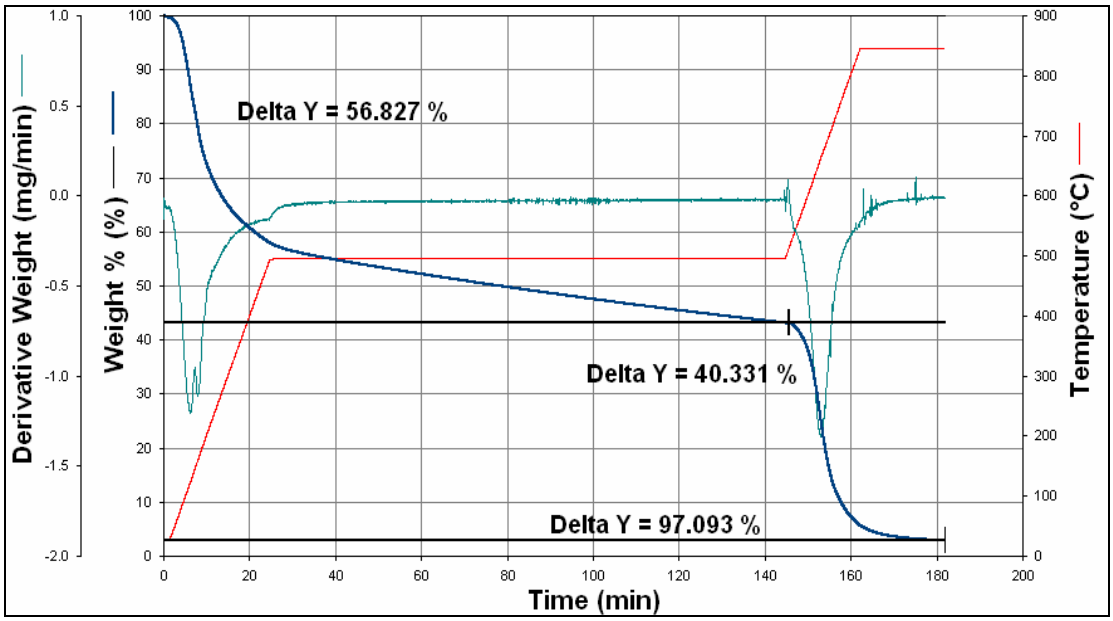

Figure E.6 TGA Result of 60% H_3PO_4 Impregnated Hazelnut Husk at 500 ºC (HH 60.5)